CZECH TECHNICAL UNIVERSITY IN PRAGUE

Faculty of Civil Engineering

Department of Sanitary and Ecological Engineering

Modelling WWTP processes using CFD methods

DOCTORAL THESIS

Ing. Ondřej Švanda

Doctoral study programme: Water Management and Water Engineering

Branch of study: Water Management and Water Engineering

Doctoral thesis tutor: prof. Ing. Jaroslav Pollert, Ph.D.

Prague, 2021

CZECH TECHNICAL UNIVERSITY IN PRAGUE
Faculty of Civil Engineering
Thákurova 7, 166 29 Prague 6

DECLARATION

Ph.D. student's name: Ing. Ondřej Švanda

Title of the doctoral thesis: Modelling WWTP processes using CFD methods

I hereby declare that this doctoral thesis is my own work and effort written under the guidance of the tutor prof. Ing. Jaroslav Pollert, Ph.D.
All sources and other materials used have been quoted in the list of references.

The doctoral thesis was written in connection with research on the project: TAČR TE02000077 Smart Regions - Buildings and Settlements Information Modelling, Technology and Infrastructure for Sustainable Development.

In Prague on ……. ……..
signature

I would like to thank my supervisor Prof. Ing. Jaroslav Pollert, Ph.D. for his consistent support and guidance during the running of this project. Furthermore, I would like to acknowledge the University of Chemistry and Technology for their participation and engagement in the experimental campaign and laboratory testing.

Abstrakt

Oblast simulace chování kalu pomocí matematického modelu je velmi dobře prozkoumána celou řadou výzkumných a aplikačních prací. Tyto modely využívají různé přístupy od snahy po čistě deterministický přístup po snahy o zobecnění kalibrovaných empirických modelů. Nicméně vzhledem k velké složitosti procesů zahrnujících například vícefázové proudění, chemické reakce, nebo nenewtonské proudění je obtížné tyto procesy simulovat a je třeba dalšího výzkumu v této oblasti. Z toho důvodu je třeba zmíněné modely verifikovat a následně validovat pomocí experimentálních měření. Tato práce se tedy zabývá vytvoření matematického modelu pro řešení dynamiky sedimentace kalu, který navazuje na předchozí výzkum a je rozšířen o vztahy získané pomocí databázového zpracování rozsáhlého experimentálního měření. Výsledným cílem je potom na základě získaných vztahů z měření vytvořit matematický CFD model použitelný pro simulaci dynamiky především dosazovacích nádrží, ale i dalších objektů na ČOV.

Abstract

The area of sludge flow modelling using numerical methods has been quite extensively explored and researched by numerous authors and papers. These developed models utilize different approaches from efforts to create a solely deterministic model to attempts to generalize calibrated empirical models. Nevertheless, the processes are not easy to simulate due to high complexity of the physics involving multiple phases, chemical reactions and non-Newtonian fluids. Therefore, additional research effort should be focused on improving these models and to verify and validate them against experimental measuring. This work is focused on creating a numerical model for sludge sedimentation dynamics which builds on the previous works and is extended with newly obtained relations from vast experimental measuring database. The objective is to create a CFD model based on obtained relations that could be primarily used for simulating the dynamics of secondary settling tanks but also for other objects at the waste water treatment plant.

Table of Content

Abbreviations

AS	Activated Sludge
CFD	Computational Fluid Dynamics
CTU	Czech Technical University
CWWTP	Central Waste Water Treatment Plant
DNS	Direct Numerical Simulation
ESS	Effluent Suspended Solids
IWA	International Water Association
LES	Large Eddy Simulation
MLSS	Mixed Liquor Suspended Solid
RANS	Reynolds Averaged Navier-Stokes
RAS	Return Activated Sludge
SLMA	Sludge Local Mean Age
SS	Suspended Solids
SST	Secondary Settling Tank
WAS	Waste Activated Sludge
WWTP	Waste Water Treatment Plant
ZSV	Zone Sedimentation Velocity

1. Introduction

It is hardly arguable that today's world is a very dynamic place driven by the technology advancement. It is more questionable whether the incredibly fast pace is good but it certainly brings new tools and ways that can be deployed into the classical design process. Such a tool that has been already successfully implemented in other industries in the recent years is numerical modelling. It has become a fundamental part of the design process in many industries including aerospace, machinery, biomedical, chemical, automotive and many others. Its' competence as a valid tool comparable to experimental measuring is the fact that major automotive companies rely on numerical models through the whole development process. The Computational Fluid Dynamics (CFD) industry is a fast-growing sector with some key players such as Siemens investing billions of dollars into their Digital Factory Division.

The usage of CFD at dealing with Waste Water Treatment Plant (WWTP) processes is nothing new. There has been lot of papers and research articles published on the topic. Those have already proven that some object at the WWTP such as pump stations, dividing objects or grits can be successfully simulated and optimized using CFD tools. Even though nearly all the processes present at WWTPs have been modelled, due to a complex physics involved in the processes there is still a lot of work that needs to be done to verify their virtual counterparts and to establish the simulation tools within the standard design process.

One of such complex processes is activated sludge sedimentation that occurs in the settling tanks. The complex dynamics that drive this process including flocculation, particles settling, non-Newtonian behaviour and different flow regimes make it difficult to simulate using a numerical model. It is believed that the field of numerical modelling of settling tanks dynamics should be explored more so better models and procedures are developed (Plósz et al, 2012).

It was also pointed out by Plósz (2012) that the problem with advanced numerical models is not in the mathematical complexity of the simulated processes but rather in the measurement quality with which those models are calibrated with. This has been true since the year 2012. In other words, the limitation of today's CFD models lays in the lack of proper experimental data methods, especially in the regions of hindered and compression settling or high-resolution concentration profiles.

1.1. Objectives

The field of numerical solutions of the sludge sedimentation and especially of the Secondary Settling Tanks (SST) has been under the scope of many researchers and over the years numerous different models were development in order to describe the driving physics underneath. Those models differ by the complexity of the physics taken into account and by the approach chosen whether they are simple empirical or complex general models. The objectives of this paper are:

1. To develop a numerical model for SST design and optimization based on the previous works and to extend it with relations obtained through experimental database.
2. To create a generalized sludge behaviour model that is applicable for different flow scenarios and that could be used for other sludge sedimentation applications.

1.2. Outline

This thesis is structured in a way that at the beginning the SST physics, different flow regimes and general behaviour are described including the flocculation and sedimentation process with brief description of the sludge non-Newtonian properties.

Following, part 2 sets its goal to describe the CFD numerical approaches for SST modelling and gives an overview of the up to the date developed models.

Part 3 describes the experimental measuring campaign that took place on the Prague central WWTP, the process of assessing the data and the constitutive relations transferred to the numerical model.

The final part 4 mostly details the results and comparison of the measured data and the numerical model behaviour. Then the assessment of the influent baffles is described leading to the design of the new baffle configuration.

The last part contains the summary and conclusions that were gathered throughout the research. Further direction of possible follow-up research is outlined.

2. Literature Overview and Works

2.1. Secondary Settling Tanks Hydraulics Overview

2.1.1. Function of SST

Secondary settling tank is part of the secondary treatment stage at WWTP. The activated sludge that inflows into the tank is usually diverted by stilling well which directs it to the main part of the SST where it settles down and is eventually draught to recirculation. The Effluent Suspended Solids (ESS) also called supernatant then continue either to tertiary treatment or straight into the water body as it is shown in Figure 1.

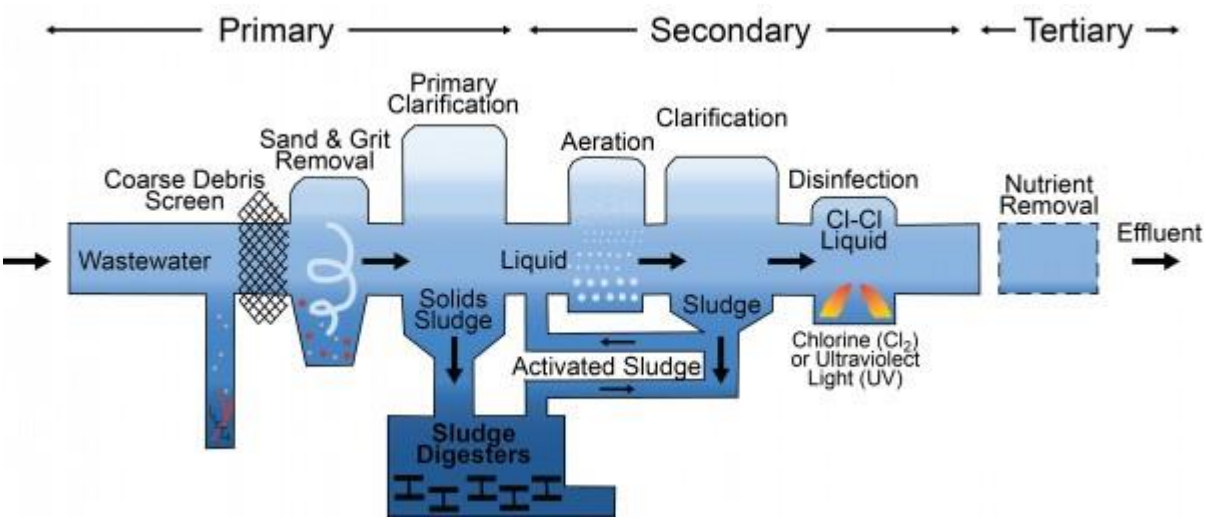

Figure 1 – Position of secondary settlement tanks within a water treatment process.

The typical circular radial flow tank design consists of several objects as it can be seen on Figure 2. The sludge influent pipe is usually located in the tank centre, where the sludge enters the stilling box or inlet zone. Its purpose is to lower the velocity and distribute the sludge to enter the main tank area – sedimentation zone. As the flow propagates through the tank to the scum or supernatant overflow, the sedimentation process takes place and the sludge blanket is created. The bottom of the tank has a gradient between 4° to 10°. The skimming blade then slowly rotates around the bottom of the tank and scrubs the well sedimented sludge to the sludge removal pit located at the bottom centre of the tank. The supernatant effluent then leaves the tank at the

outer rim through different types of an overflow and continues to the tertiary treatment or directly to the recipient.

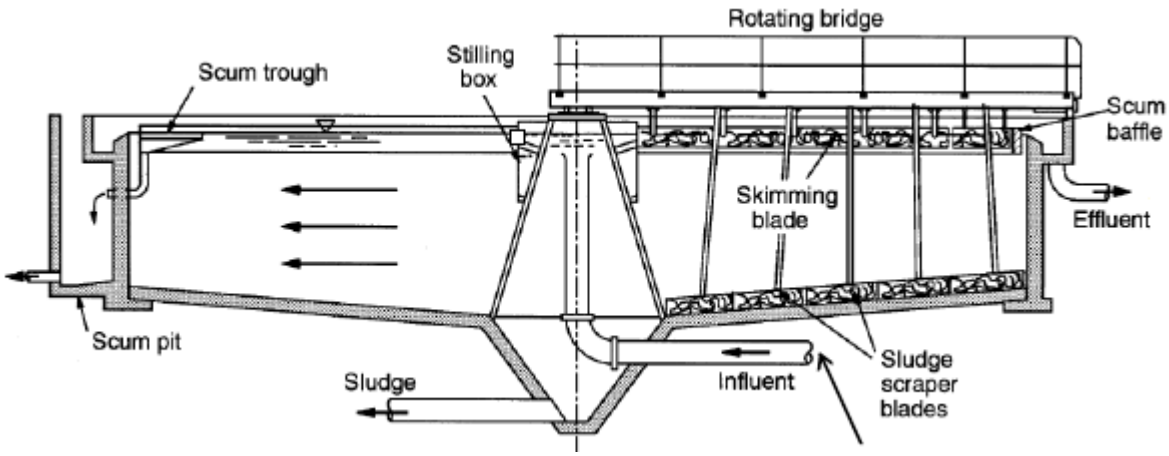

Figure 2 – Cross section of the secondary settling tank (Monash University, 2003).

The role of SST in the treatment process can be split into several functions that SST are designed to fulfil. The first function is the thickening process at which the settling sludge is compressed under its own weight and creates a thick layer at the bottom of the SST. This high-concentration sludge that can reach up to the value of 20 g/l is drained back for recirculation to the activation tanks by the mechanical removal system. This ability of sludge thickening plays an important role in the WWTP performance. Second function is the clarification ability. Most of the solids settle in the SST and only a small fraction of approximately 1-2 % of SS reaches the effluent. The SST efficiency is expressed in terms of ESS concentration. Well-designed SST then should provide low ESS concentrations even at wet flow conditions. Also, keeping the sludge in the SST at these high hydraulic loadings is the third objective of SST. It acts as a storage, where it should restrict an excessive leakage of SS over the effluent weirs. (Ekama et al, 1997).

A standard measure of the characteristics of activated sludge solids is the Sludge Volume Index (SVI). It is defined as "the volume in ml occupied by 1 g activated sludge after settling the aerated liquor for 30 min" (Dick & Vesilind, 1969).

Stirred Sludge Volume Index (SSVI) is then a SVI modification where slow stirring is used to minimize wall effects on the settled sludge volume.

Effluent Suspended Solids (ESS) is the most important metric in determining the SST performance as it represents the number of suspended solids that didn't settle and is transported to the outflow.

The key factors influencing the SST performance according to (Voutchkov, 2005) are:

1. Solids accumulated in the SST which can be expressed as the ratio of the Returned Activated Sludge (RAS) concentration and Waste Activated Sludge (WAS) concentration.
2. The number of solids in the aeration basins, which is established by measuring the Mixed Liquor Suspended Solids (MLSS) concentration and the RAS flow rate.
3. The settleability of the sludge.
4. The plant influent waste load and flow.

These factors are related in a way that the sludge characteristics and the design of the SST results in certain hydraulic behaviour that has a major influence on the settleability and thickening process. The physical phenomena that play a key role in these processes are settling and flocculation behaviour. (Ekama et al., 1997).

2.1.2. Sedimentation process

The settling that occurs in the tank is a result of gravitational force, buoyant force and opposite drag force acting on the suspended solids. There are 4 types of different settling regimes identified (IWA, 2008).

- Discrete particle settling – this regime is typical for low concentrations in the upper part of the tank, where the number of particles per litre is small and thus the particles (flocs) settle individually without any interaction. The velocity at which the flocs settle is constant.
- Flocculent particles settling – as the number of flocs per volume increases, they agglomerate and create bigger flocs that have increased mass and settle at a faster rate. This process depends also on the biological and chemical properties of the sludge.
- Hindered or Zone settling – with the increased solid concentration of about 0.6 – 0.7 g/l (Mancell-egala et al., 2012) the aggregated flocs settle as a unit. The settling velocity decreases due to the increased drag caused by the water being pushed outwards the zone as

the mass becomes denser. This mass creates a blanket with a recognizable interface with the low concentration supernatant.

- Compression settling – this regime occurs at the bottom of the SST as sedimentation can be only done through compression of the layer. This process continues to the point, where the density of the sludge is at the level, that doesn't allow for any further compression and the packing limit is reached. Compression settling can be identified by the decrease of the settling velocity.

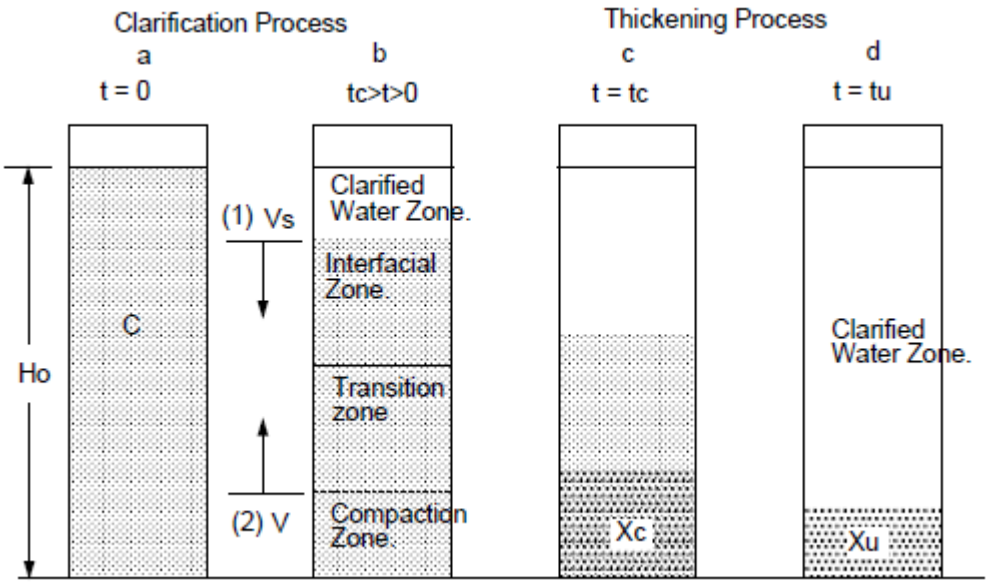

Figure 3 – Sludge settling stages in batch experiment (source: Brennan 2001)

The forces acting on a single discrete particle are the gravitational force F_g, frictional force F_f and the lifting force F_l. Putting these forces together gives us the Newton second law:

$$m\frac{d_v}{dt} = F_g - F_f - F_l \tag{1}$$

Where v is the particle velocity and m is the mass of the particle.

The gravity force F_g, frictional force F_f and lifting force F_l are given by

$$F_g = m.g \tag{2}$$

$$F_f = \frac{C_D . A . \rho_f . v^2}{2} \quad (3)$$

$$F_l = \rho_f . V_p . g \quad (4)$$

Where C_D is the drag coefficient, A is the particle projected area and ρ_f is the fluid density.

Putting these equations together and given the $d_v/dt = 0$ gives us the general particle sedimentation velocity

$$v = \sqrt{\frac{2g(\rho_p - \rho_f)V_p}{C_D . A . \rho_f}} \quad (5)$$

This general term can be expressed assuming a laminar flow, where

$$C_D = \frac{24}{R_N} \quad (6)$$

Where R_N is the Reynolds number

$$R_N = \frac{v . D . \rho_f}{\mu} \quad (7)$$

and μ is the dynamic viscosity. For a spherical particle, the equations (5), (6), (7) gives us a well-known Stokes law:

$$v = \frac{g(\rho_p - \rho_f)D^2}{18\mu} \quad (8)$$

2.1.3. Flocculation

Flocculation can be described as a process where small particles of an Activated Sludge (AS) group together and create bigger flocs. For a proper function of SST, it is fundamental that the micro-organisms have the ability to form large structures that settle well and are resistant to

breakage due to higher shear stresses (Das et al. 1993). The rate at which the flocculation occurs is dependent on biological and physical properties of the flocs (Ekama et al., 1997). The biological properties of AS include different types of microorganisms, number of filament bacteria, adsorbed matter, organic material and inorganic articles such as Ca^{2+} and Mg^{2+} (Govoreanu et al., 2004).

It has been suggested that the settling properties also depend on the physical properties of the flocs, the floc surface in particular. It was confirmed by the work of (Steiner et al., 1976) that the sludge volume index is directly related to the surface charge carried by the sludge particles and thus the settleability is strongly affected by the physical and chemical composition of the flocs. (Steiner et al., 1976).

Extensive research into activated sludge floc characteristics and their impact on settleability and compressibility was done by (Jin et al., 2003), where the authors collected samples from 7 different WWTPs and carried a series of tests to look into the biological, chemical and physical properties of the flocs. The factors influencing activate sludge properties are shown in Figure 4. It is apparent from the figure, that the sludge settling and compressing abilities are influenced by numerous different parameters such as chemical composition of the sludge, microbial population with strong influence of the filament bacteria, size distribution, structure, rheological properties etc.

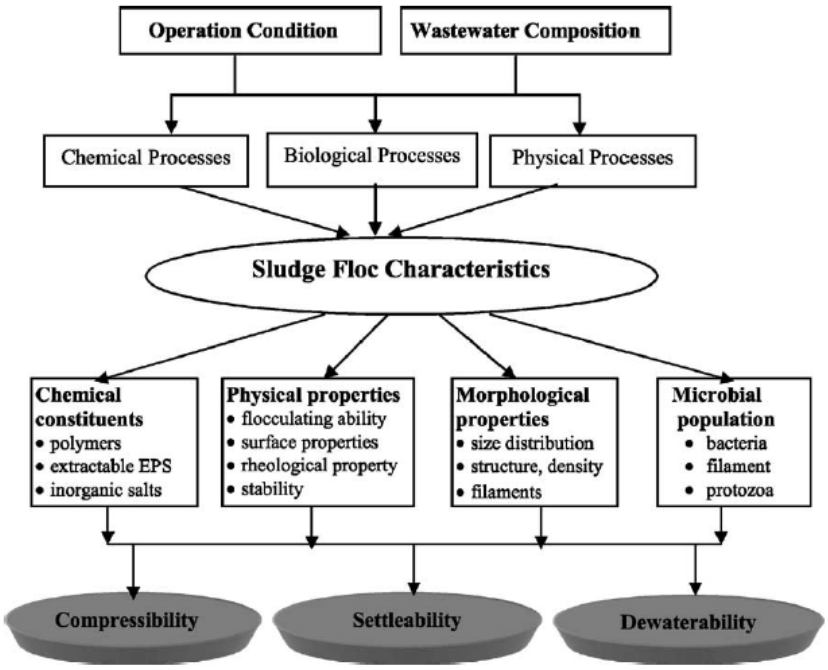

Figure 4 – Chemical, physical and biological factors influencing the settleability and compressibility of the activated sludge (Jin et al., 2003)

In their study, they measured flocculating ability, floc size distribution, relative hydrophobicity, fractal dimension, surface charge, filament index, SVI and ZSV of all the samples. From the results it is apparent, that different samples varied in terms of SVI from 40 to 260 ml/g and ZSV from 0.3 m/h to 6.6 m/h and showed a clear non-linear correlation with R^2= 0.8249. Samples with SVI higher than 150 ml/g were settling at very low velocities whereas low SVI samples showed a much faster settling velocity (Figure 5).

It has to be taken into consideration, that both SVI and ZSV values could be influenced by different settling device configurations and geometry, sludge volume, floc structure and temperature and therefore the results from different researchers will not be consistent (Dick & Vesilind, 1969), (Daigger & Roper, 1985). The opinions on the possibility of using a relationship between SVI and ZSV vary as some researches find it questionable (Dick & Vesilind, 1969). On the other hand, many researches claim that there is at least some correlation between SVI and ZSV (Vanderhasselt et al., 2000), (Ozinsky, Ekama, 1995). Nevertheless, as it was aforementioned, there are numerous parameters influencing the compressibility and settleability and thus either SVI and ZSV is governed by different sludge properties (Jin et al., 2003).

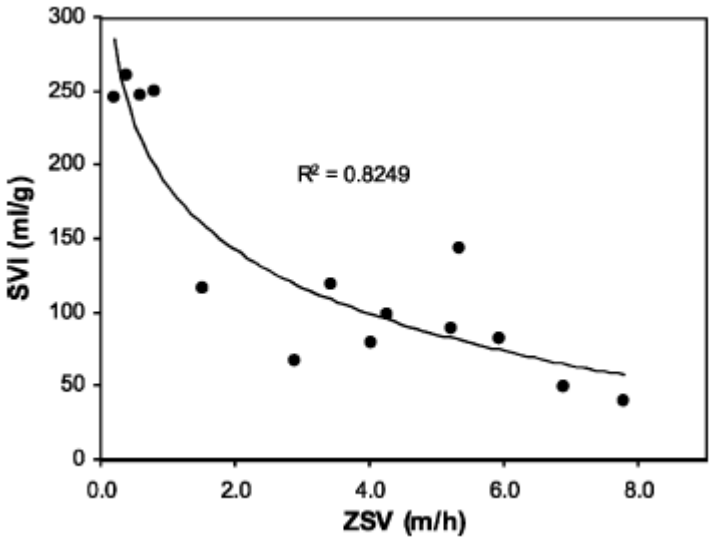

Figure 5 – Relationship between SVI and ZSV (Jin et al., 2003)

Based of statistical analysis using Pearson's correlation it seems that the most influencing parameters to settleability and compressibility are floc size and filament index showing significant correlation of $P < 0.05$ (Jin et al., 2003).

2.1.4. Sludge rheology

It is a well-known observation that sludge can be described as non-Newtonian fluid, meaning that the shear rate is not linearly proportional to shear stress. Different types of behaviour for sewage sludges were observed and described by (Casey, 1983). It turns out, that the linear Newtonian behaviour can be observed within the sludge of lower weight concentrations up to approximately 4 %. Sludges with concentration above this threshold then behave as either plastic or pseudo-plastic (Dick & Ewing, 1967).

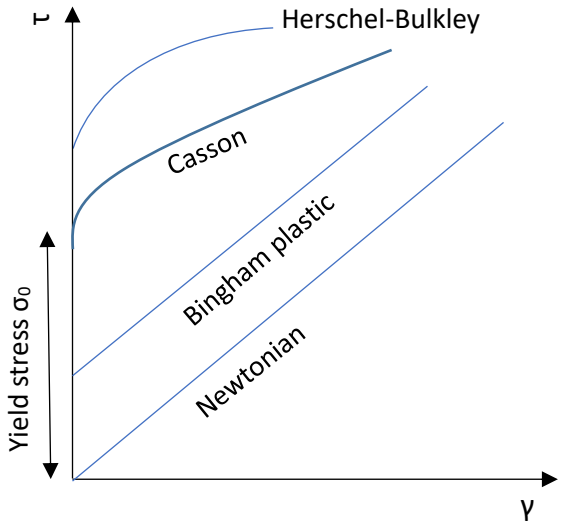

Figure 6 – Rheological models typical for sewage sludge behaviour (source: own)

Sewage sludges can be often characterized with shear-thinning behaviour which is typical for Bingham pseudo-plastic, Herschel-Bulkley or Casson rheology model. All these models are considered to be time independent and inhibit yield stress and pseudo-plastic relation between shear stress and apparent viscosity. Nevertheless, the sludges having high Deborah Number (response time / observation time) are called thixotropic (time dependant) as the internal structure of the sludge changes over time and thus changing the rheological behaviour. Various models for rheological data approximation are power-law models since the shearing behaviour of the fluids tends to be naturally approximated applying the power law (Alcantara, Moura, 1999). Mathematical models for flow behaviour applicable for sewage sludge description are Newtonian (9), shear thinning (10), Bingham (11), Herschel-Bulkley (12) and Casson (13).

$$\tau = h.\dot{\gamma} \tag{9}$$

$$\tau = K.\dot{\gamma}^n \ (n < 1) \tag{10}$$

$$\tau = \tau_0 + \eta_p.\dot{\gamma} \tag{11}$$

$$\tau = \tau_0 + K\dot{\gamma}^n \tag{12}$$

$$\tau^{1/2} = {\tau_0}^{1/2} + {\eta_\infty}^{1/2}.\dot{\gamma}^{1/2} \tag{13}$$

Yield stress τ_0 is defined as a minimum shear stress that need to be applied to initiate fluid deformation and is related to the structure of the sludge and aggregation of primary particles. These particles form a three-dimensional grid that has to be initially broken down before the fluid starts to flow (Casey, 1983).

2.2. Numerical models overview

2.2.1. Previous works

Numerous works and papers have been published on the topic of using CFD techniques to model activated sludge systems. These researches cover all the standard CFD approaches from basic single phase flow models using scalar equation to deal with the multiphase nature of the problem, to the mostly used mixture model and its modification, where some of the researches used computationally intensive Lagrange drift flux model or the general Eulerian multiphase model. Also, the general numerical models were introduced. The most relevant works and ideas are briefly described.

The comprehensive summary of early works in SST modelling was done by Ekama (1997) and was later extended by Samstag (2016). Firstly, he mentions the historically first attempts to use CFD for sedimentation purposes done by McCorquodale and his student using method of Roache (1982) and Patankar (1980). Later Zhou & McCorquodale (1992) used standard k-e turbulence model with the incorporation of solids transport and settling model using double exponential equation of Takacs (1991). They concluded, that the velocity pattern of the water-only flow is significantly different from the one containing solids.

More advanced model was introduced by Griborio (2004) who developed a model that included also flocculation and used vorticity/stream function to model the fluid pressure correctly. The impact of flocculation in the centre-well design tank was studied in Griborio & McCorquodale (2006) and stated that the flocculation influence on the hydraulic performance is low. A recognizable author is De Clercq (2003) who introduced a 2D model based on a commercial solver that took into account flocculation, solids transport, density coupling and Herschel Bulkley rheological model.

The possibilities of using a mixture model are well described in a PhD thesis by Burt (2010), where the author tries to extensively validate and verify an extended drift flux model to be used

in clarifier processes modelling. As a result, he points out that improved models are required for flocculent and discrete settling since those cannot be captured by the standard Takács settling function.

In the process of sedimentation model development, the General Sedimentation Model (GSM) that includes flocculation and all phases of settling – discrete, hindered and compressive would have been a significant improvement (Samstag et al., 2016).

The models differ by the complexity of the physics taken into account and by the chosen approach. One type of the models is focused on discrete particle settling using different particle classes and modelling their kinematics which does not capture the hindered phase correctly. The second type of models considers the sludge phase as monodisperse which is beneficial for the hindered phase but does not account for the discrete particle phase. There have been some attempts to create a generalized hybrid models but these eventually require numerous parameters as input which complicates its use outside the laboratory. What all these models share in common is that their performance decreases when used outside the sludge parameters they were calibrated on or require to obtain the sludge parameters for every settling tank they are trying to assess. Also, very limited number of models are applied in 3D, which is a considerable limitation in cases where the tank geometry doesn't have a rotational symmetry.

2.2.2. Conservation equations

In the real world, the movement of fluids can be described by partial differential equations ensuring the mass, momentum and energy conservation. The basic concept of CFD counts on the procedure of removing these PDE by a set of algebraic equations. Those equations can then be solved by computers. Applying the momentum vector leads after adjustments to a well-known governing Navier-Stokes set of equations (Daly & Harlow, 1970):

$$\frac{\partial u}{\partial t}+\frac{\partial(uu)}{\partial x}+\frac{\partial(uv)}{\partial y}+\frac{\partial(uw)}{\partial z}=-\frac{\partial p}{p\partial x}+v\left(\frac{\partial^2 u}{\partial x^2}+\frac{\partial^2 u}{\partial y^2}+\frac{\partial^2 u}{\partial z^2}\right)+f_x \tag{14}$$

$$\frac{\partial v}{\partial t}+\frac{\partial(vu)}{\partial x}+\frac{\partial(vv)}{\partial y}+\frac{\partial(vw)}{\partial z}=-\frac{\partial p}{p\partial y}+v\left(\frac{\partial^2 v}{\partial x^2}+\frac{\partial^2 v}{\partial y^2}+\frac{\partial^2 v}{\partial z^2}\right)+f_y \tag{15}$$

$$\frac{\partial w}{\partial t}+\frac{\partial(wu)}{\partial x}+\frac{\partial(wv)}{\partial y}+\frac{\partial(ww)}{\partial z}=-\frac{\partial p}{p\partial z}+v\left(\frac{\partial^2 w}{\partial x^2}+\frac{\partial^2 w}{\partial y^2}+\frac{\partial^2 w}{\partial z^2}\right)+f_z \tag{16}$$

Where u, v, w are velocity components, p is pressure, Fx,y,z are the components of external forces, ρ is the density and v is kinematic viscosity.

2.2.3. Turbulence

The problem with solving the flow field is the presence of turbulence. That can be tackled by several numerical approaches that vary in the required computational power and level of accuracy respectively. The main 3 approached are listed below:

- Direct Numerical Simulation (DNS)
- Large Eddy Simulation (LES)
- Reynolds Averaged Navier-Stokes (RANS)

DNS

The most precise and most demanding is the Direct Numerical Simulation (DNS) method. It basically involves the solution of the Navier-Stokes time dependent equations without the need of any turbulence model. It means that the entire spatial scale of the turbulence must be resolved from the largest eddies carrying the most energy down to the smallest dissipative scales called Kolmogorov scales. Therefore, even today it is too demanding to be used for industrial analyses and thus it remains in the military and supercomputing research applications.

LES

One step down the ladder of computational requirements stands Large Eddy Simulation method. The idea behind this model is that according to Kolmogorov, the largest eddies are induced by the geometry whereas the smaller scales could be considered isotropic and therefore have small impact on the momentum of the fluid. Thus, the biggest eddies are calculated directly and the small eddies are resolved using a sub-grid scale (SGS) models. This filtration significantly lowers the computational power and it still offers a solution that is not time averaged. Nevertheless, this approach is not suitable for the purposes of this work.

RANS

The most used turbulence model is generally based on the assumption that in global measure the characteristics of the turbulence could be averaged in time and then only statistical methods can be used to provide closure to the equations.

The basic assumption behind the Bousinesq model is that shear stress tensor can be substituted with the Newton law:

$$\tau = \eta . \frac{du}{dy} \tag{17}$$

Where τ is shear stress and η is the dynamic viscosity.

Without this generalization, all nine turbulent stresses would must have been counted for which adds significantly to the computational requirement. Nevertheless, it introduces a new quantity called turbulent viscosity that adds for another equations to be solved.

One-Equation Models

These models are the simplest models for handling turbulent viscosity as it only introduces the velocity scale k. Thus, they are suitable for low-Re number. The most common model is Spalart-Allmaras but its usage is not very common as there are more advanced models with only slight increase in complexity.

K-e and k-w turbulent models

Generally, two equation models include two extra transport equations besides the Navier-Stokes to compute the turbulent properties of the flow. Thanks to that, the diffusion and convection effects can be included.

Both of the models rely on the Boussinesq eddy viscosity assumption which states that the Reynolds stress tensor T_{ij} is proportional to the mean strain rate tensor S_{ij} and therefore can be written in the following way (Schmitt, 2007):

$$\tau_{ij} = 2\mu_t S_{ij} - \frac{2}{3}\rho k \delta_{ij} \tag{18}$$

Where μ_t is the eddy viscosity.

The advantage of this assumption is that it handles the effects of turbulence in a way similar to how molecular viscosity affects a laminar flow. That significantly reduces the computational requirements as it is a huge simplification and that brings also the downsides. The Reynolds stress tensor is not always proportional to the strain rate tensor and therefore it is not valid for

the complex flows with strong curvature and wakes. That results in the models not being able to properly handle rotating flows and stagnation flows (Anon., n.d.).

The k-ε model

The k–ε model is by far the most widely used and tested two-equation model, with many improvements incorporated over the years. The standard k–ε model of Launder and Sharma is specified as follows:

Kinematic eddy viscosity (v_t) equation:

$$v_t = C_\mu \frac{k^2}{\varepsilon} \tag{19}$$

Turbulence kinetic energy (k) equation:

$$\frac{\partial k}{\partial t} + \bar{u_j} \frac{\partial k}{\partial x_j} = \frac{\partial}{\partial x_j}\left[\frac{(v + v_t)}{\sigma_k}\frac{\partial k}{\partial x_j}\right] - \varepsilon + \tau_{ij}\frac{\partial \bar{u_i}}{\partial x_j} \tag{20}$$

Turbulence dissipation rate (ε) equation:

$$\frac{\partial \varepsilon}{\partial t} + \bar{u_j} \frac{\partial \varepsilon}{\partial x_j} = \frac{\partial}{\partial x_j}\left[\frac{(v + v_t)}{\sigma_k}\frac{\partial \varepsilon}{\partial x_j}\right] - C_{\varepsilon 1}\frac{\varepsilon}{k}\tau_{ij}\frac{\partial \bar{u_i}}{\partial x_j} - C_{\varepsilon 2}\frac{\varepsilon^2}{k} \tag{21}$$

where $\sigma k = 1.0$ and $\sigma\varepsilon = 1.3$ are the Prandtl numbers for k and ε, respectively. The remaining model constants are: $C_\mu = 0.09$, $C_{\varepsilon 1} = 1.44$, $C_{\varepsilon 2} = 1.92$. The standard k-e model is well known for good prediction of turbulent shear flows (free shear) which is of the interest in most of the applications. On the other side, the prediction of great pressure gradients and side strains lags behind which results in poor separated flow behaviour (Ansys Inc., 2013).

The k–ω model

This model is also widely used and it has been around for some time already. The roots of this model reach back to Kolmogorov, who introduced it in 1942. Imperial College group under Prof. B. Spalding then proposed improved version of the model. Over the time many applications of k–ω model were performed by many scientists and engineers, but the most important development was by well-known Wilcox (Argyropoulos & Markatos, 2014).

Kinematic eddy viscosity (v_t) equation:

$$v_t = \frac{k}{\omega}, \quad \omega = max\left\{\omega, C_{lim}\sqrt{\frac{2S_{ij}S_{ij}}{\beta^*}}\right\}, \quad C_{lim} = \frac{7}{8} \tag{22}$$

Turbulence kinetic energy (k) equation:

$$\frac{\partial k}{\partial t} + \overline{u_j}\frac{\partial k}{\partial x_j} = \frac{\partial}{\partial x_j}\left[\left(v + \sigma^*\frac{k}{\omega}\right)\frac{\partial k}{\partial x_j}\right] - \beta^* k\omega + \tau_{ij}\frac{\partial \overline{u_\iota}}{\partial x_j} \tag{23}$$

Specific dissipation rate (ω) equation:

$$\frac{\partial \omega}{\partial t} + \overline{u_j}\frac{\partial \omega}{\partial x_j} = \frac{\partial}{\partial x_j}\left[\left(v + \sigma\frac{k}{\omega}\right)\frac{\partial \omega}{\partial x_j}\right] - \beta\omega^2 + \frac{\sigma_d}{\omega}\frac{\partial k}{\partial x_j}\frac{\partial \omega}{\partial x_j} + a\frac{\omega}{k}\tau_{ij}\frac{\partial \overline{u_\iota}}{\partial x_j} \tag{24}$$

The k–ω model is superior to the standard k–ε model for several reasons. For instance, it achieves higher accuracy for boundary layers with high pressure gradient and therefore better predicts separation of the boundary layer. The model suffers from weaknesses when applied to flows with free-stream boundaries such as jets, but that is not the case for sedimentation tank flows.

2.2.4. Numerical multiphase approaches

Multiphase flows are often present in engineering and research applications and therefore the numerical approaches have been developed and put in use. Due to an extensive complexity of the multiphase flows, it is not possible to develop a general model that would cover all regimes and fluid types. That is mainly because of several reasons. Firstly, the flow type is dependent on the compounds of the multiphase – solid-gas, liquid-gas, liquid-solid, etc. and within the flow, also numerous regimes occur such as annular flow, bubbly flow, slug flow, etc. Another difficulty arise from diverse physical phenomena can has to be modelled such as break-up, flocculation, drag and others. Last, but not least, the overall diversity of the multiphase models projects into the complexity of numerics which often leads to convergence difficulties, short time steps and CFL number (Wachem & Almstedt, 2003).

First attempts of modelling multiphase were made by Anderson & Jackson (1967) with gas-particle flow and later numerous authors had been developing the constitutive relation like Gidaspow (1994), Kuipers (1990), Ding (1992), Sinclair (1989) and many others. A significant work to notice was done by Ishii (1975) who derived the multiphase fluid-fluid governing equations with different assumptions from those used by Anderson and Jackson enabling him to overcome the constraints limiting the usage of the model only to certain flow types and offers closures for various gas-liquid regimes.

It should be noticed, that until 1980's all the multiphase models were assumed to be Eulerian models meaning that all of the phases were modelled as continuous, therefore average volume fractions are obtained rather than properties of dispersed particles and droplets (Wachem, Alms, 2003). The other, Lagrangian approach, on the other hand, tracks every discrete particle separately and governs the motion and trajectory using own equation of motion within the continuous phase. The basics approach widely used for multiphase modelling can be summed up in to following list:

- Eulerian-Eulerian approach, also called full multi-phase model
- Eulerian-Langrangian approach, or discrete particle tracking model
- Mixture model approach, known as drift flux model.

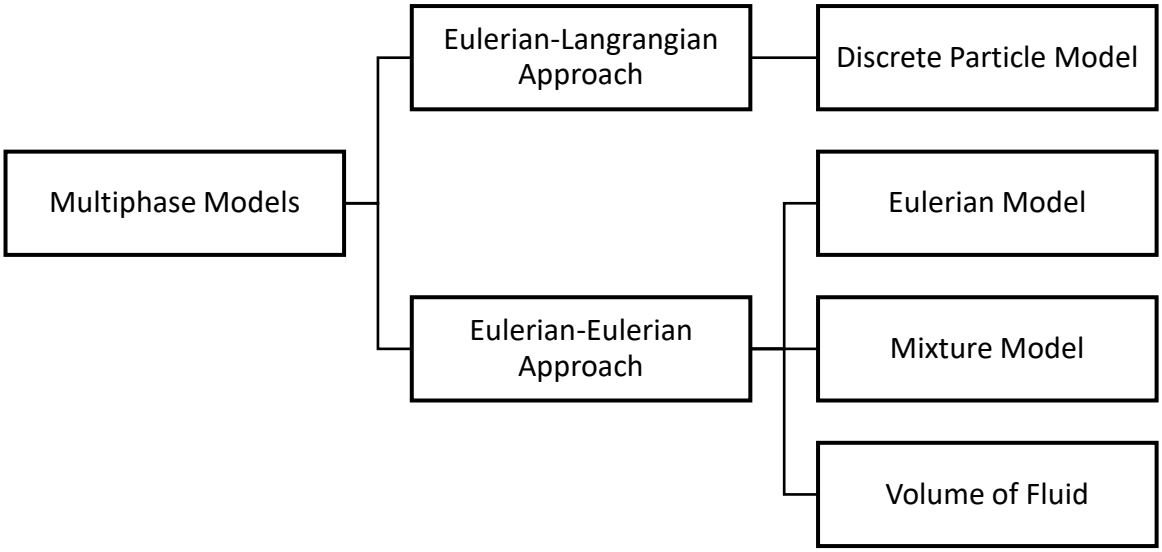

Figure 7 – Structure of multiphase models (source: own)

Eulerian-Eulerian Approach

In Eulerian-Eulerian frame all the phases including the dispersed phase are considered to be continuous. Thus, the conservation equations for mass, momentum and energy are solved separately for each phase which increases the computational requirements.

The phases in the Eulerian-Lagrangian frame are governed by the standard continuity and mass conservation equations

$$\frac{\partial \epsilon_g \rho_g}{\partial t} + \nabla . \epsilon_g \rho_g \upsilon_g = 0 \tag{25}$$

$$\frac{\partial \epsilon_g \rho_g \upsilon_g}{\partial_t} + \nabla . \left(\epsilon_g \rho_g {\upsilon_g}^2\right) = -\epsilon_g \nabla \mathrm{P} + \varepsilon_g \nabla \bar{\bar{\tau}}_g + \epsilon_g \rho_g g - {}_k I \tag{26}$$

Where k in the phase index and I represents the interphase momentum transfer between the phases. It provides the coupling between independent conservation equation for each phase.

$$I = I_{drag} + I_{am} + I_{hist} + I_{turb} + I_{lift} \tag{27}$$

Where I_{drag} is the viscous drag force, I_{am} represents added mass, I_{hist} is Basset force, I_{turb} stands for turbulent fluctuations and I_{lift} is the force denotating rotational strain, velocity gradient or wall.

In case of SST, the movement of each phase can be independent and there is momentum exchange between the phases in terms of drag, lift and buoyancy. That enables to solve the settling behaviour of the sludge in deterministic manner. It is possible to specify the drag force for spherical particles using correlations of Ishii and Zuber (1979). It is also possible to define irregular particle shape and use correlations to determine the relevant drag force. The inter-particle forces present is denser sludge bed were then solved by increasing the effective mixture viscosity by Gidaspow (1994). Compression settling correlations based on solids pressure were presented by Witt (1995). Despite the fact, that various Eulerian-Eulerian models were developed, the limitation of this approach is that these particulate properties such as density, shape and length scale can be defined only as a single value for a single solid phase (Burt 2010). That is a huge simplification given the fact, that the sludge flocs are very diverse in terms of sizes and floc shapes (CIWEM, 1997). Realizing the complexity of the flocculation, zone and compression settling, floc break up, agglomeration and all other phenomena occurring in SST, it is not possible to use this deterministic approach to model sludge behaviour within SST.

Eulerian-Lagrangian Approach

Lagrangian models are very useful for solving particulate flows but since the equations of motions are solved for each particle and also the collision model is included, limiting factor for the usage is the computational power.

The fluid phase is modelled using the governing equation stated in Equation 25.

The motion of the particle is governed by Newton's second law of motion solving for the forces acting upon the particle such as gravity and drag.

$$m_s m_a = m_s g + V_s \nabla . \bar{\bar{\tau}}_g - V_s \nabla P + \beta \frac{V_s}{\epsilon_s} (v_g - v_s) \tag{28}$$

Where a is the particle acceleration, V_s is the volume of one particle, P is the local pressure ε_s the local solids volume fraction, β the interphase momentum transfer coefficient and $\bar{\bar{\tau}}_g$ represents the fluid phase stress tensor.

The collisions of the particles can be described using two different approaches called hard-sphere and soft-sphere. In the hard-sphere approach the collisions are calculated based on the linear and angular momentum in the collision. Energy transfer during the collision is assumed to be elastic deformation with prescribed coefficient affecting the velocity of the rebound. This type of collision is used for both particle-particle and particle-wall collisions. The idea behind the soft-sphere approach is that the collision of two particles results in deformation and loss of some of the kinetic energy. (Wachem, Almstedt, 2003).

The use of Lagrangian framework for particle modelling and Eulerian frame for solving the fluid phase has been used by researchers to model waste water systems (Stovin, 1998) and a detailed study of using the multiphase models for combined sewer overflow modelling was done by (Burt et al, 2002). The outline of that study suggests that Lagrangian frame is not appropriate for modelling SST. The major drawback is that particles numerically disappear from the simulation when they terminate which doesn't allow for forming sedimentation body as it happens in reality. This method is very limited in prediction of solids retention and thus not suitable for SST modelling (Burt, 2010).

Mixture Model Approach

The idea behind the mixture model is that both the fluid and solids phase is considered as one – mixture phase. This concept was originally proposed by Wallis (1969) and was later developed by Ishii (1975). This method assumes that the momentum equations of both phases are merged to form a single mixture momentum equation and as it is with the continuity equations becoming one mixture continuity equation. The dispersed phase distribution is then expressed through convection diffusion equation. This method reduces the number of solved equations by eliminating the interphase momentum exchange terms. The benefit arising from this simplification is that the numerical instabilities associated with the interphase exchange terms are now eliminated leaving a more robust set of equations and decreasing the computational efforts. On the other hand, the deterministic behaviour achieved through specification of drag, density and shape of the particle is lost to the constitutive relations. In case of SST, the velocity difference of the dispersed phase is caused mainly due to gravitational settling which is inhibited in the model as slip velocity. Therefore, the horizontal velocity difference is neglected and it is assumed that the phases move together in this direction. That assumption can cause some

problems in the areas of high velocity gradients. The slip velocity is often obtained through experimental data collection and testing using batch settling procedures.

Since the mixture model is based on centre of mass conservation equations, the mixture velocity is defined as:

$$v_m = \frac{\epsilon_1 \rho_1 v_1 + \epsilon_2 \rho_2 v_2}{\rho_m} \tag{29}$$

The relationship between mixture velocity v_m and the velocities of each phase $v_{1,2}$ is shown in Figure 8.

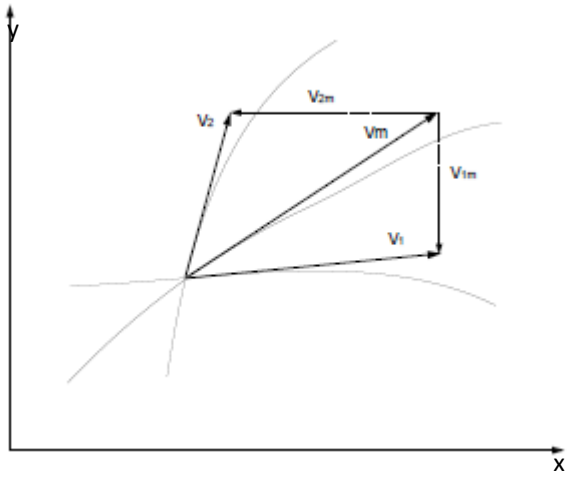

Figure 8 – Velocity relationship in mixture model (Ishii, 1975)

The slip velocity is then expressed as;

$$v_{2m} = -\frac{\epsilon_1 \rho_1}{\rho_m} (v_1 - v_2) \tag{30}$$

The mixture model's slip velocity concept is a widely used and cited in sludge sedimentation works and its versions are often included in commercial CFD solvers, for example the algebraic slip model implemented in Ansys Fluent and CFX (Ansys Inc., 2013).

In this section, Eulerian-Eulerian, Eulerian-Langrangian and Mixture model multiphase approaches were briefly introduced in order to summarize their effectiveness, complexity and applicability in SST modelling. The most complex approach is the Eulerian-Eulerian where each

phase is solved separately and their interaction is defined through interphase exchange source/sink terms. This approach enables for deterministic description of the dispersed phase but in reality, it is difficult to obtain these terms. Also, they cannot be specified for different sludge particle sizes densities etc. On the other hand, the mixture model phase interaction is defined only through slip velocity, which is a considerable simplification in general but it is not that restrictive in the way of SST modelling. The mixture model is often used and is the best choice for accomplishing the objectives of this dissertation.

2.2.5. Hindered settling

Hindered or zone settling regime is typical for a clear interface between sludge and water and the particles settle as a zone. The majority of the hindered sedimentation models are based on the solid flux theory which was pioneered by Kynch (1952). This theory is wrapped around the idea that the total flux of solids is given by

$$j_m = X.v \tag{31}$$

Where X is the suspended solids concentration and v is the hindered settling velocity and depends on X, giving us

$$j_m = X.v(X) \tag{32}$$

meaning that gravitational hindered settling velocity depends only on the local suspended solids concentration X. The total solid flux j_t including the bulk flux withdrawing from the domain can be then expressed as

$$j_t = \left(v_g(X) + \frac{Q_u}{A}\right)X \tag{33}$$

Where v_g is the velocity of the withdrawing sludge and Q_u is the withdrawal rate.

An easy determination of the hindered settling velocity is to perform a batch column settling test for different concentrations. During the test a glass column with the height of 3 m is filled with sludge mixture from the SST and then the creation of the interface between water and sludge is observed. Later on, this interface starts to settle down and its height in the column is

recorded over time. The detailed methodology of the performed tests is described in 3.2.1 Hindered settling velocity . This test is then repeated with different concentrations of the suspended solids. The hindered velocity (V_s) is then calculated from the slope of the linear part of the curve as it is shown in Figure 9.

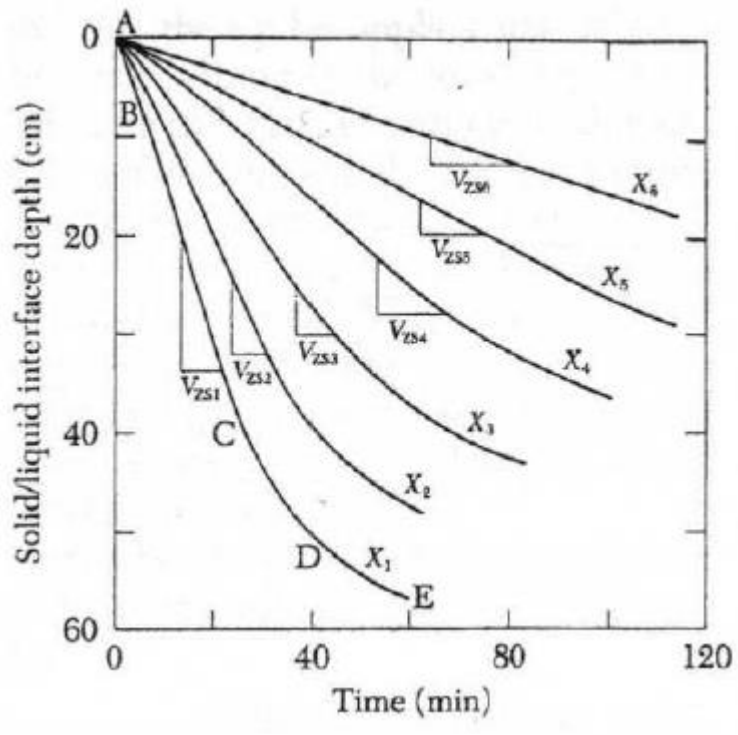

Figure 9 – The function of the sludge/water interface height in time for different solids concentration (X), The hindered velocity is the slope of the linear part of the curve (Ekama et al., 1997)

Therefore, most of the numerical models that were introduced are based on this empirical relation of the settling velocity (V_s) and solids concentration (X). Since now, lot of models were introduced such as Vesilind (1986); Takács et al. (1991); Cho et al. (1993); Dick and Young (1972); Watts et al. (1996) etc. Until the introduction of the Takács model, the Vesilind model was widely used and accepted.

Vesilind formulated the hindered velocity and solids concentration relation as an exponential function

$$V_s = V_0 e^{(-r_V X)} \tag{34}$$

where V_0 is the maximum settling velocity or the slope of the linear part of the curve (Figure 9) and r_v is the Vesilind parameter influencing how fast the velocity decreases with increasing solids concentration (X). This parameter can be easily obtained by linear regression of the batch column settling tests data. The setback of this approach is that with solids concentrations close to 0 the velocity still increases which is contrary to the observations, where very small concentration tend to settle at small velocities.

To account for that inconsistency, Takács et al. (1991) proposed a modified version of the Vesilind function by introducing another exponential term to the function.

$$V_s = V_0 e^{(-r_H \cdot (X - X_{min}))} - V_0 e^{(-r_p \cdot (X - X_{\min}))} \quad (35)$$

Where X_{min} is the minimum solids concentration at which settling occurs, r_H is a parameter describing the hindered zone and r_p is a parameter characterizing the low concentration settling. These parameters can be deducted from the batch column test data by linear regression same as the Vesilind parameters.

2.2.6. Rheology modelling

One of the early rheology models used was the Standard Model by Bokil and Bewtra (1972) which puts into linear log relation sludge solids concentration and apparent viscosity as shown in 23.

$$\mu_m = \frac{\tau}{\dot{\gamma}} = 0.00327.\,10^{0.132X} \quad (36)$$

Bolik and Bewtra used an extended number of 65 different sludge samples into consideration. Nevertheless, the general usage of the model is questionable as the correlation coefficient R^2 = 0.854 is valid only for solids concentrations higher than 700 mg/l. This shortcoming was later compensated for by Lakehal (1999) who introduced a linear fit for low concentration sludges as it is apparent in Figure 10.

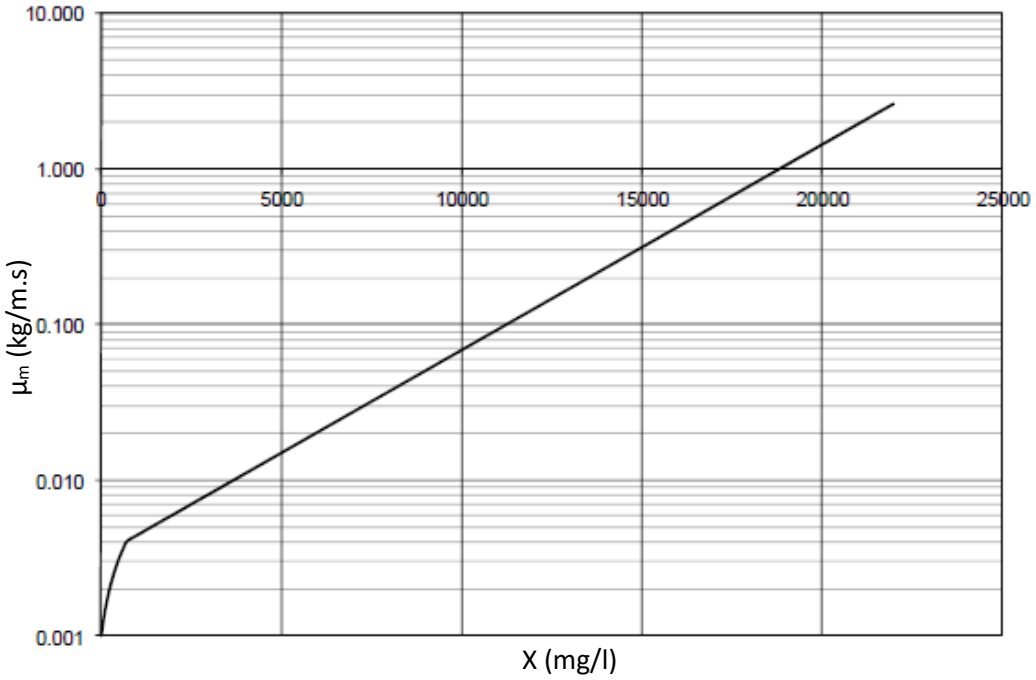

Figure 10 – Mixture viscosity function introduced by Bolik and Bewtra (1972) and later modified by Lakehal (1999)

It was stated in chapter 2.1.4 Sludge rheology that sewage sludge may indicates similar behaviour to Bingham plastic model. That wasn't left unnoticed and Lakehal (1999), who proposed a model with yield stress that must be initially overcome to set the fluid to motion. Thus, the relation 11 is modified into

$$\mu_m = \mu_0 + \frac{\tau_0}{\dot{\gamma}} \tag{37}$$

where the plastic yield stress τ_0 is given by Dick and Ewing (1967) as

$$\sigma_0 = \beta_1 e^{\beta_2 X} \tag{38}$$

Extensive research in yield stress parameters (β_1, β_2) fitting was done by Dick and Ewing (1967) who also proposed that the sludge is thixotropic as the measured viscosity decreased after some time using the same viscometer.

One of the latest significant contributions to rheology models is the one from De-Clerq (2003) who modified the Bingham plastic model to fit the Herschel Bulkley model characteristics

$$\mu_m = \frac{\tau_0}{\dot{\gamma}}\left(1 - e^{(-m\dot{\gamma})}\right) + \mu_0 \dot{\gamma}^{n-1} \tag{39}$$

where *m* compensates for the stress growth over the time. The experimentally derived constants by De-Clerc for this relation are m = 163.4 s, n = 0.777. De-Clerc also proposed a modified equation for the yield stress which is as follows

$$\tau_0 = \beta_1 (\frac{X}{\beta_3})^{\beta_2} \tag{40}$$

Where the fitted coefficient are β_1 =9.036e^{-4} kg/m.s^2, β_2 = 1.12 and β_3 =1 kg/m^3 based on three sites experimental campaign.

2.2.7. Closure

The area of modelling SST processes using CFD has been extensively researched by many authors. They try to develop and improve the methods aiming at generally two different outcomes. First group of researches focuses on the development of general sludge behaviour model that could be deployed without the necessity of vast experimental measuring. Even though this deterministic approach is possible, the difficulty associated with obtaining interphase exchange terms seems to be still too big to climb. The other group of academics aim at finding relationships through experimental data regression. The relationships are then put together in an attempt to provide a model that is as generic as possible. The mostly used phase interaction model is the mixture model which seems to be the best option for SST modelling as it has been already proven many times. This model relies on the slip velocity assumption providing an easy way for fitting experimental settling data. This straightforwardness then makes it easy to extend the model by additional sub-models for solving rheology and flocculation. Nevertheless, the authors generally agree, that the sludge sedimentation process is complex and more effort should be put into creating a model that accounts for different sedimentation regimes and would be valid outside its calibration data.

3. Methodology and Experimental Data Gathering

The methodology consisted of several subsequent steps. First, the experimental data of sludge properties of interest were gathered at the Central Waste Water Treatment Plant in Prague (CWWTP) from two different SSTs. Subsequently, the measured data were evaluated partly on-situ and partly in the laboratory. For each sample a report including all measured and calculated properties was made. Due to an extensive amount of data gathered over two years, a database framework was created to process that data and to find sludge sedimentation dependencies and relations which were then used as an input for the CFD model.

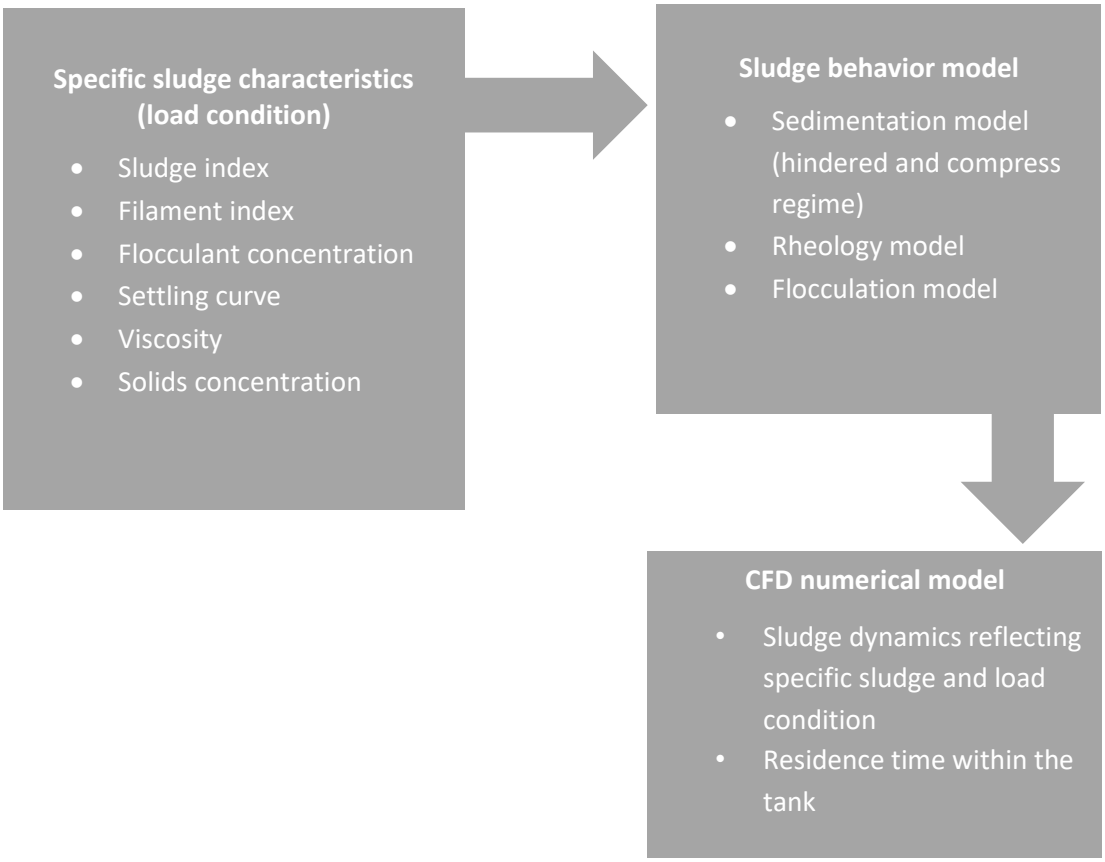

Figure 11 – Schematics of the CFD model development

3.1. Experimental site

For the data gathering purposes, the CWWTP in Prague was chosen primarily thanks to its close proximity to the Czech Technical University (CTU) so the samples that could not be examined in-situ were not affected by long transport times to the lab.

At the WWTP, there are 8 old and 4 new circular SSTs with the diameter of 43 m and outer wall depth of 2.5 m. The influent type is central stirring well having octagonal shape. The cleared water outflows through an annulus to the drain at the outer perimeter of the tank. Settled sludge at the bottom of the tank is transported to the sludge collection pit by a bottom scrapper and removed. The geometry of the SST with major dimensions is shown in Figure 13.

Figure 12 – Secondary settling tank at the CWWTP in Prague

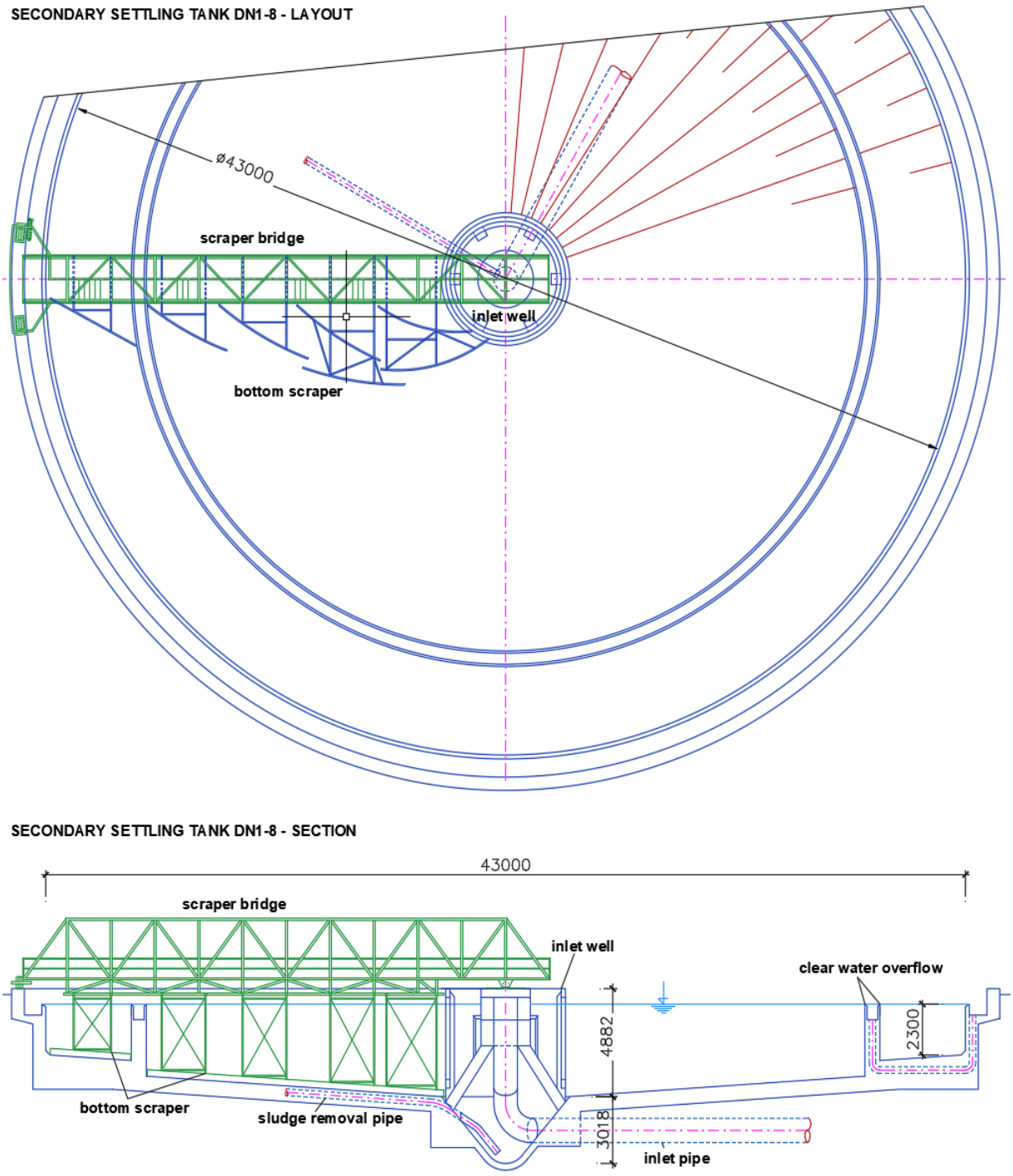

Figure 13 – Drawing of the secondary settling tank at the CWWTP in Prague

For the purposes of running the tests in-situ, a temporary field lab was erected next to the SSTs. It houses two settling columns for batch sedimentation tests, viscosimeter, sludge pump and other accessories necessary for the samples collection.

Figure 14 – Field lab built for tests data collection at the CWWTP in Prague

3.2. Methodology of sludge properties measuring

There were total of 9 data gathering campaigns from April to October 2017 from SST DN1 and then from April to September 2018 from tank DN3. Specific data for the need of the numerical model were also measured in 2019. Total of 136 complex samplings were conducted. The extent of data analysed for each sample is summarized in Table 1.

Table 1 – Recorded sludge and external properties

Properties recorded for every sample	**External properties**
Sampling – depth in the tank	SST inlet flow rate
Sampling – radial coordinate of the tank	SST outlet flow rate
Time and date	SST sludge removal flow rate
Temperature	SST inlet suspended solids concentration
Hindered sedimentation velocity	SST outlet suspended solids concentration
Viscosity	SST flocculant dosage
Sludge volume index	Weather (dry/rain)
Density	SST suspended solids concentration profile
Suspended solids concentration	
Flocs size distribution (small, medium, large)	
Microflocs	
Core consistency (compactness)	
Filament index	
Fragmentation	
Buoyancy	
Turbidity	

3.2.1. Hindered settling velocity column tests

One of the main tests was the settling column test conducted in the field lab (Figure 15). Two, 3 m high cylindrical columns with a diameter of 0.15 m were used. The sludge from a certain location in the SST was pumped into the columns up to the height of 2.8 m using a standard submerged sludge pump. Before initiating the settling test, the column was aerated using a compressor to stir the sludge so the start of the sedimentation was not affected by the delay while filling the column. The height of the interface between water and sludge was recorded every 5 minutes for the entire length of the test, taking 1 or 2 hours. The outcome from this test was the Hindered Settling Velocity (HSV) taken as the slope of the curve's linear part (m/h). The same sludge sample used for the test was concurrently analysed in the means of its viscosity,

sludge index, density and temperature. Later in the CTU lab, spectrophotometry was used to obtain the concentration of extracellular polymers (carbohydrates, proteins and humic substances). The suspended solids concentration was measured gravimetrically.

Figure 15 – Batch settling columns

3.2.2. Viscosity measuring

Rheological properties of the samples were measured using the rotary viscometer Rheometer RC20. The tests were conducted in a cylinder/cylinder setup and is suitable for non-Newtonian fluids. The strain rate range was chosen to be 0 – 1000 s^{-1} during the tests in 2017 and then changed to 3.5 – 500 s^{-1} during 2018. The overall time of the test was 300 s with the resolution of 50 values per test. The postprocessing of the data was done in Rheotec 3000, v2.0. The dynamic viscosity was calculated as:

$$\mu = \frac{\tau}{\frac{\partial u}{\partial y}} \tag{41}$$

Where μ is dynamic viscosity (Pa.s), τ is shear stress and du/dy is strain rate.

The maximum strain rate in the SST obtained from a CFD simulation was around 20 s^{-1}, meaning that the resolution from the Rheometer RC20 was not sufficient for analysing sludge in the SST as there was only 1 value between 0 and 20 s^{-1}. Changing the maximum test strain rate and/or sample resolution did not lead to usable results with the Rheometer RC20. Consequently, in 2019 a new viscometer Brookfield DV2TLV was obtained in order to measure the viscosity in the interested range of 0 – 50 s^{-1}.

Figure 16 – Rhometer RC20 (left), Brookfield DV2TLV (right)

3.2.3. Density measuring

The density of the sludge was measured using a 100 ml pycnometer. The weight of a dry pycnometer was recorded and then it was filled with the sample and closed. The redundant

sample overflowed through capillary and its weight was measured. The density was then calculated from the weight difference of dry and full pycnometer. Also, the temperature of the sample was recorded using WTW Multi 3430 multimeter.

3.2.4. Sludge volume index measuring

SVI was determined as specific volume of activated sludge after 30 minutes of settling in a 1 l container related to the suspended solid concentration.

$$SVI = \frac{V_{30}}{X} \tag{42}$$

Where V_{30} is the settled sludge volume and X is the suspended solids concentration.

3.2.5. Suspended solids measuring

The concentration of suspended solids was measured gravimetrically according to Horáková a spol. (2005). As a filter, Pragopor nitrocellulose 0.4 um was used, pre-dried at 105 °C. The filtered volume was chosen based on the suspended solids concentration. It ranged between 5 – 20 ml for sludge samples, 50 ml for supernatant and 100 ml for the water outflow.

3.2.6. ECPs

Spectrophotometry was used to obtain the concentration of extracellular polymers such as carbohydrates, proteins and humic substances. Free and bonded ECPs were separated using a centrifuge. Bonded ECPs were thermally extracted and centrifuged.

3.2.7. Sludge Concentration Profile

For the numerical model validation, it is important to capture the distribution and depth of the sludge blanket. For that purpose, an innovative approach was developed. It is based on the suspended solids concentration profile measuring using the Cerlic Multitracker and then postprocessing the data in Matlab to visualize the concentrations in the SST (Švanda, et al., 2018).

Figure 17 – Cerlic Multitracker used for obtaining suspended solids concentration

The handheld multitracker consists of a probe connected to the device through a several meter long cable. As the probe is being submerged in to the tank to the bottom, it continuously records the suspended solids concentration creating a vertical concentration profile.

This profile was measured at the SST at the radial distance of 3 meters from the tank's centre and then at each 2 m increment until the outer wall of the SST with last profile being taken at the radial distance of 21 m. These data were then assembled in Matlab to create a 2D concentration map. It vividly displays the position of the sludge blanket and provides more insight into the state of the sludge in the tank during different events such as rain flow etc. It can be seen in Figure 18 and Figure 19 that during the rainless flow, the sludge blanket interface is clear, whether during the rain flow the sludge is in the buoyancy and no clear interface is visible. It serves as a main validation tool to compare the CFD model results with as these distributions can be taken at any moment to validate different flow scenarios and tank states.

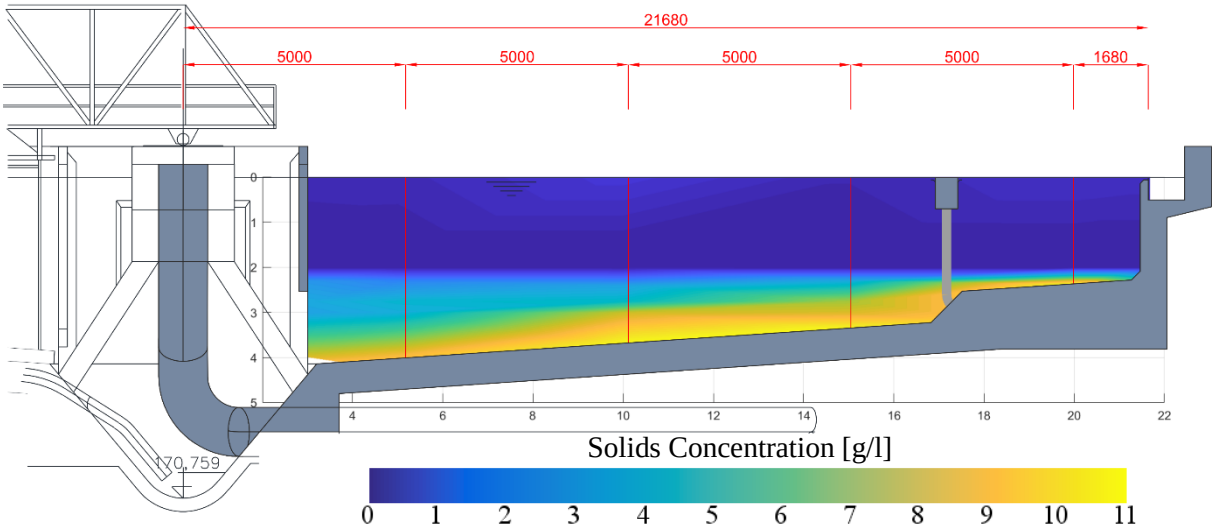

Figure 18 – Distribution of suspended solids concentration in the SST – rainless flow

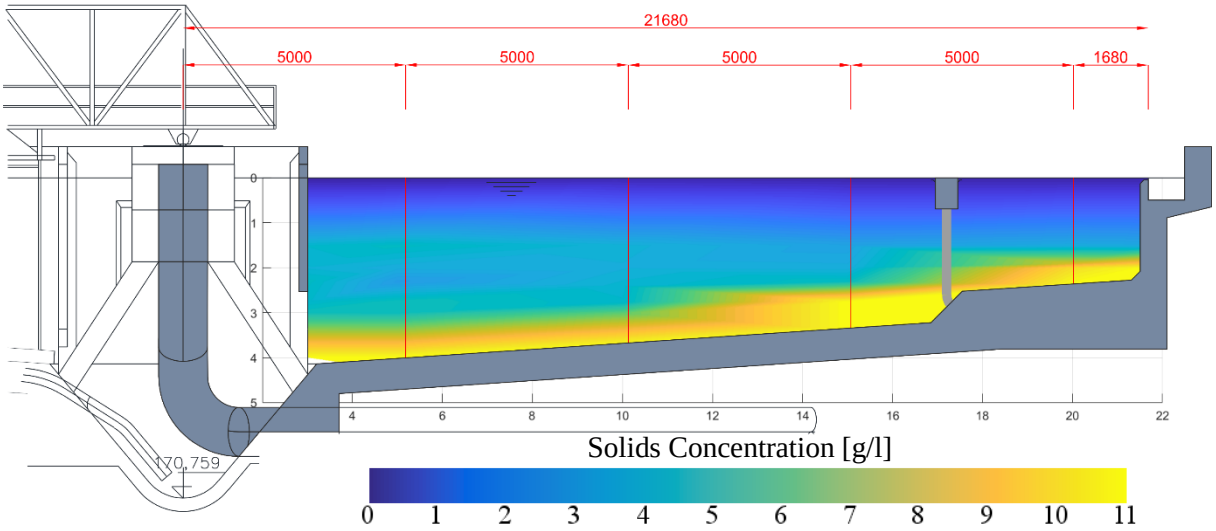

Figure 19 - Distribution of suspended solids concentration in the SST – rain flow

3.2.8. Camera Tests

To get a better understanding of the sludge flow field, especially in the critical areas such as the inlet zone, a special camera was constructed. It consists of a GoPro camera mounted to a tube with plastic plates serving as stabilizers and preventing the assembly to rotate when being submerged. To ensure good visibility, a powerful flash light is angled to the field of view of the camera. It is then possible to visually analyse the flow behaviour and understand the influence of the change of the geometry or change of the inlet flow rates.

Figure 20 – Camera assembly

3.3. Sludge Properties Database

To consolidate the big amount of data obtained during the campaigns, a database system was developed. For that purpose, a commercial software Microsoft Access was used as a platform. Developing the database system was both beneficial and necessary from several aspects.

- Ability to sort and show all properties and values from a certain sample
- Possibility to easily compare samples and to find relations between properties
- Ability to categorize and to create sludge groups based on the settling properties

Each sample underwent several different tests. The settling column test and viscosity measuring was done in-situ, where microscopic test, sludge volume index, ECPs and densities were analysed in the CTU lab. On top of that, external parameters such as SST inlet and outlet flows and concentrations, flocculant dosage and weather information needed to be included as well. For that purpose, each sampling was given an ID through which all the tests can be connected together in the database. Choosing a certain sampling ID brings all the parameters associated with that sampling in a well-arranged matter.

Plotting the properties from all samplings at once enabled to identify wrong data and obviously erroneous measurements and to exclude them from the database in order not to influence the relations.

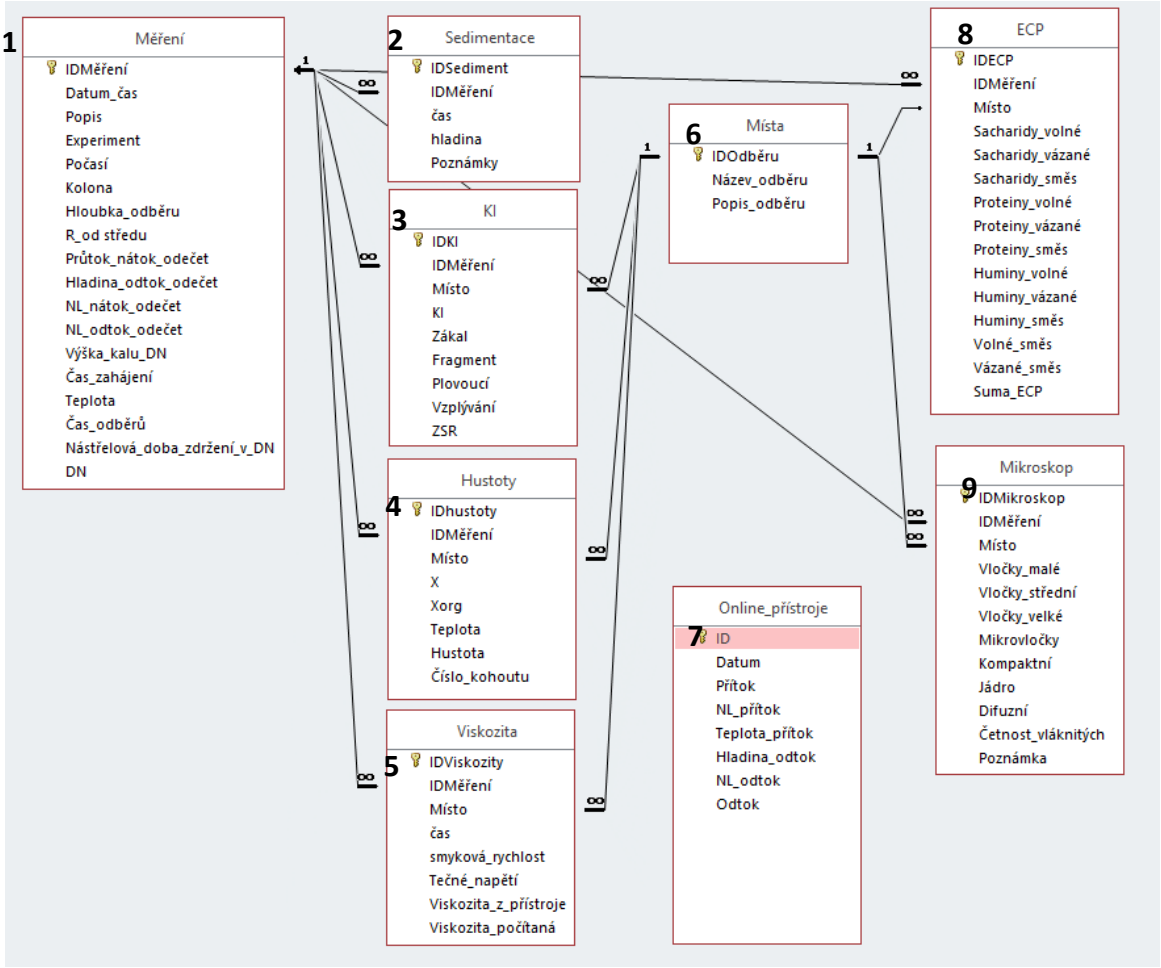

Figure 21 – Database data and relations

Creating the database required an extensive amount of man hours and thus was developed with a collaboration of a small team who went through the input data and cleaned them from any corrupted measurements, wrong readings and other misplaced data. That is also the reason for the database being written in Czech language. The data processed in the database that are relevant to the development of the numerical model are:

1. Měření – Measurements, properties of sludge that was taken from a tank
    - IDMěření – unique ID to connect all the data sources
    - Datum_čas – date and time of the measuring

- Počasí – weather conditions – important when raining
- Kolona – sedimentation column, matches the No. 2 Sedimentation data
- Hloubka odběru – depth of sampling relative to the water surface level
- R_od středu – radial distance of the sampling from the tank center
- Průtok_nátok_odečet – tank inlet volumetric flow from a probe
- NL_nátok_odečet – suspended solids concentration at the tank inlet
- NL_odtok_odečet – suspended solids concentration at the tank outlet
- Teplota – temperature of the sample

2. Sedimentace – Sedimentation, data taken from the sedimentation columns
    - Čas – time from the start of the sedimentation
    - Hladina – water surface level recorded every 5 minutes
3. KI – Sludge volume index
4. Hustoty – density of the sample
    - X – suspended solids concentration
    - Hustota – density
5. Viskozita – viscosity of the sample
    - Smyková_rychlost – strain rate
    - Tečné_napětí – shear stress
    - Viskozita_počítaná – calculated viscosity from strain rate and shear stress
6. Místa – location, description of the sample location
7. Online_přístroje – online measuring probes dedicated especially for flow rate and suspended solids concentration measuring
    - Přítok – tank inlet flow rate
    - NL_přítok – tank inlet suspended solids concentration
    - Odtok - tank outlet flow rate
    - NL_odtok - tank outlet suspended solids concentration
8. ECP - extracellular polymers
9. Mikrokop – sample properties determined using microscope
    - Vločky malé/střední/velké – sludge flakes small/medium/large
    - Četnost vláknitých – number of fibrous flakes

4. Developing of the numerical model

4.1. General framework

The framework on which the numerical model is built is the commercial CFD software Ansys Fluent. It is not the goal of this work to develop a CFD code from scratch but to extend the ability of a widely used CFD code to simulate the specific behaviour of sludge in SSTs. That enables an easy deployment of the sludge settling model to any user with the Ansys Software package. The Ansys software package provides all the necessary tools for creating geometry, meshing, post-processing and already implements transient implicit solver, multi-phase models and common turbulence models.

The CFD sedimentation model is implemented through utilization of user defined functions (UDFs) to handle the flocculation, sedimentation and rheology of the sludge. This model can be easily adjusted through parameters to respect different sludge types and behaviour which extends its usage to be applied to any settling tank beyond the experimental one.

The developed numerical model consists of several sub-models each handling different part of the sludge behaviour:

- Flocculation sub-model handles the initial phase of the settling process, the flocculation.
- Sedimentation sub-model is responsible for hindered zone and compress zone sedimentation.
- Rheology sub-model is based on the non-Newtonian characteristics of the sludge.
- Sludge residence time distribution adds a time level into the model and provides additional insight.

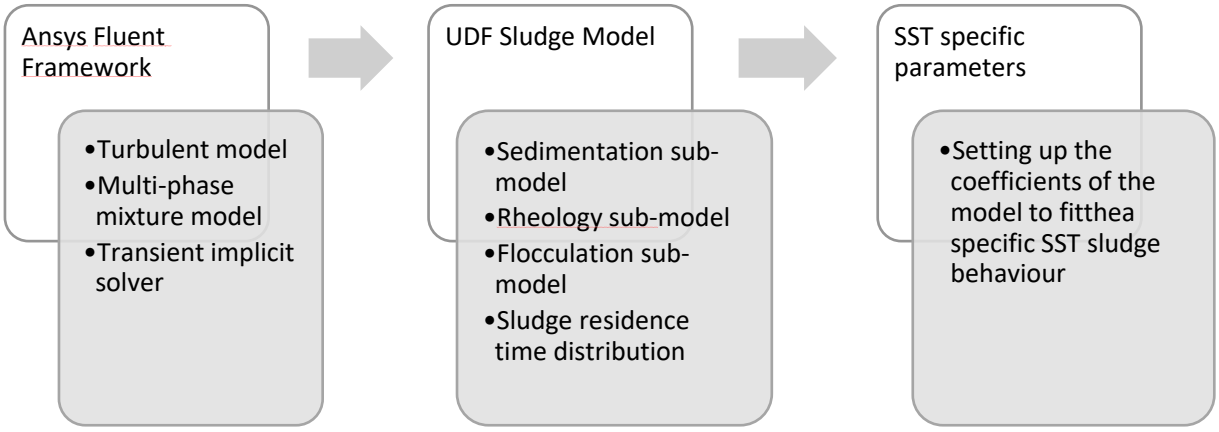

Figure 22 – CFD sludge sedimentation model implementation

4.1.1. Turbulent model

The most widely used turbulent model for RANS is the k- ε model. This model uses two variables to provide a closure to the equations. The k is the turbulent kinetic energy and ε is the dissipation rate of the kinetic energy. The model uses logarithmic wall function to predict the generation or dissipation of the turbulence in near wall regions. The wall function approach has its limits in cases of a close to laminar flow (low Reynolds numbers), which is observed in the SSTs outside the inlet zone or in cases where steep velocity gradients are present. For those reasons a low-Reynolds modification of the SST k-ω turbulent model was used as it is described by Wilcox. Consequently, during the meshing process, the first layer cell height was adapted to have value of $y^+ < 3$ (< 1 is theoretical optimum) to accommodate for the turbulent model.

4.1.2. Transient solver

The transient solver was used in order to obtain sludge residence time distribution in the tank which is lately used to modify the sludge settling parameters based on the time the sludge spends in the tank. The pressure based implicit Iterative Time-Advancement Scheme (ITAS) was chosen as it is more suitable for high viscous flow than the Non-Iterative Time-Advancement Scheme that is available in Fluent.

The ITAS is based on the idea, that all the equations are solved iteratively for as long as it takes to meet the convergence criteria for a given time step. Meaning, it requires multiple inner iterations within one time step to progress the solution in time. The ITAS algorithm for segregated solver implemented in Fluent is shown in Figure 23.

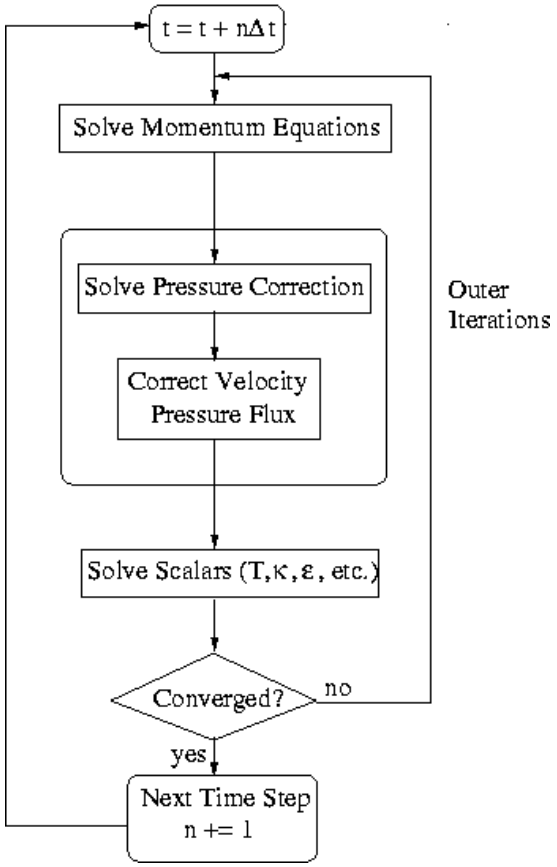

Figure 23 – Iterative Time Advancement Solution Method (ANSYS Fluent Manual 12.0)

4.1.3. Multi-phase mixture model

In the Chapter 2.2.4 Numerical multiphase approaches, different multi-phase approaches are evaluated resulting in the selection of using the Mixture model and its slip velocity implementation. For detailed information about the Mixture model, please refer to the aforementioned Chapter.

4.2. Rheology

Since the activated sludge often behaves as a non-Newtonian fluid, it is necessary to precisely capture the non-linear relationship between strain rate and shear stress. That is important because in the inlet flocculation zone there are an order of magnitude higher velocities than in the rest of the tank and therefore higher strain rates as well. Thus, the sludge in the inlet zone has a different viscosity than in the rest of the tank. Also, the apparent viscosity changes with the suspended solids concentration – higher concentration results in higher viscosity and the

sludge blanket at the bottom of the tank shows radically different behaviour than the supernatant at the sludge-water interface. Therefore, the purpose of the rheology sub-model is to find a relation between suspended solids concentration and strain rate. In the CFD model, both the strain rate and concentration are known so a viscosity can be calculated and assigned accordingly to each cell.

A total of 41 samples were analysed using the viscometer which outputs the relation between strain rate and shear stress. Using the well-known equation, the apparent viscosity was calculated.

$$\mu_m = \frac{\tau}{\dot{\gamma}} \tag{43}$$

All of the raw data of strain rate vs shear stress were plotted and are shown in Figure 24.

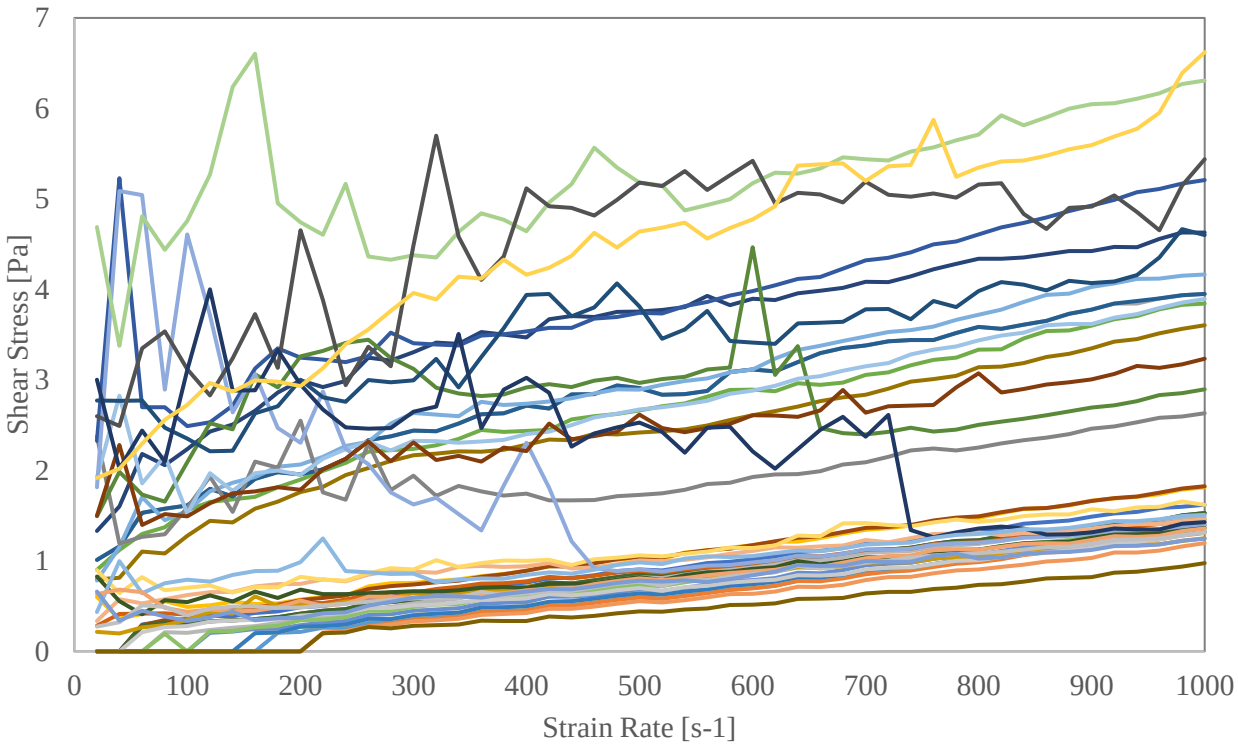

Figure 24 – Shear Stress vs. Strain Rate of measured samples

From the figure, there are several things worth noting. Firstly, the data scatter in two different zones, first zone represents the bottom part of the figure with samples showing rather linear,

close to Newtonian behaviour. On the other hand, the upper two thirds of the Figure show strong non-Newtonian behaviour following either Herschel-Bulkley or Casson behaviour. Secondly, it is obvious that some of data were not recorded correctly and show low consistency with high bias, especially the ones with high suspended solids concentration. The probable cause is the heterogeneity of the sludge with high solids concentrations. The viscometer works with a small sample volume of the sludge that may consist of bigger floc agglomerates that move within the sample and influence the precise measuring process. Together with a generally low viscosity of the sludge that is difficult to measure, inaccurate results may be produced. Even though the biased data fit in the tendency, they were not used further on.

After discarding the erroneous samples, the data showed a good correlation with the Casson sludge type, that is described by the equation

$$\tau^{1/2} = {\tau_0}^{1/2} + {\eta_\infty}^{1/2}.\dot{\gamma}^{1/2} \quad (44)$$

where τ_0 is the Casson yield stress that needs to be overcome at zero strain rate and n_∞ is the Casson plastic viscosity. These parameters differ for each sample based on the solids concentration, so we can obtain the function from a regression analysis of the data. The selected data to extract the dependency are the curves with c= 4,9 g/l and c= 13,5 g/l to capture both the low and high concentration profiles.

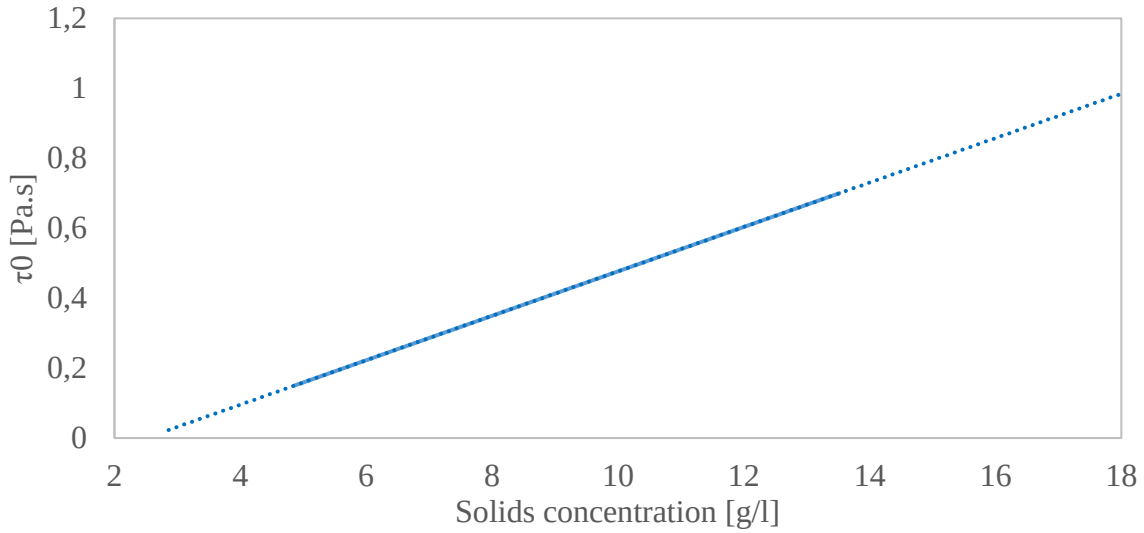

Figure 25 – Data regression curve of τ_0

The τ_0 parameter shows a linear dependency on the solids concentration that can be described as:

$$\tau_0 = 6.35 \cdot 10^{-2} \cdot c - 1.58 \cdot 10^{-1} \quad (45)$$

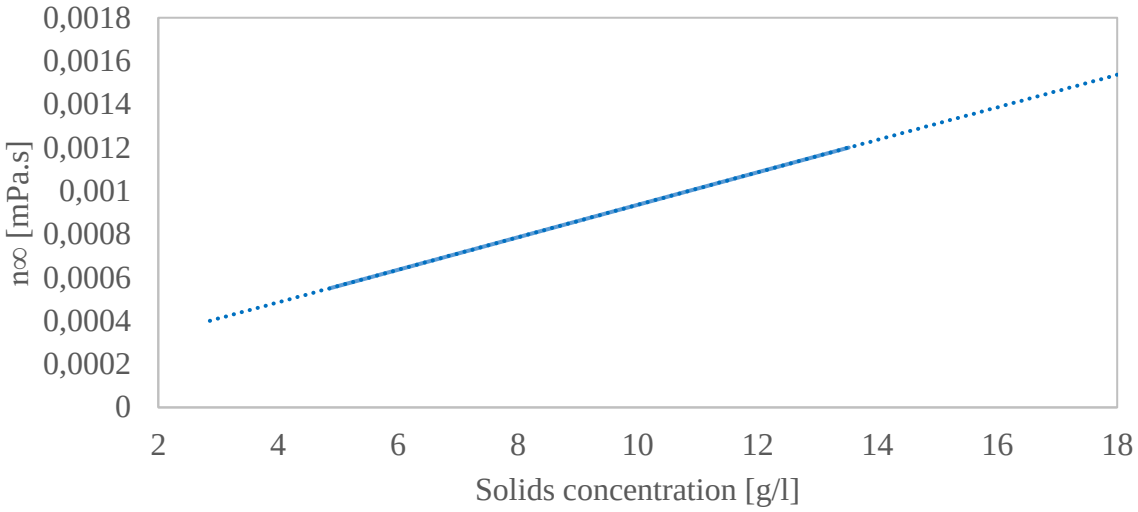

Figure 26 – Data regression curve of n_∞

Also, the n_∞ can be described using a linear function:

$$\eta_\infty = 7.51 \cdot 10^{-5} \cdot c + 1.85 \cdot 10^{-4} \quad (46)$$

Eventually, we can create a viscosity function based on the solids concentration.

$$\tau^{1/2} = (6.35 \cdot 10^{-2} \cdot c - 1.58 \cdot 10^{-1})^{1/2} + (7.51 \cdot 10^{-5} \cdot c + 1.85 \cdot 10^{-4})^{1/2} . \dot{\gamma}^{1/2} \quad (47)$$

In the

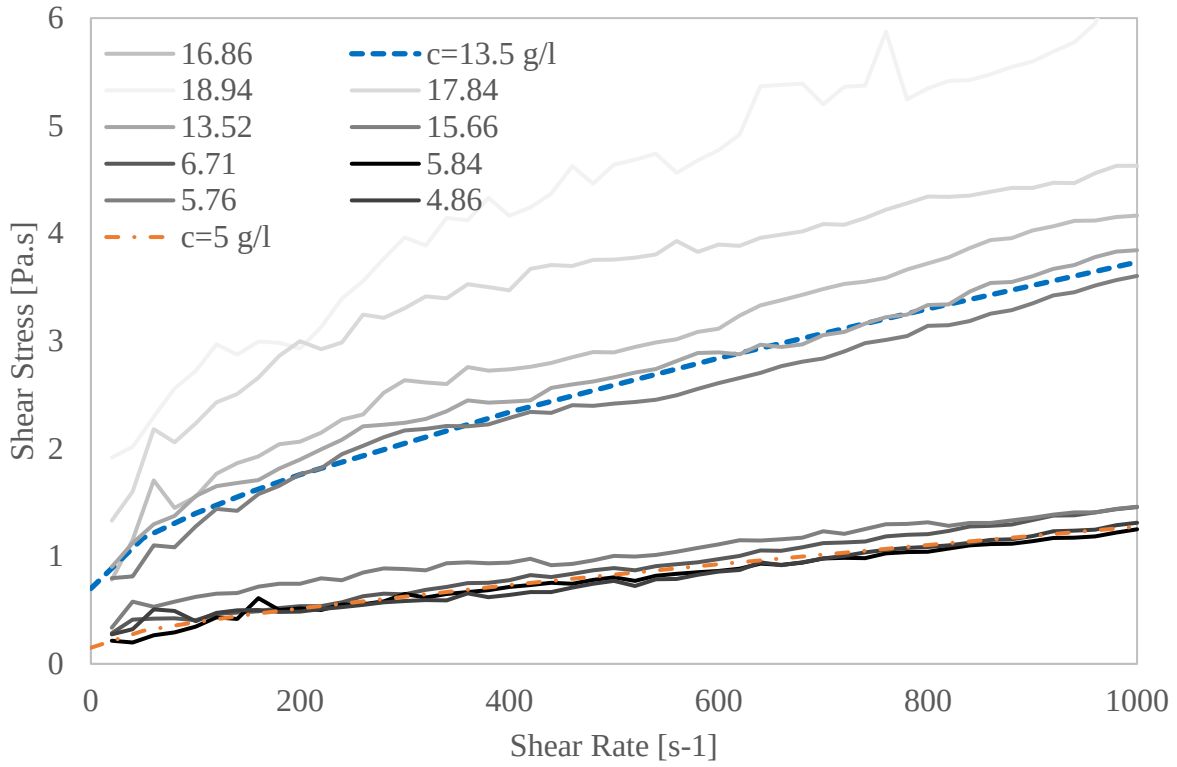

Figure 27, the aforementioned function is plotted against experimental data. One is constructed for c = 4.9 g/l with $\tau_0 = 0.15$ and $n_\infty = 5.5.10^{-4}$ to show low solids concentration region fitting and one for c = 13.5 g/l with $\tau_0 = 0.7$ and $n_\infty = 1.2.10^{-3}$ to show high solids concentration fitting. Only some of the sampling data are shown for better clarity.

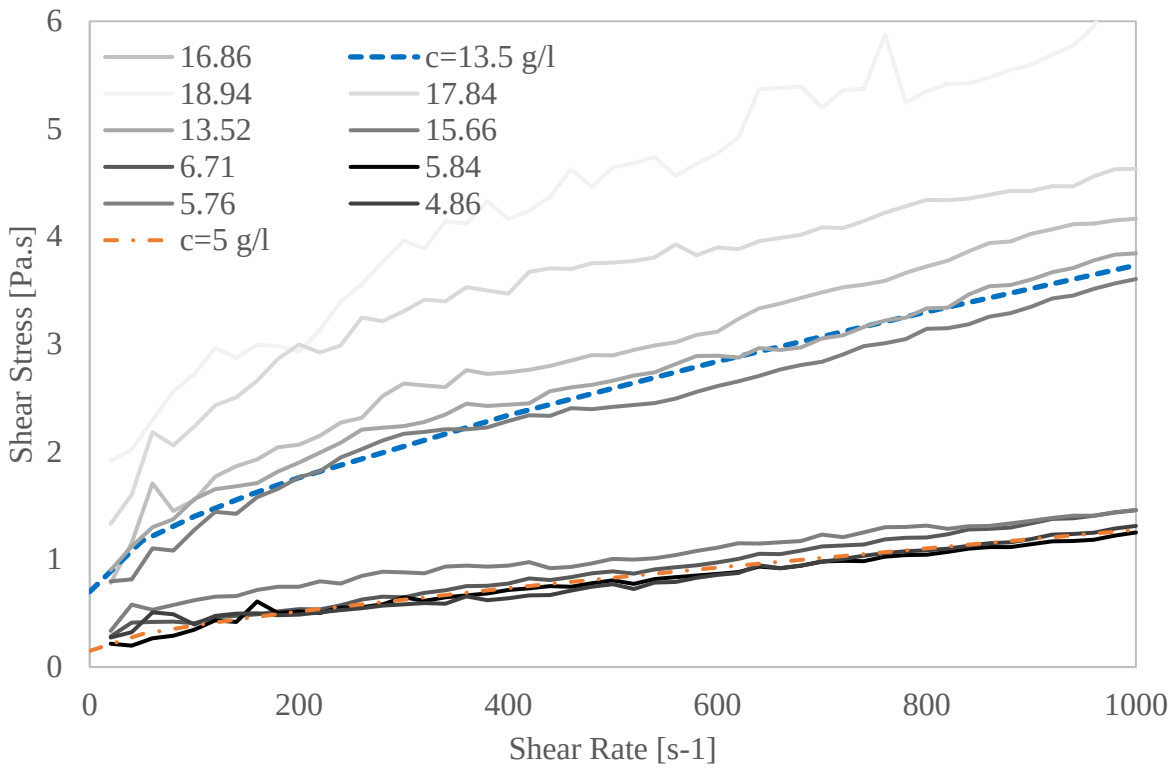

Figure 27 – Fitting of the obtained equation to the experiment

It is apparent, that the Casson sludge type matches the experimental data well. The only complication is that as mentioned earlier, the shear rates in the settling tank are in the range up to 30 – 40 s^{-1} and this range is not captured well by the viscosimeter. In 2019 a new viscosimeter was purchased by the department that should be able to measure low shear rates. A test sample was made in order to confirm the suitability of the Casson sludge type. The sample solids concentration was c = 2,9 g/l and the results are plotted in Figure 28. The Casson model seems to fit the data well, nevertheless the repeated measurement of one sample shows quite a big difference in shear stresses. That is caused by the combination of very low viscosities at these low shear rates that are at the sensitivity limit of the viscosimeter and also by the fact, that the sludge sample is not completely homogenous which leads to small blobs affecting the measurement. For these reasons, no further measurements were made as the described rheology model servers the purposes of this work well.

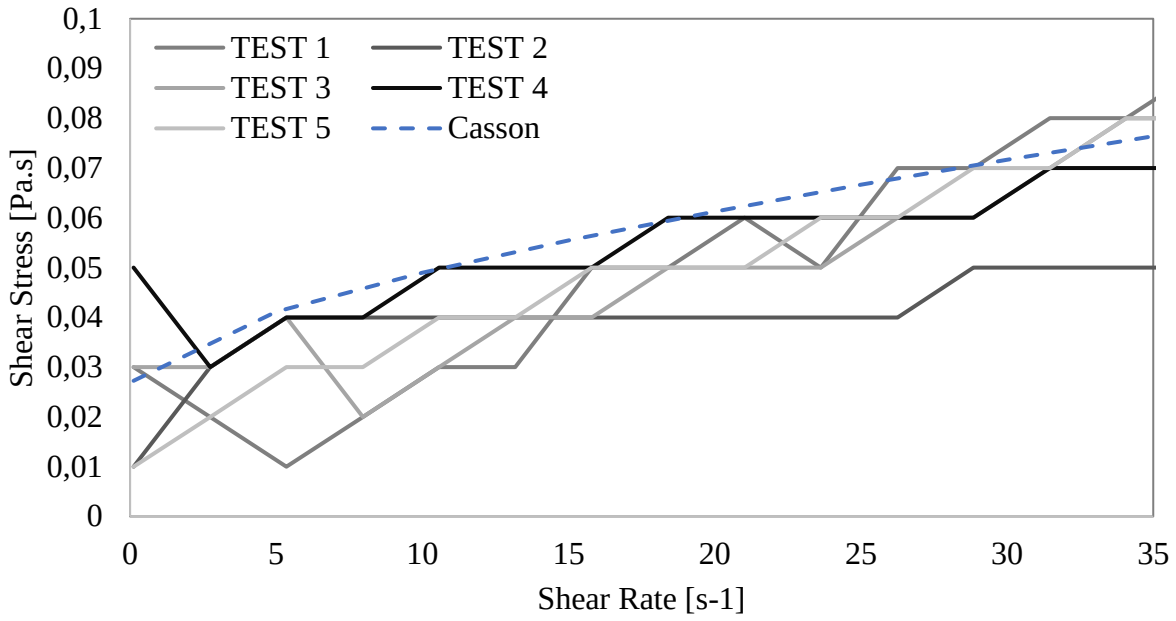

Figure 28 – Low shear rate measurements in 2019

4.3. Sludge Retention Time

Another implemented sub-model is a sludge retention time (SRT) model. The purpose of this model is to calculate the sludge local mean age (SLMA) in every cell of the domain and create a global scalar field. The gain of knowing the SLMA at every location within the tank brings two benefits:

1. To evaluate potential dead zones within the tank and to bring another level of information for a better tank performance evaluation.
2. To assess the dependency between SLMA and settling velocity – it is a widely accepted fact, that the age of sludge affects its settleability.

The idea behind the determination of the sludge age influence to its settling velocity is based on the following thoughts. The SLMA is extracted from the CFD model at the same locations as the samples with similar concentrations were taken – groups of sludge concentrations are created to neglect the influence of the concentration on the settling velocity. Based on that we can create a plot of SLMA and its corresponding settling velocity. Then the data regression can be done to analyse any dependency.

To be able to assess the SLMA at any location within the SST, following equations were introduced to the model:

To be able to track the flow from the inlet and calculate its age, additional convection-diffusion scalar transport equation must be introduced:

$$\frac{\partial \rho \varphi}{\partial t} + \nabla \cdot (\rho \vec{v} \varphi - \Gamma \nabla \varphi) = S \tag{48}$$

Where S is the source term, φ is the SLMA and Γ is the diffusion coefficient for turbulent flow:

$$\Gamma = \frac{\mu}{SC} \tag{49}$$

Where μ is the turbulent viscosity and SC is the Schmidt number (Karches & Buzas, 2011).

The source term initialization is then applied at the inlet boundary where the SLMA is always 0.

4.4. Sedimentation

The sedimentation sub-model consists of two parts. The settling phase that is resolved by the well-known Takacs-Vesilind model is the hindered phase, where the sludge settles at maximum velocity. But that is not true for the initial phase when flocs aggregate after entering the tank. It can be seen in the batch settling column test that after aeration of the sample, it takes several minutes before the sludge-water interface is created and settling process begins. To avoid immediate high velocity sedimentation caused by the hindered model approach a function is added to the model that restricts sedimentation during the first 3 minutes based on the sludge residence time obtained through the SLMA.

Also, the floc breakup under high shear rates is captured by the model. The effect of high shear rates on floc aggregation and breakup has been investigated by (Das, 1993) with a conclusion that the break up process dominates at shear rates higher than 70 s^{-1} which negatively affects the sedimentation process. This effect is implemented in the model in a way that the settling velocity is set to 0 when the shear rate exceeds 70 s^{-1}. That is not of a big relevance for the settling tanks, where the shear rates usually don't exceed 20 s-1 but plays an important role in other WWTP processes that include sludge flows such as the pipe flow or dividing objects and galleries.

The main sedimentation model origins from the well-known Takacs-Vesilind model – for reference please see Chapter 2.2.5 Hindered settling. The data needed for this model comes from the settling columns' experiments. The total height of the column is 280 cm and every 5 minutes

over a total time of 60 minutes a sludge-water interface height was recorded. That outputs into a set of sedimentation curves, one for each sludge sample as these raw data can be seen in Figure 29. Overall, 108 samples were measured using the settling columns. However, 20 of the samples did not create a sludge-water interface and were therefore omitted from the data. The reason for this behaviour is usually a very high suspended solids concentration over 14 g/l under which sedimentation does not occur anymore or a strongly fibrous sludge. Afterall, a total of 88 samples were proceeded for further use.

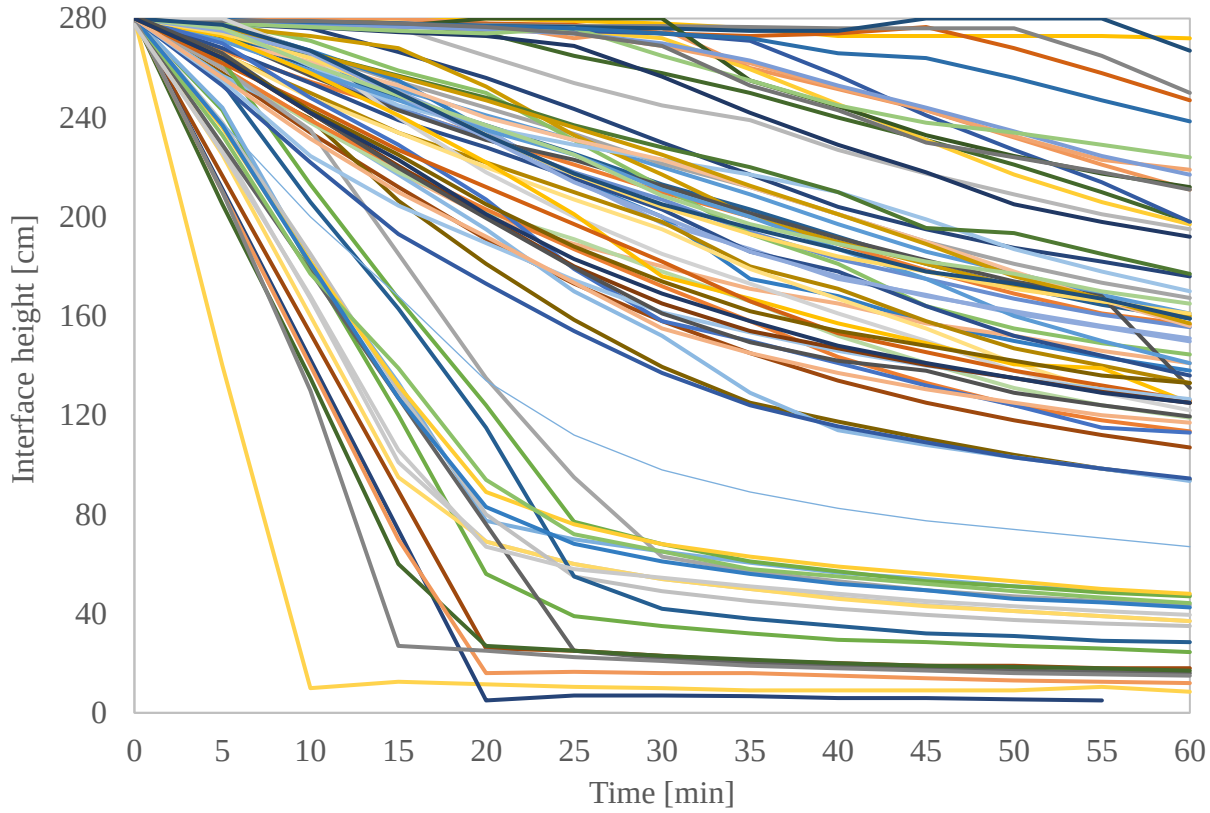

Figure 29 – Settling column sedimentation curves

The Takacs-Vesilind equation

$$V_s = V_0 e^{(-r_H.(X-X_{min}))} - V_0 e^{(-r_p.(X-X_{\min}))} \quad (50)$$

describes the settling velocity against suspended solids concentration and consists of 4 parameters where V_0 is the maximum settling velocity, X_{min} is the minimum solids concentration at which settling occurs, r_H is a parameter describing the hindered zone and r_p is a parameter

characterizing the low concentration settling. These parameters can be deducted from the batch column test data by linear regression same as the Vesilind parameters.

The settling velocity against suspended solids concentration was plotted on a natural log to linear scale. The gradient of the slope and the intercept of the curve are the V_0 and r_H coefficient respectively as shown in Figure 30.

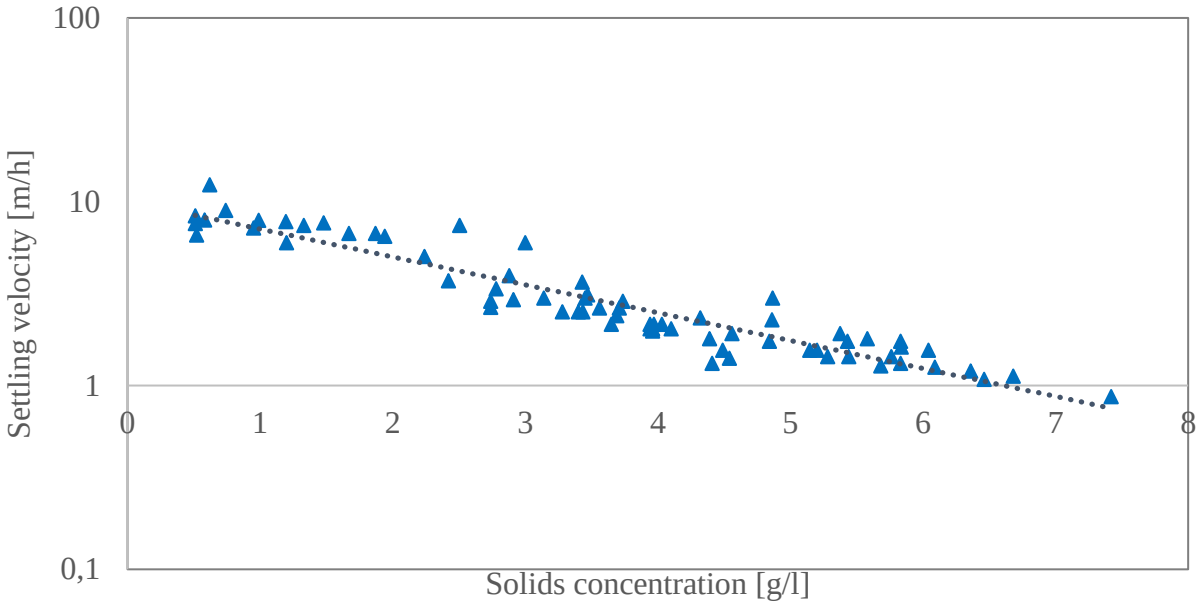

Figure 30 – Settling velocity on solids concentration dependency

From the linear regression the V_0 = 10.08 m/h and r_H = 0.35 m^3/kg. The X_{min} parameter was measured by using decantation and resulted in 8 x 10^{-3} m^3/kg. The last parameter r_p is generally considered to be a one order of magnitude larger than r_h, thus r_p = 3.5 m^3/kg. The summary of the coefficients is presented in Table 2.

Table 2 – Takacs–Vesilind parameters

V_0 [m/h]	r_h [m^3/kg]	X_{min} [m/h]	r_p [m^3/kg]
10.08	0.35	0.008	3.5

Using the coefficients, finally the Takacs-Vesilind double exponential equation can be plotted (Figure 31).

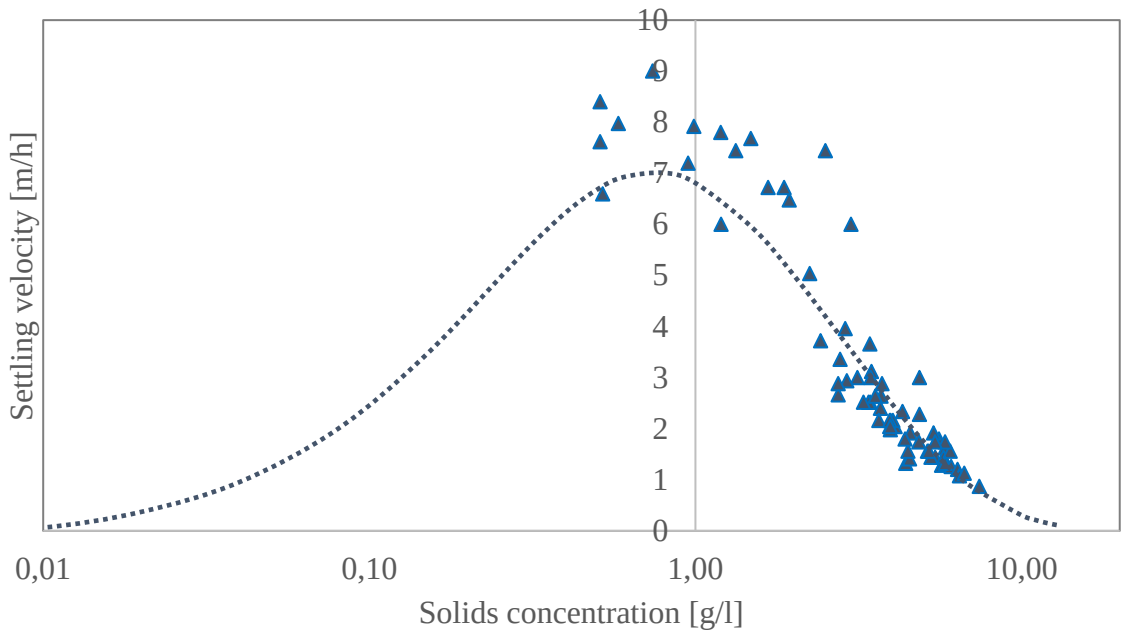

Figure 31 – Takacs-Vesilind double exponential sedimentation equation

It is apparent from the plot that the curve does not perfectly copy the shape of the source data. The settling velocity of the samples with low suspended solids concentration of x<2 g/l are undervalued where the velocity of the samples with higher concentration of x>3 g/l are slightly overvalued. There are several reasons for this discrepancy:

- First, the exponential type of the curve is not fully convenient in this case and some higher order polynomial curve may fit the data better. Nevertheless, the Takacs-Vesilind model has been tested against numerous independent studies and even though not all researches concluded its superiority, it is considered a good trade-off between complexity and accuracy which makes it easily usable for real applications.
- The samples were taken over a long period of time (almost 2 years) and although they all come from a single WWTP, the properties of the sludge and especially the settleability may vary depending on the actual load and sludge conditions and thus creating a significant variance. This is very important to notice as this is actually the cumber stone of sludge settling models and should be more deeply discussed:

Most of the models, Takacs-Vesilind included are valid only for a specific WWTP and specific load conditions under which the samples were taken. Unfortunately, that restrains all these hardly produced settling curves from any practical applications outside the experimental site. It

can be contradicted that there exist settling models which have been developed with an intend for a general use in mind, especially the using Eulerian – Eulerian multiphase models, but these models share a common and underlying downside being way too complex for any practical use and require many different parameters that are difficult to obtain experimentally.

The extensive number of samples that have been taken and measured in the batch settling tanks in this study is unique in a way that these samples represent all different combination of conditions under which they were taken – samples were taken during spring/summer/autumn, rain, different flow rates, different dosage of floculants etc.

That leads to an idea to categorize the samples based on their settleability (influence of different conditions) rather than average them into a single settling curve as it is common.

4.4.1. Sludge Settling Envelope

It becomes apparent from Figure 31, that a single averaged settling curve cannot enclose all the different sludge conditions and differentiate between well settling and badly settling sludge relatively to the suspended solids concentration. A single settling curve represents a single settling condition. Therefore, it is questionable whether such a model can be used for a real application such as secondary settling tank optimization where the conditions principally vary. It is very common, that the sludge in the SST does not settle well for example under high flow (rain) rates because its properties influencing the settleability are different. In order to be able to utilize the CFD model for a optimization purpose, the sludge samples would have to be taken under the actual high flow rate conditions. Otherwise, batch settling curves from a different tank condition would result in different settling characteristics.

In order to be able to compensate the settling curves for different condition without the need to rerun the time-consuming batch settling measurement every time, an envelope is created to mark the maximum and minimum settling boundary. That produces two new sets of settling curves as can be seen in Figure 32.

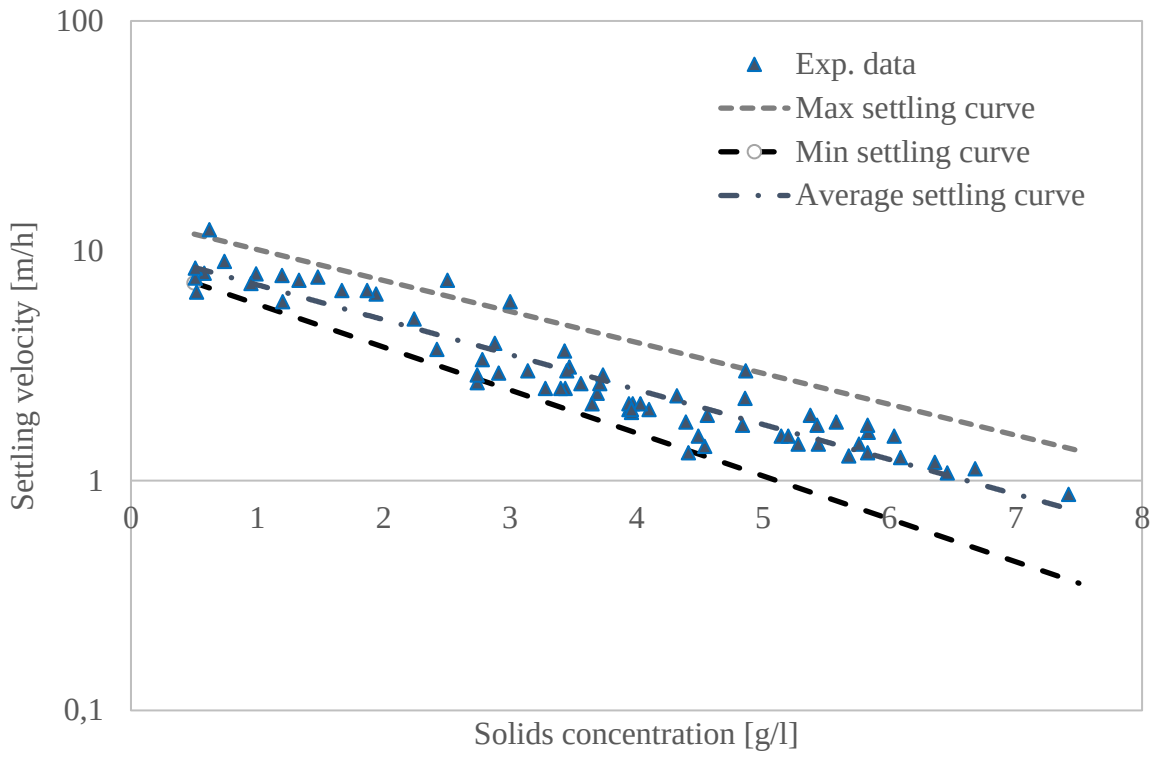

Figure 32 – Sludge settling envelope

From the regression of the Vesilind parameters for maximum settling curve V_0 = 13.8 m/h and r_H = 0.31 m^3/kg and for the minimum settling curve V_0 = 9 m/h and r_H = 0.43 m^3/kg.

The summary of the coefficients is presented in Table 3.

Table 3 – Takacs-Vesilind parameters for Min, Max and Average settling curves

	V_0 [m/h]	r_h [m^3/kg]	X_{min} [m/h]	r_p [m^3/kg]
Average	10.08	0.35	0.008	3.5
Max	13.81	0.31	0.008	3.1
Min	9.02	0.43	0.008	4.3

With the envelope curves created, we can plot the Takacs-Vesilind double exponential equation again (Figure 33).

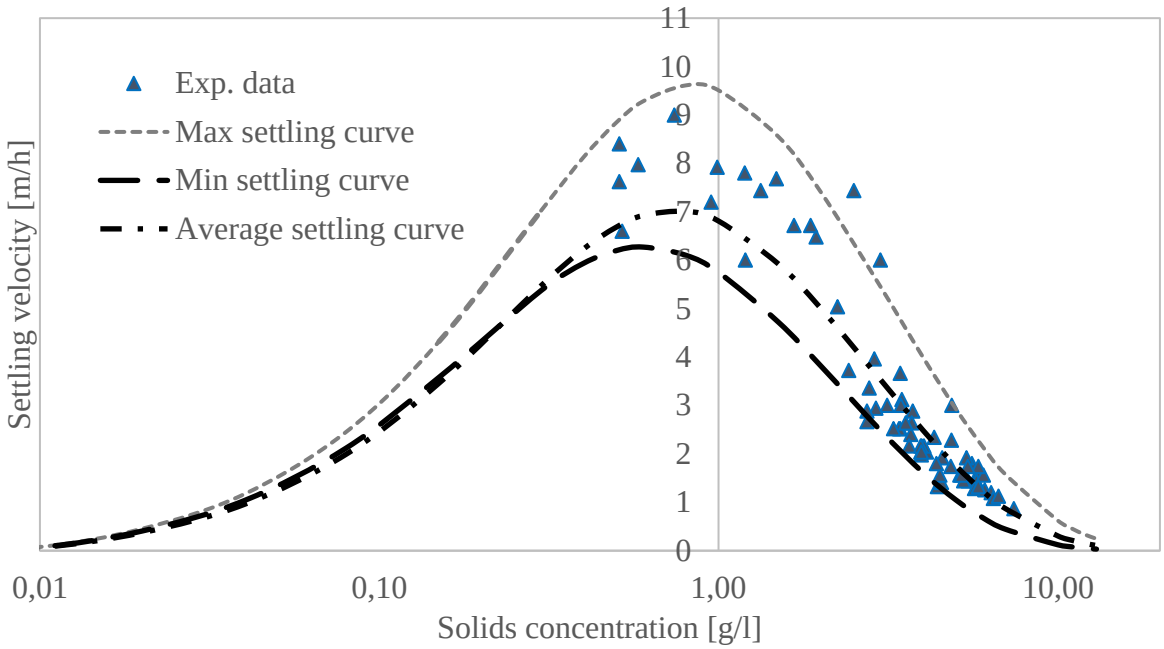

Figure 33 – Takacs-Vesilind Min, Average and Max settling curves

It is apparent from the range of min and max curves, that the settling velocity for the same sludge solids concentration may differ significantly. That corresponds to the fact, that there are other factors with a strong influence on the settleability of the sludge.

In order to be able to adjust the settling curve precisely to reflect the actual sludge behaviour at the time of the sample extraction (and not use averaged long-time data), another parameter must be added to the equation.

4.4.2. Sludge Settling Factors

The settling curves are based on the ZSV which is considered to be a lumped parameter that inherently embeds sludge morphological, physical and chemical factors. Given the fact that a sludge property database was created during the sampling campaign, it is possible to try to find other relations between sludge settleability and other factors such as SVI, rain conditions, filament index, flocculant and coagulant dosages or retention time.

The problem arises when we try to directly compare settleability (ZSV) with other parameters because the ZSV also depends on the SS concentration that is given by the Takacs-Vesilind equation. In other words, a sample with a ZSV of 5 m/h will be consider a poorly sedimenting sludge at the SS concentration of 1.5 g/l but a very well sedimenting sludge at the concentration

of 3.5 g/l as is demonstrated in the Figure 34. It is apparent now that we need to compare entire settling curves rather than just the ZSV.

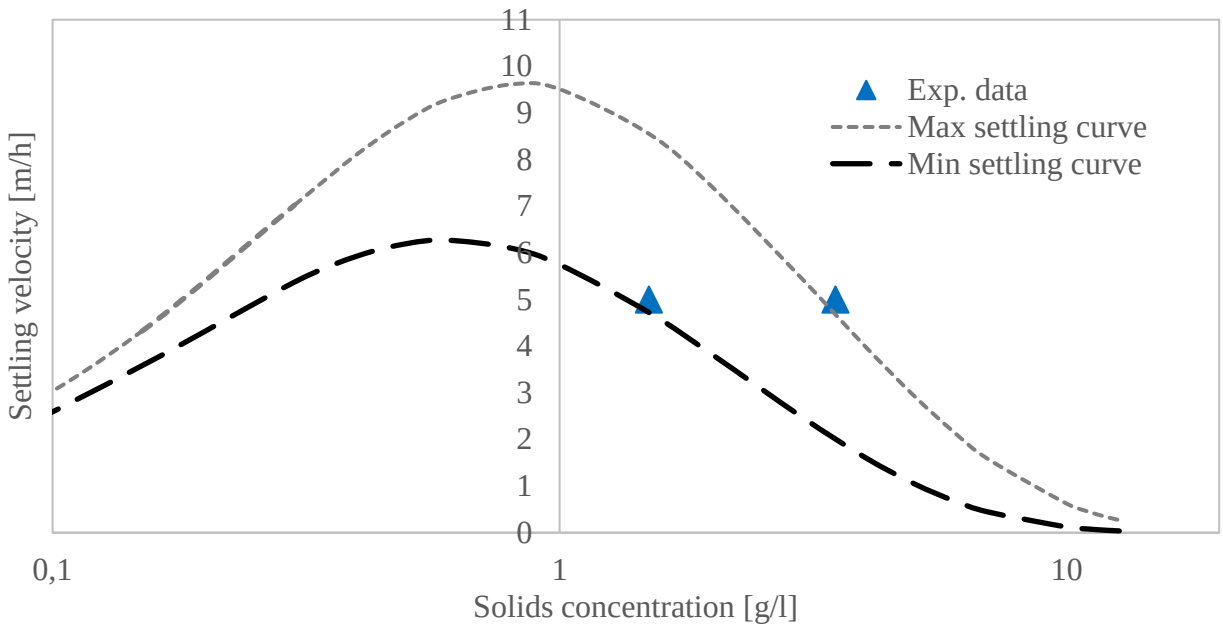

Figure 34 – Comparison of differently settling sludge having the same solids concentration

That can be done if we put in use the maximum settling velocity parameter from the Vesilind equation. This parameter effectively shifts the entire settling curve vertically and thus can be considered a good measure to compare the settling behaviour of different samples. We can take the Vesilind equation

$$V_s = V_0 e^{(-r_V X)} \tag{51}$$

and reverse it so the maximum settling velocity parameter V_0 is on the left side of the equation

$$V_0 = \frac{V_s}{e^{(-r_V X)}} \tag{52}$$

From the Table 3, we can see that the sludge from poorly settling curve will have the V_0 close to 9 and below, whereas a sludge that lays on the well settling curve will have V_0 values close to 14 and above. The r_V parameter is chosen to be an average of the r_V parameters for Min and Max curve: -0,37. That will affect the data in a way, that well sedimenting sludge will appear to be even better sedimenting and low settling samples will appear to be even less sedimenting.

That does not influence the function for our purposes and the resultant data will be only stretched along the y axis.

Using this method, we can now directly compare the settling ability (expressed as V_0) against the influencing factors.

Rain condition

Rain is one of the external parameters that influences the settling ability in terms of increased flow rate, velocities and shear rates in the tank which ultimately leads to the changes in the settling behaviour.

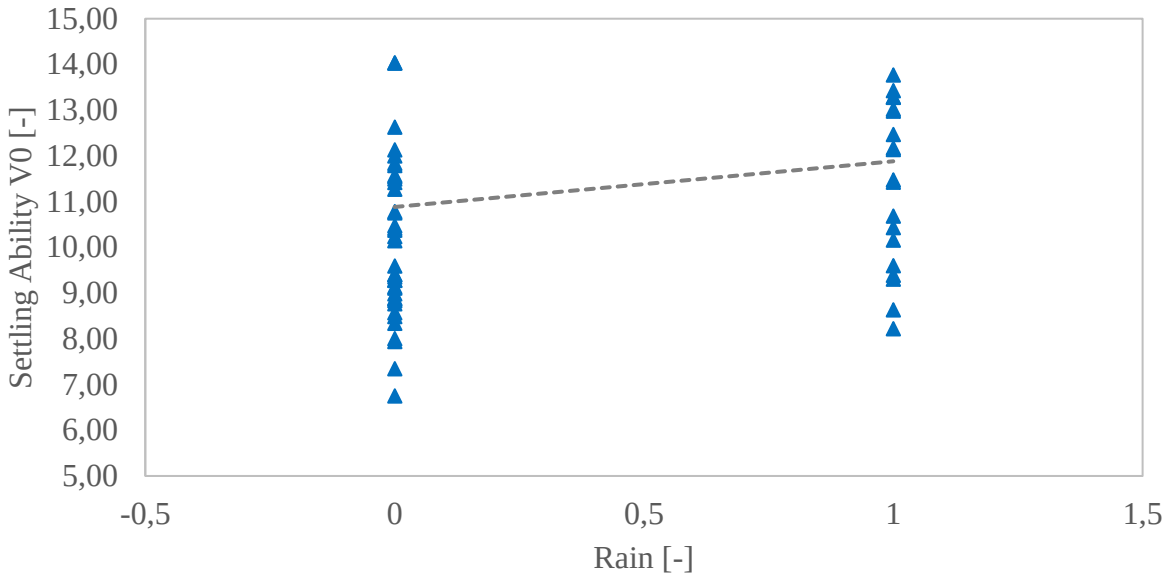

Figure 35 – Dependency of settling ability and rain conditions

In the graph above, the rain conditions are symbolized by 1 on the X-axis where the standard flow conditions are given 0. It is apparent that the settling ability is similar for samples under both conditions, even statistically a slightly better settling behaviour can be observed form the rain-loaded samples. That can be explained by the fact, that during the rain the flocculants and coagulants are added to the sludge which leads to better settling ability. To support this theory, a rain vs. flocculant dosage was plotted (Figure 36) – none added with dry conditions.

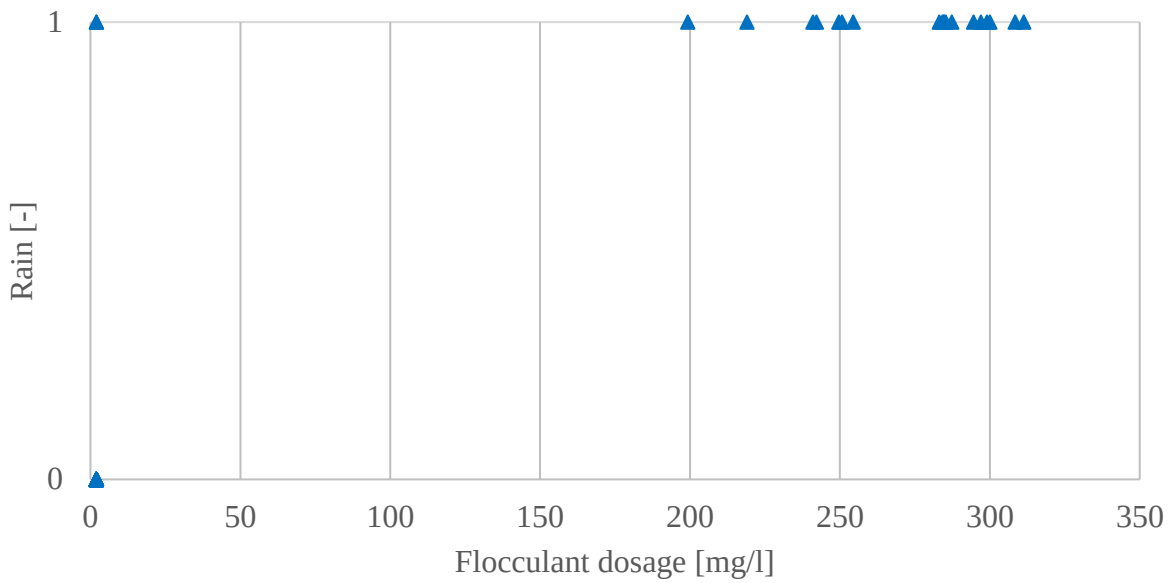

Figure 36 – Dependency of flocculant dosage and rain conditions

To better understand the relation between rain and flocculant dosage, we need to take a closer look at the latter.

Flocculant dosage

Taking look at the flocculant dosage graph reveals that the settling ability does not differ with different dosage ratios. The flocculant dosage is tightly bonded with the rain flow since it is only added to the inlet under that circumstance. The obvious explanation is, that the rain flow negatively affects the settling ability (which is genuinely accepted) and the flocculant counter affects that.

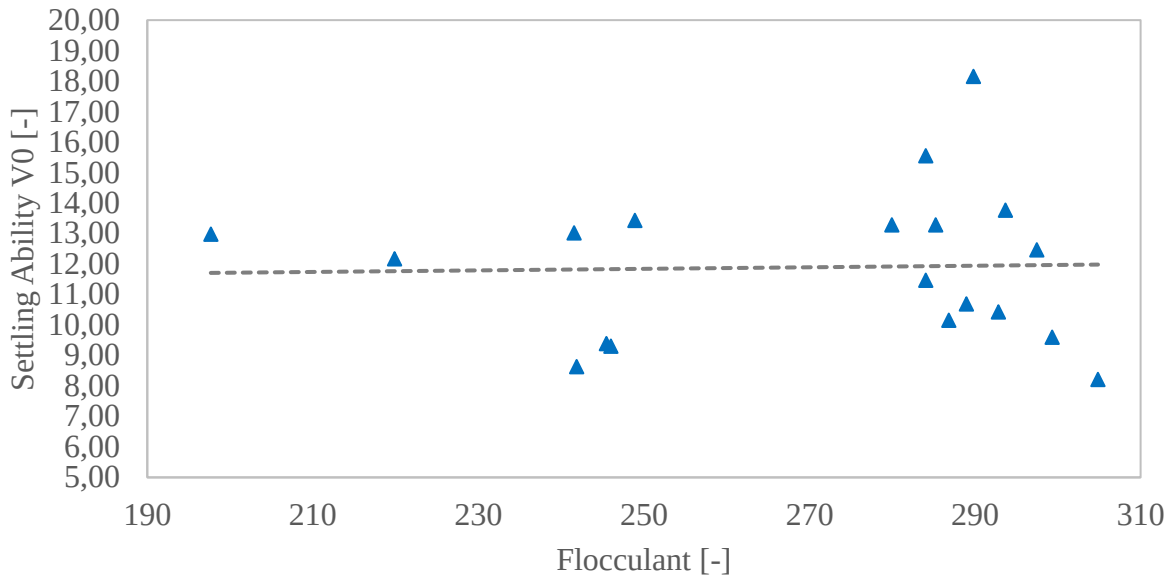

Figure 37 – Dependency of settling ability and flocculant dosage

Since those two influences go against each other, it is not possible to use either of it for our purposes.

Coagulant dosage

Another factor presumably influencing the settleability is coagulant admixing. Contrarily, the Figure 38 shows otherwise as there is no evident connection between coagulant dosage and settling performance.

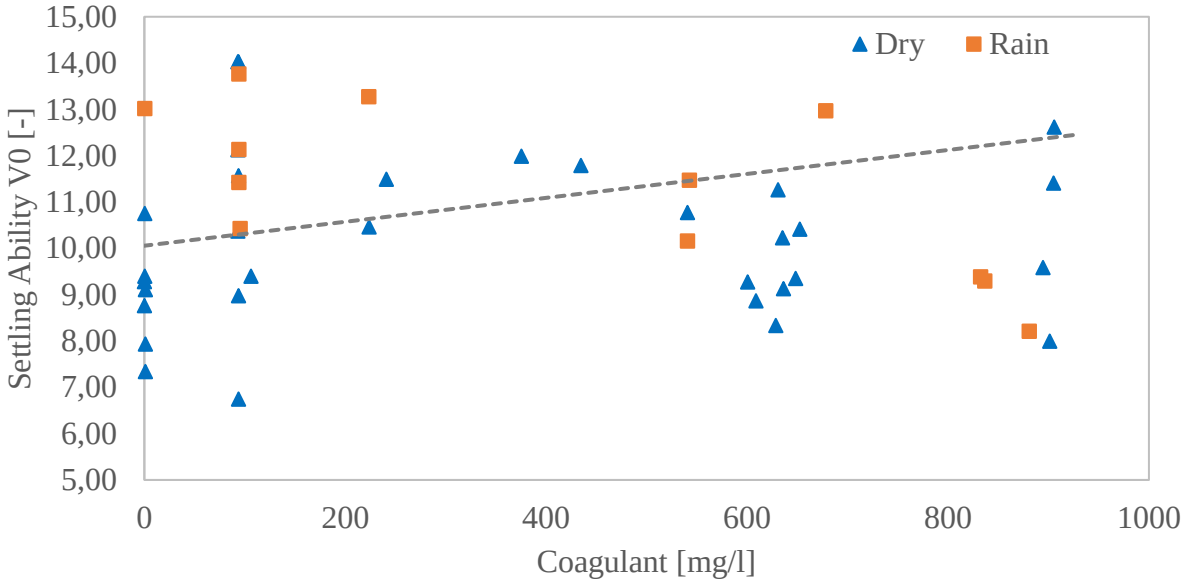

Figure 38 – Dependency of settling ability and coagulant dosage

The color mark in the graph differentiate samples under dry and rain conditions as the coagulant is added independently of the rain. Nevertheless, there is no statistically significant dependency between either set of data and settling ability.

SVI

Sludge Volume Index is a standard sludge criterion that is usually measured at the WTTP directly which enables to assess the data time series.

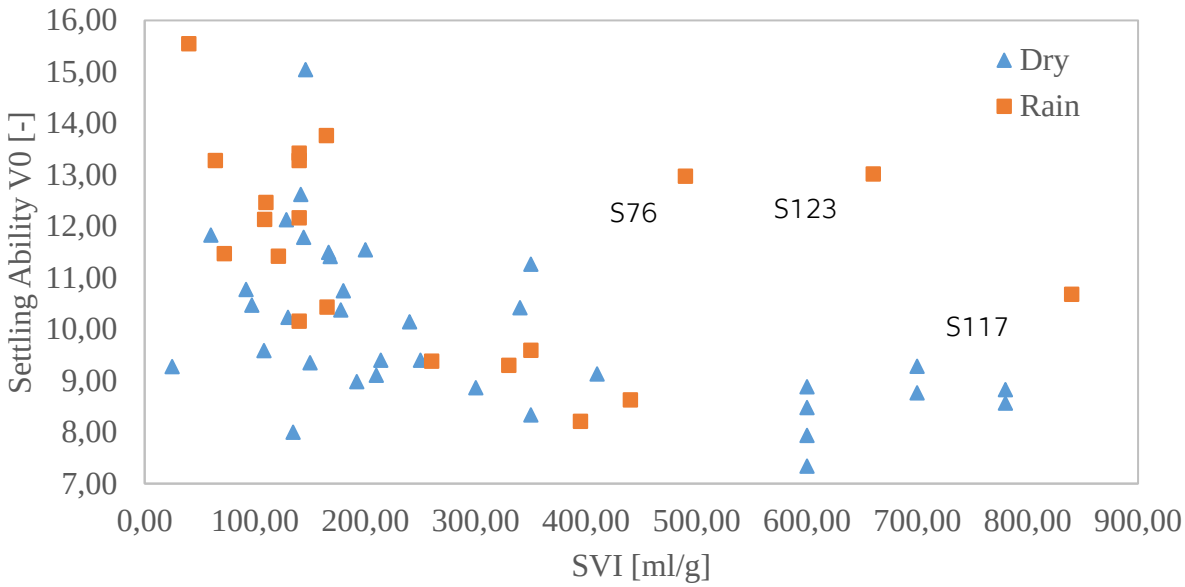

Figure 39 – Dependency of settling ability and SVI

The SVI vs. Settling Ability plot shows a logarithmic correlation of the data. Low SVI results in better settling performance and vice versa which corresponds to the general experience (Jin et al., 2003). This correlation is valid for both dry and rain samples. Since the rain samples are affected by the flocculant dosing increasing the settleability, some of the samples may tend not to follow the dependency as is probably the case for samples s76, s123 and s117 and thus these samples were excluded from the data set.

From the graph we can distinguish the regions corresponding to the different settling curves as is shown in Figure 40. Zone 1 corresponds to the maximum settling curve, Zone 2 to standard settling curve and Zone 3 to minimum settling curve.

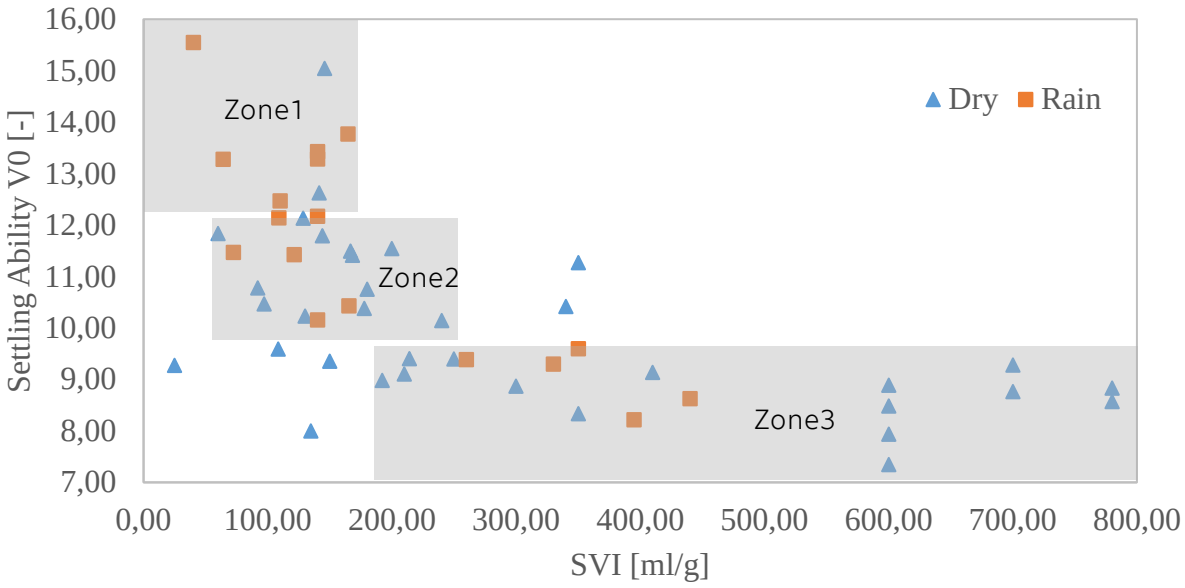

Figure 40 – Dividing the SVI vs. settling ability into separate zones

Now we can transform the Y-axis into a V_0 Correction Coefficient and add another parameter called r_H Correction Coefficient. These coefficients will serve as modifiers to the original Takacs-Vesilind exponential function to adjust the settling curve.

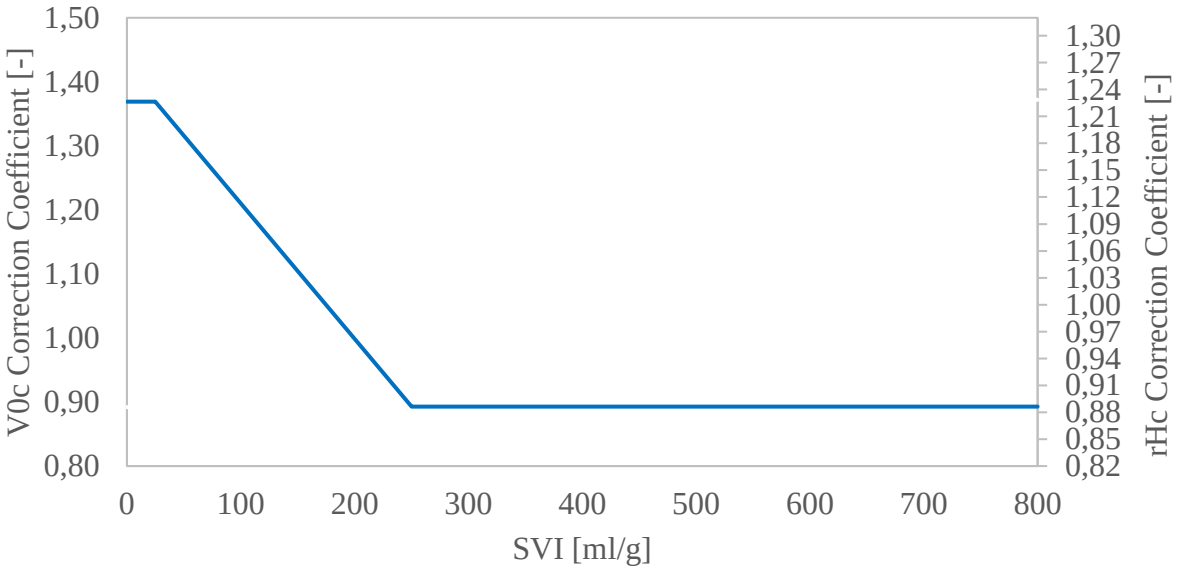

Figure 41 – Correction coefficients to the Takacs-Vesilind settling equation

We can rewrite the Takacs-Vesilind equation with the added correction coefficients as follows:

$$V_s = 10.08 \cdot V_{0c} e^{(-0.35 \cdot r_{Hc} \cdot (X - 0.008))} - 10.08 \cdot V_{0c} e^{(-3.5 \cdot r_{Hc} \cdot (X - 0.008))} \quad (53)$$

The benefit of this extended equation is that we can now construct a custom settling curve based on a suspended solids concentration and SVI. Given that, we can easily adjust the settling model regarding the current tank conditions, such as for rain flow where the sludge parameters differ without the need to run the batch settling test again for the specific condition. That significantly simplifies the preparation work that is needed to run a CFD simulation of a settling tank that is different than the experimental one and brings the model closer to the engineering practise (Švanda & Pollert, 2021).

3. Model validation

The first part of the model validation was conducted using the settling columns. The sludge is poured into the settling column and then the water-sludge interface level is monitored in time. That gives a simple validation of the implemented settling and rheological models in (simplified) 1D space. After that, the validation of the CFD model was done on two settling tanks in the Prague WWTP, marked as DN1 and DN3 for two different rain and dry conditions.

With a legacy, basic CFD model a new inlet object was designed to better handle rain flows. Based on the proposed design, the DN1 tank was modified and thus differs from DN3. Therefore, it is also a good potential for a comparison between the preceding CFD model and this newly developed one.

3.1. Settling Column Validation

The settling column was used during the data gathering campaign in order to measure settling velocities. The sludge was pumped into the column and stirred properly by aeration. Then the water-sludge interface was measured every 5 minutes and recorded.

The CFD model replicated the scenario. The domain is a cylinder with a height of 3 m and a diameter of 0.3 m. The domain was then meshed using quad type cells to obtain a structured mesh which is suitable for this type of simulation and can be seen on Figure 42.

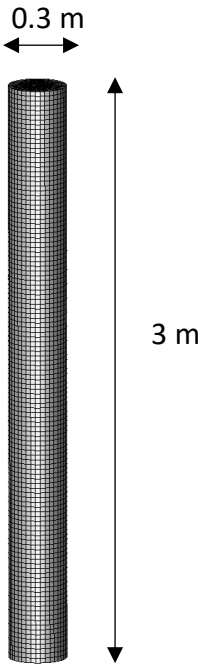

Figure 42 – Settling column CFD model mesh

The multiphase Mixture model was used and the slip velocity (velocity difference between water and sludge) is defined using the sedimentation and rheology sub-models. Turbulent model was used k-ω SST with prism layer mesh done accordingly (y+ < 1). The simulation was carried out as transient with a timestep of 0.5 s and 1 hr total physical time. The initial SS concentration set to 5.7 g/l to match the experiment and the SVI in this case was 600 ml/g which corresponds to factors V_{0c} = 0.89 and r_{Hc} = 0.89. The sludge-water interface and solids concentration were then observed. From the comparison of the measured sedimentation and CFD model (Figure 43) it can be seen that the evolution of the water-sludge interface in time and the concentration profile matches very well.

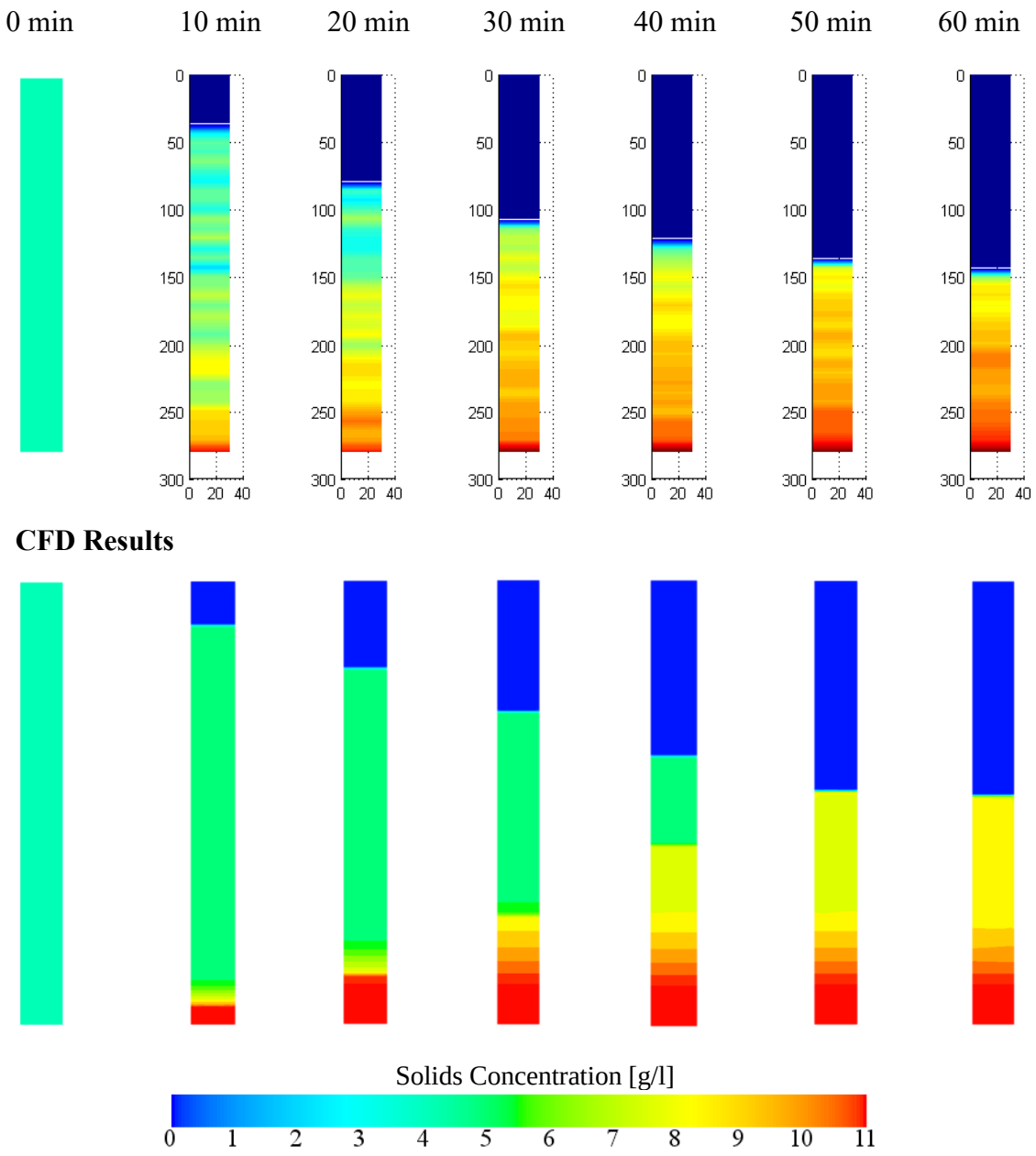

Figure 43 – Comparison of settling column sedimentation between CFD and experiment

The water-sludge interface height evolution in time was plotted. The match between experiment and CFD model can be seen in Figure 44.

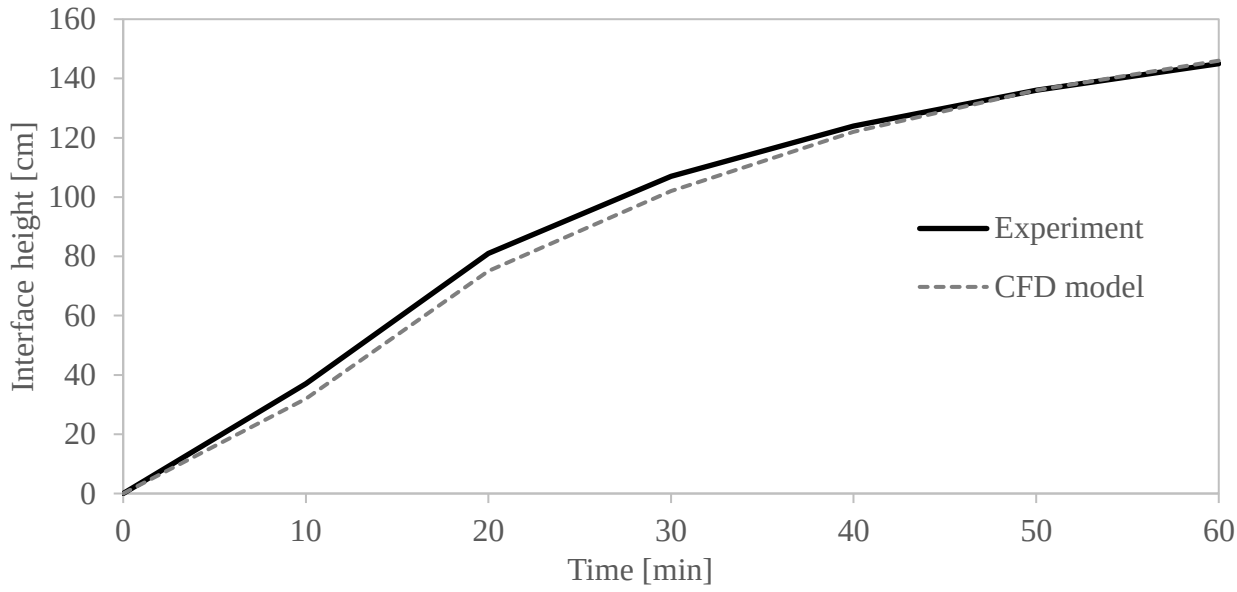

Figure 44 – Interface height evolution comparison between CFD and experiment

This initial validation shows that the CFD model behaves well in this simple scenario. To test it under real conditions and flow rates, it is necessary to deploy it to the actual settling tank geometry in 3D.

3.2. Settling Tank DN3 Validation

The settling tank DN3 is located at the Prague WWTP within the old treatment plant. The radius of the tank is 21 m and depths are 5 m at the sludge removal pit and 2.1 m at the outer rim. The influent is a pipe located traditionally in the centre area. The inlet zone is bounded by 8 pillars supporting metal plates. The outlet area is located 17 m from the centre and consists of two circular weirs.

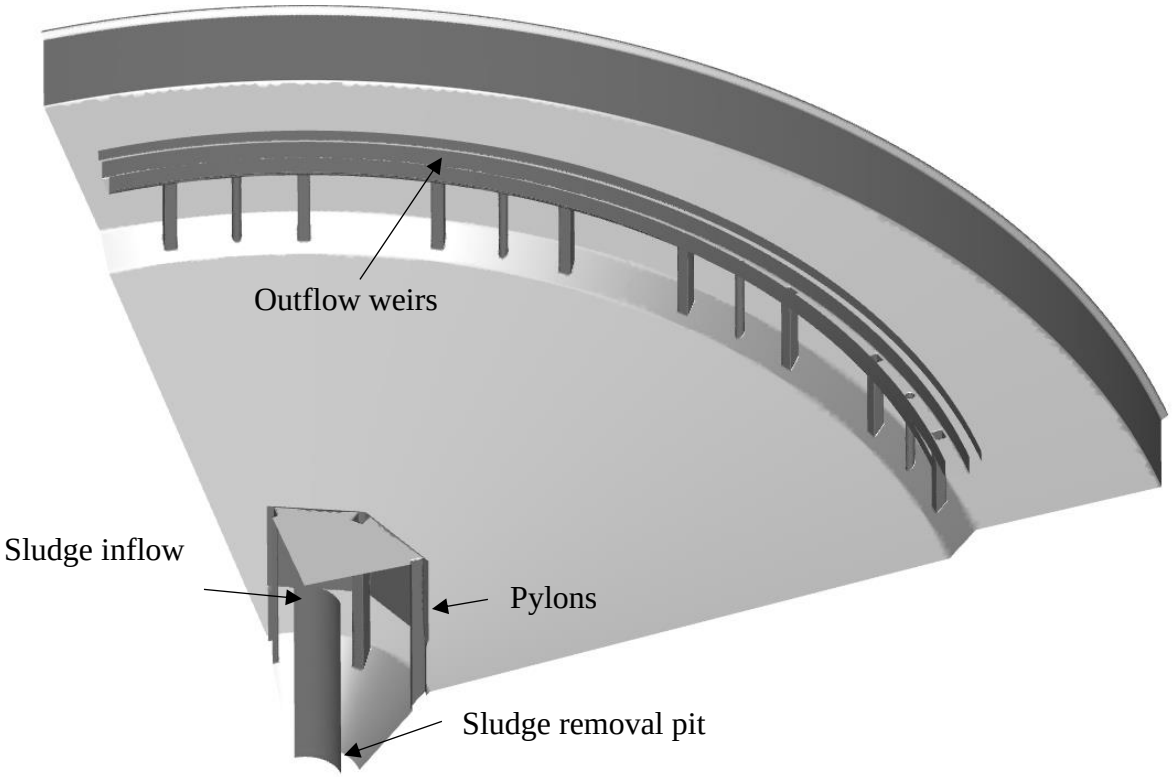

Figure 45 – Settling tank DN3 model geometry

3.2.1. Model setup

The geometry of the tank has a cylindrical periodicity and therefore only ¼ of the geometry was modelled. The inlet is considered to be a mass flow inlet and atmospheric pressure is setup at the outlet. Sludge removal is modelled as mass flow outlet. The side walls of the model are modelled as periodic to capture the symmetry. Top boundary that represents water-air interface is modelled as symmetry boundary condition – it ensures a non-zero wall velocity at the boundary.

Table 4 – Boundary conditions used in the model

Feature	Boundary Type
Influent	Mass Flow Inlet
Overflow	Pressure Outlet
Sludge Removal	Mass Flow Inlet (reversed)
Water-air Interface	Symmetry Plane
Cylindrical symmetry	Periodicity
Multiphase Model	Mixture
Turbulent Model	SST k-w
Submodels	UDF

The mesh type is polyhedral as it well suited for this type of simulation. Also, prismatic layer is modelled at all walls to correctly capture the near wall velocity profile. The prismatic layer is modelled to have a $y+ < 1$ to be suitable for the turbulent model SST k-w. This model was chosen because it resolves the boundary layer that is of an importance due to the presence of the sludge blanket and low velocities close to the bottom of the tank.

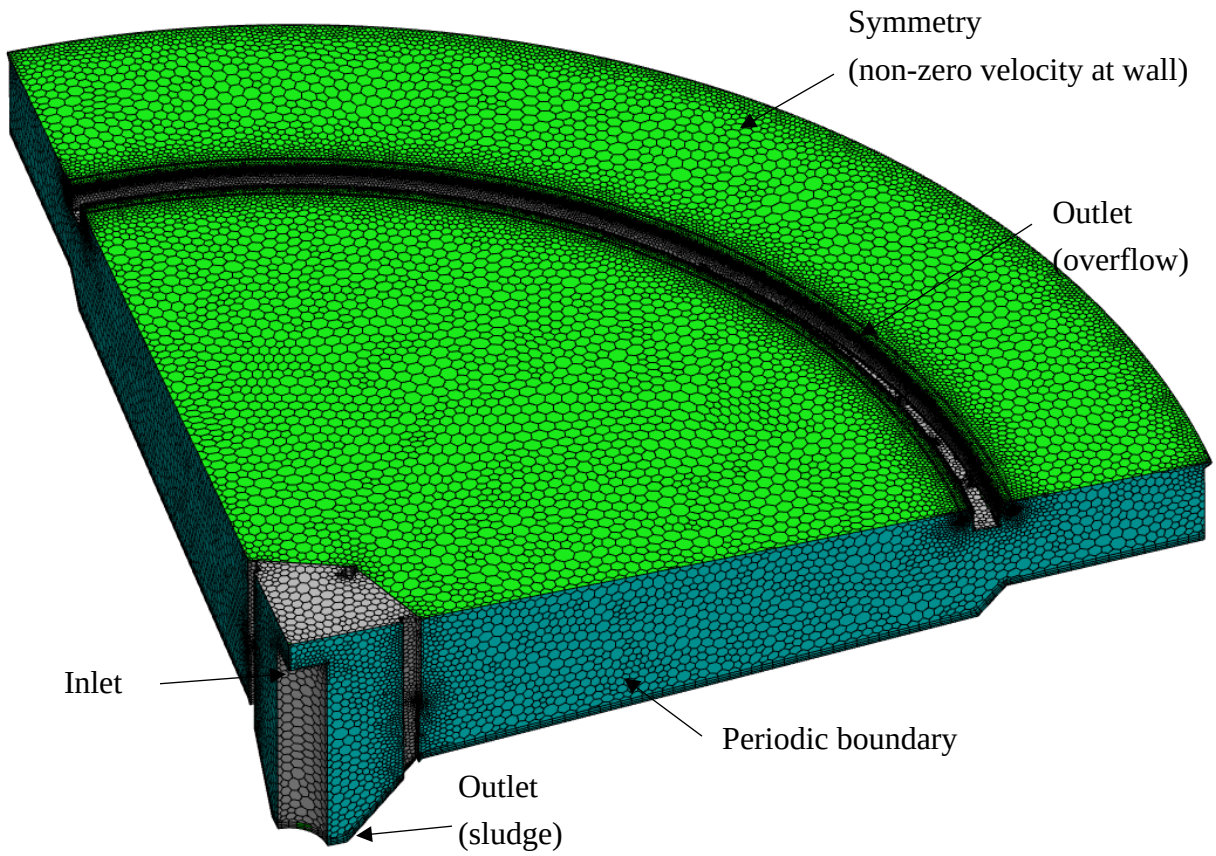

Figure 46 – Settling tank DN3 computational mesh

The developed sub-models for sedimentation, rheology and sludge local mean age were implemented using User Defined Functions (UDFs). The source code was written in C programming language, compiled and loaded into the CFD simulation. The sedimentation sub-model is implemented into the solver as a slip velocity, rheology sub-model calculates viscosity based on the solids concentration and shear rate and the SLMA is implemented as a User Defined Scalar (UDM).

For the tank DN3, two different flow rates were simulated and compared to the experimental measurements. A flow rate Q = 0,635 m3/s represents the nominal flow at the tank during normal conditions and was measured on 16.06.2016. The SVI at the tank inlet was 55 ml/g, which corresponds to the V_{0c} = 1.31 and r_{Hc} = 1.18. The increased flow rate Q = 0,870 m^3/s represents rain conditions and was measured on 16.4.2018 with the inlet suspended solids concentration of c = 3,3 g/l. The SVI in this case was 270 ml/g with corresponding factors V_{0c} = 0.89 and r_{Hc} = 0.89.

Table 5 – Validation cases for DN3

	Flow Rate [m^3/s]	**SVI [ml/g]**	**V_{0c} [-]**	**r_{Hc} [-]**
DN3 Nominal Flow Rate	0,635	55	1.31	1.18
DN3 Increased Flow Rate	0,870	270	0.89	0.89

3.2.2. Results DN3 - Nominal Flow Rate

The comparison of the suspended solids concentration between CFD and experiment can be seen on Figure 47. It can be seen that the CFD model shows a good match with the experiment. Right after the inlet zone, there is a rising sludge eddy which is well-captured by the model (1). Also, the sludge blanket height and concentration matches the experiment.

CFD Model

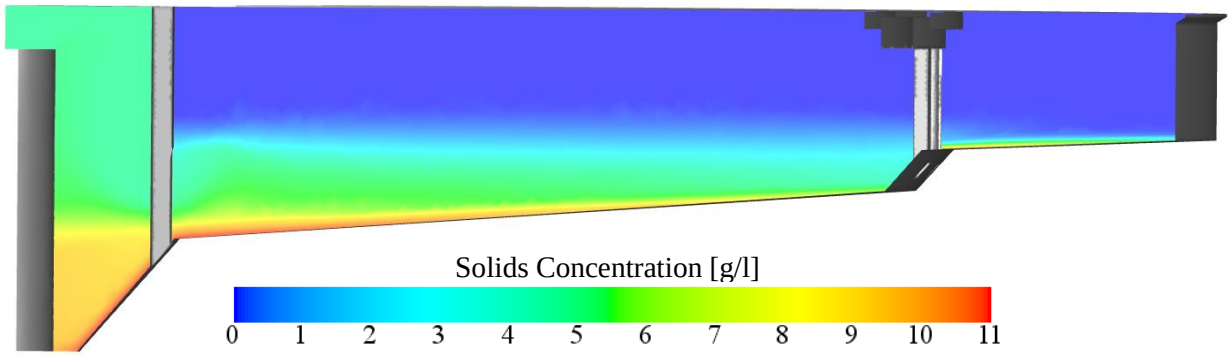

Experiment

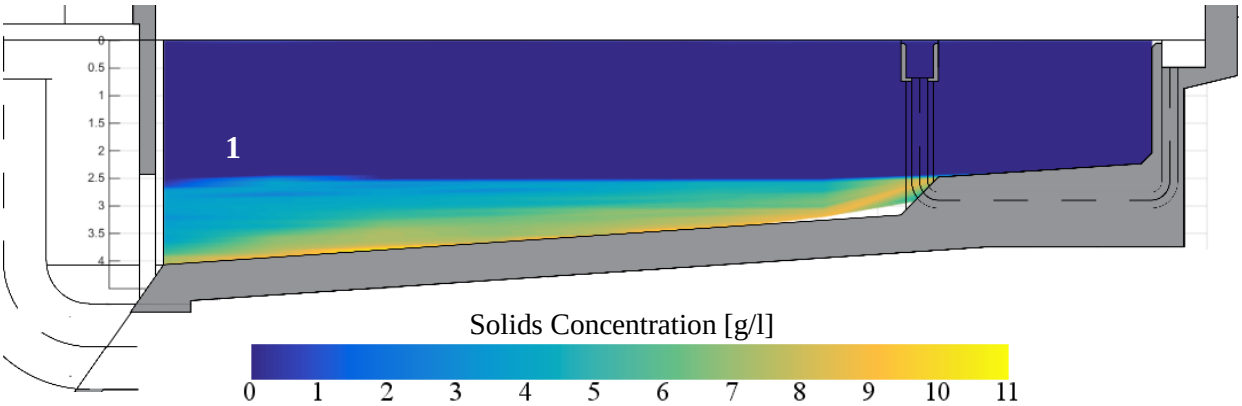

Figure 47 – Comparison of CFD model (top) and experiment (bottom) for DN3 nominal flow

Figure 48 shows scalar velocity field together with velocity vectors shown as black arrows. It can be seen that the sludge is stirred up when leaving the inlet zone. Also, there is a region with very small velocities at the top of the tank creating a dead zone.

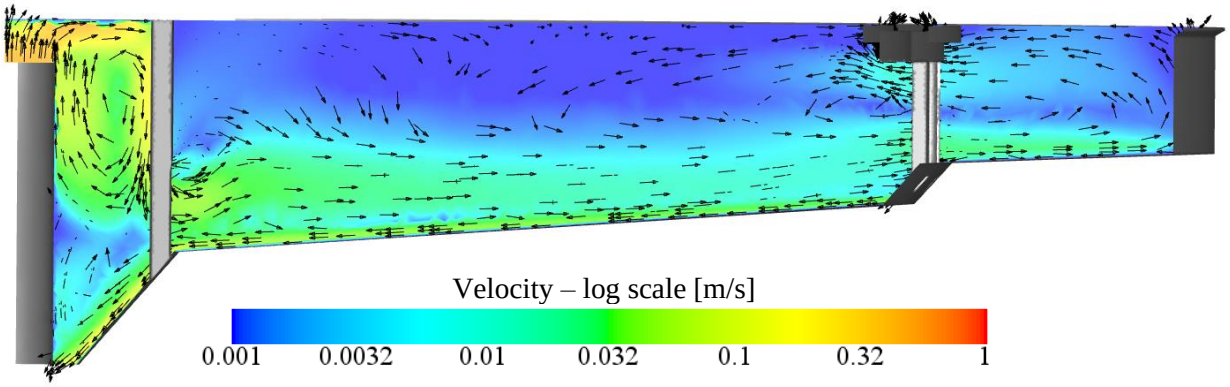

Figure 48 – Velocity vectors for the DN3 nominal flow

Looking at the SLMA field, sludge leaves the inlet zone after proximately 15 min which points to a good design of the tank. Then the sludge continues into the tank and most of it settles down and is removed from the tank after 1 hr. What can be also seen is a fact, that at the top of the tank, the SLMA is high and close to 2 hr which confirms the suspicion of the recirculation zone.

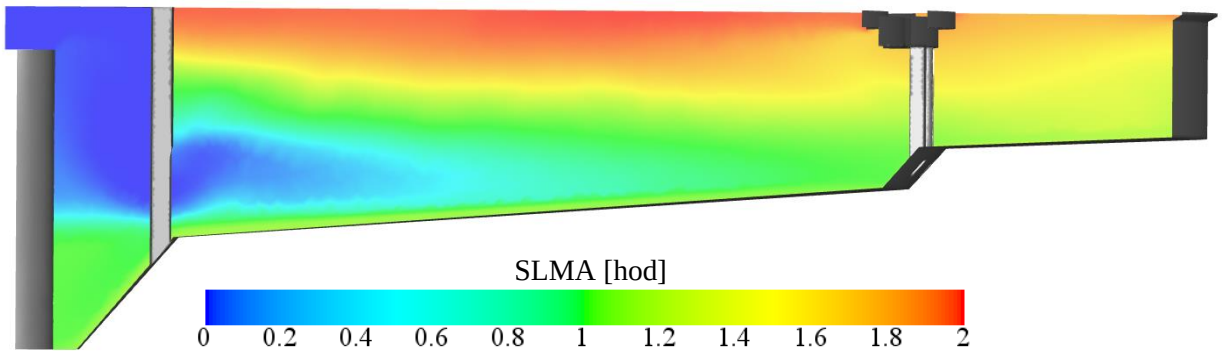

Figure 49 – Sludge local mean age scalar field for DN3 nominal flow

On the Figure 50 the streamlines are shown and also the low velocity dead zone is apparent here. Otherwise, most of the flow traverse the entire tank to the end and then to the overflow which means the tank is working well for the nominal flow rate.

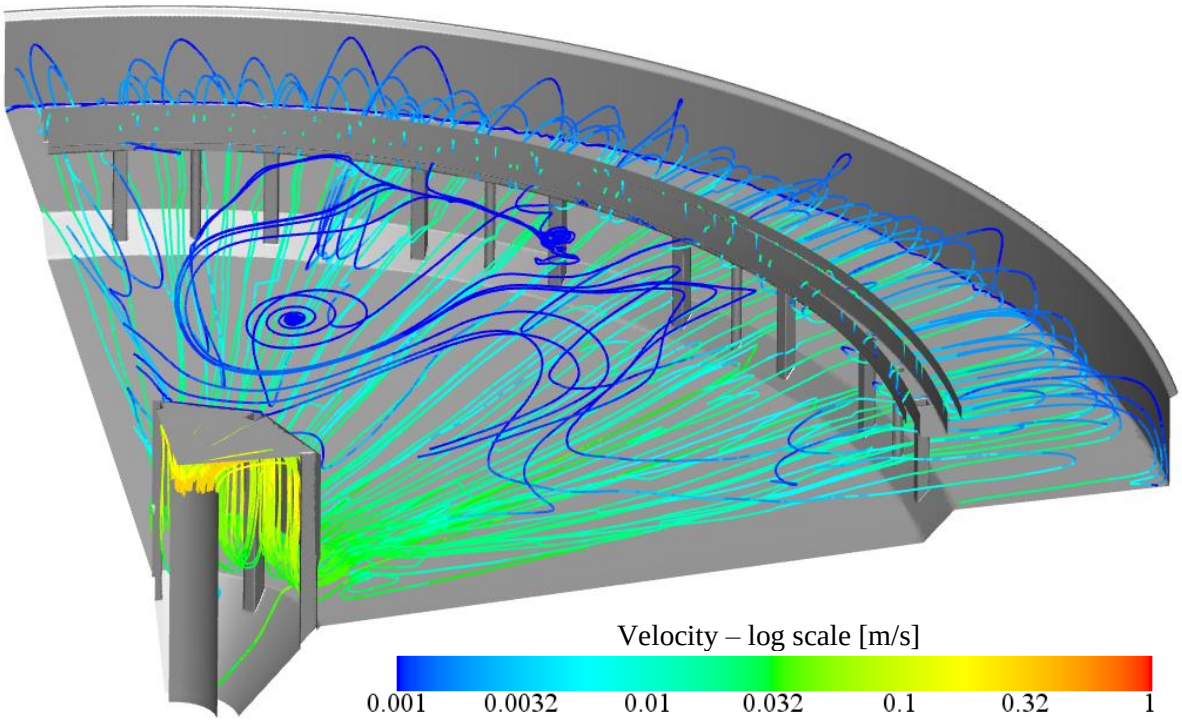

Figure 50 – Streamlines coloured by velocity for DN3 nominal flow

3.2.3. Influence of the pillars

The pillars supporting the inlet zone have a negative impact on flow as can be seen from the camera probes. The pillars are contracting the flow leaving inlet zone resulting in local velocity increase. Thin increased velocity then causes the sludge to stir the already settled returning sludge which decreases the tank efficiency. The same phenomenon can be observed from the CFD model Figure 52.

Figure 51 – Camera probe picture of the pillar exit

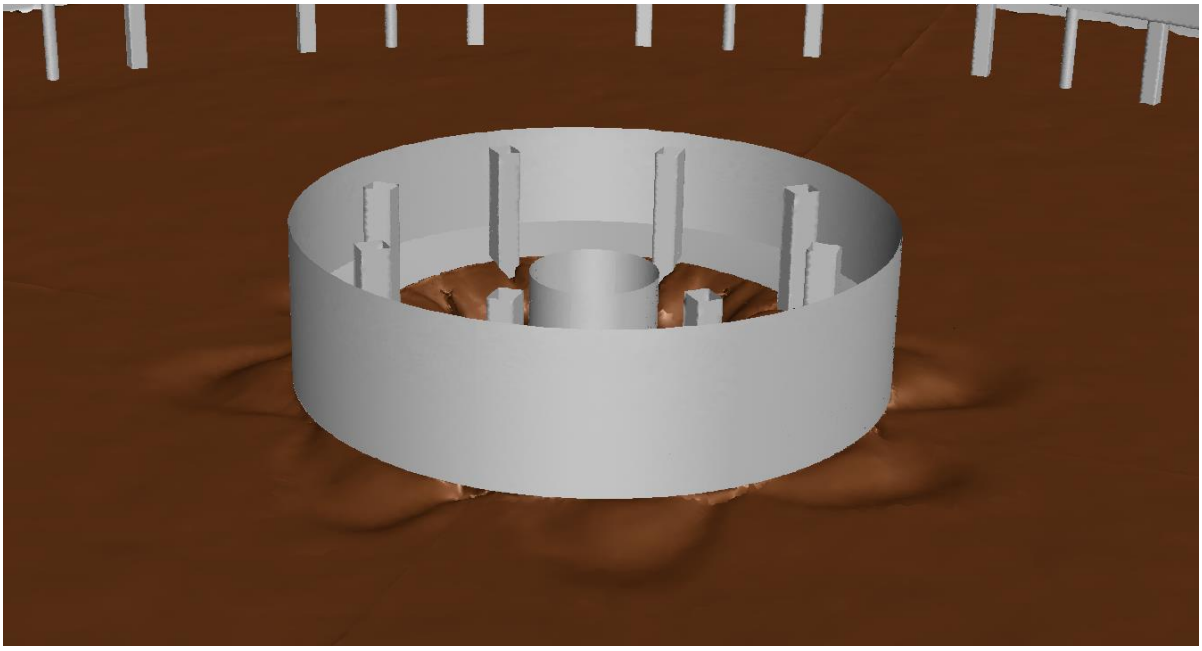

Figure 52 – Detail of the water-sludge interface for DN3 nominal flow

3.2.4. Results DN3 – Increased Flow Rate

Another validation was done after a rain event when the profile of the DN3 tank was measured on the day of 16.4.2018. The increased flow rate was Q = 0,87 m^3/s and the concentration of suspended solids at the tank inlet was c = 3,3 g/l.

The comparison of the suspended solids concentration between CFD and experiment is shown on Figure 53. It can be seen that the CFD model shows also a good match with the experiment regarding the sludge blanket height. The concentration of suspended solids is quite homogenous in the entire tank as is captured by both the measurement and CFD model. At the end of the inlet zone the sludge blanket rises which can be seen on both CFD and experimental results.

CFD Model

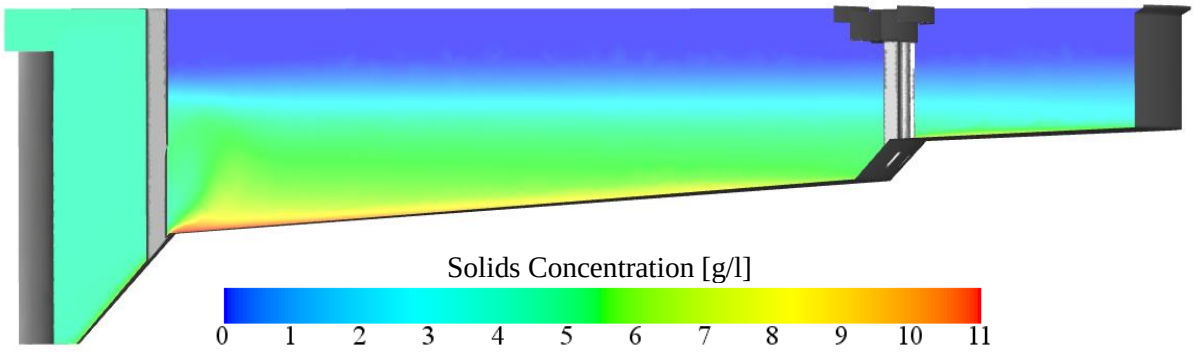

Experiment

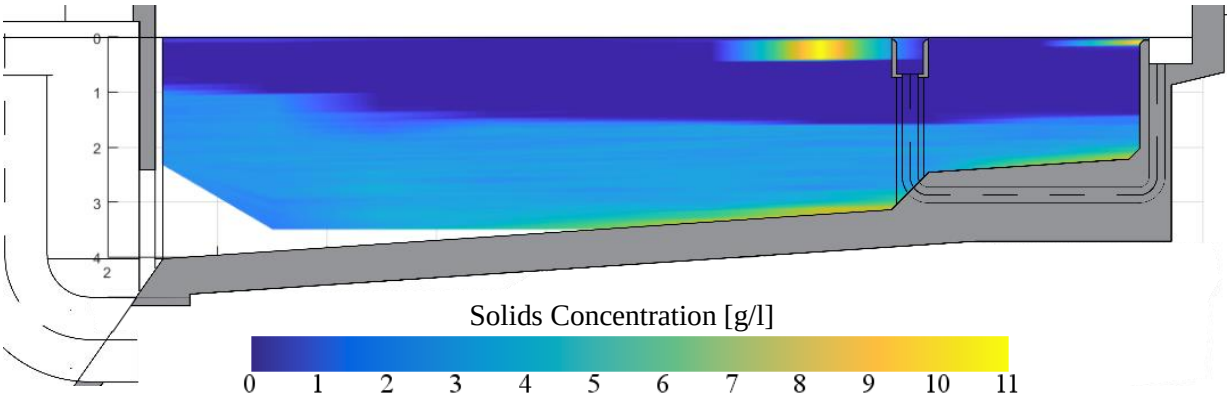

Figure 53 – Comparison of CFD model (top) and experiment (bottom) for DN3 rain flow

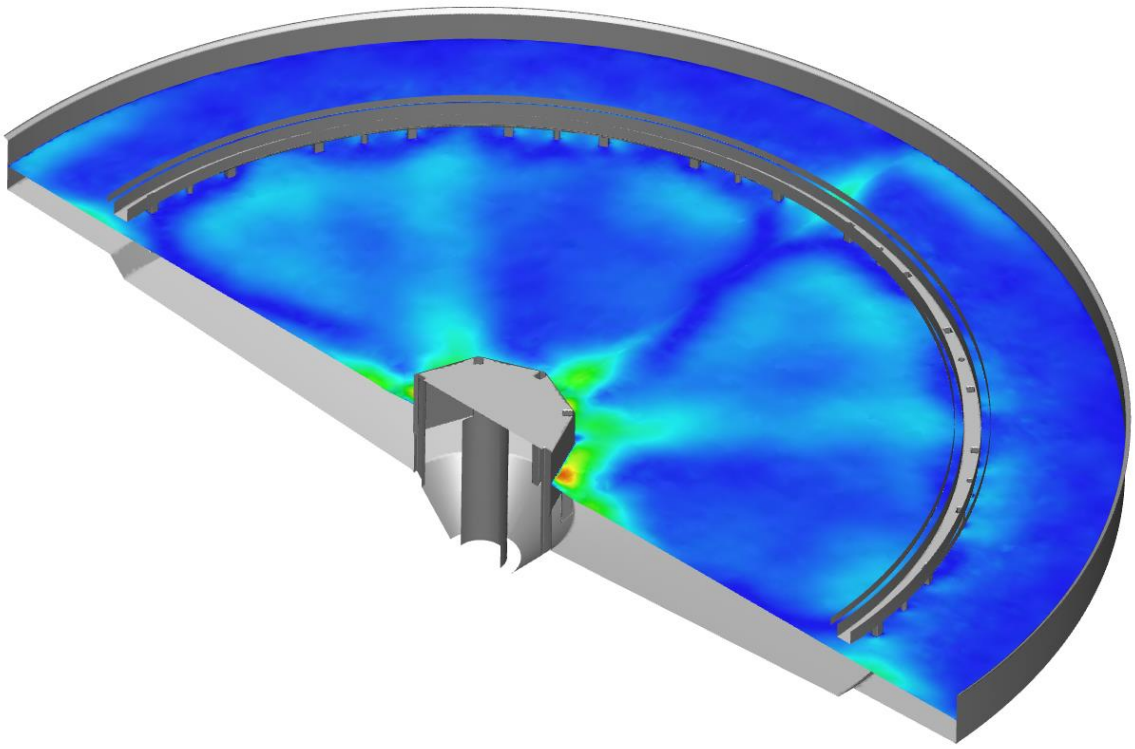

Figure 54 – Isosurface of the c = 2 g/l interpreting the sludge-water interface for DN3 rain flow

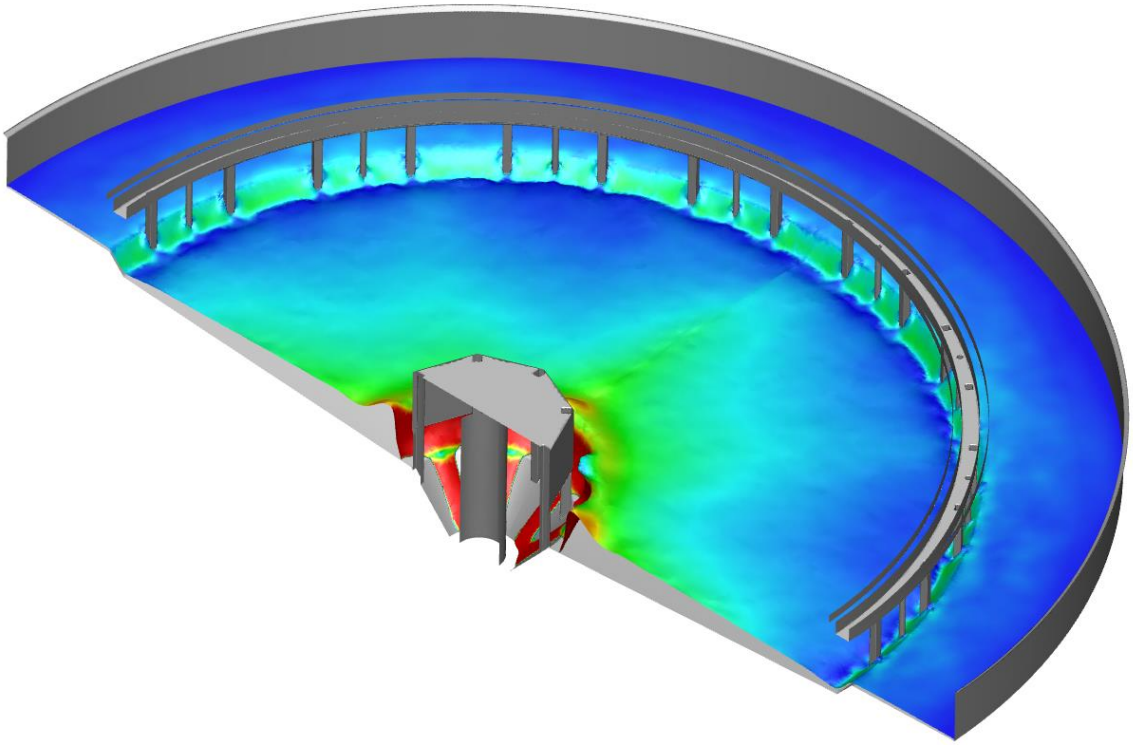

Figure 55 – Isosurface of the c = 6 g/l interpreting the hindered and compression regions interface for DN3 rain flow

As it can be seen from both the vector field (Figure 56) and isosurfaces (Figure 54 and Figure 55), the increased flow causes the inflow to rise when leaving the inlet zone because it is confronted with the returning sludge at the bottom. That is not optimal as higher velocities restrict good settleability of the sludge.

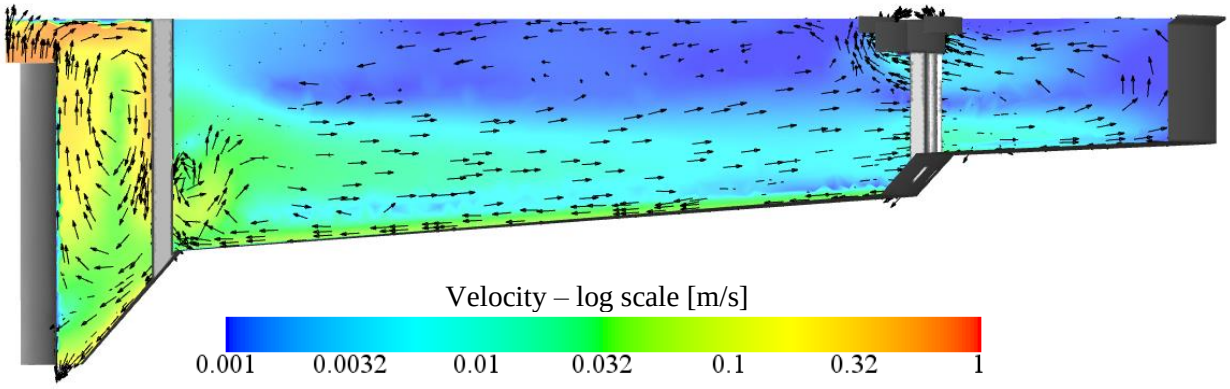

Figure 56 – Velocity vectors for the DN3 rain flow

The difference in SLMA can be observed compared to the nominal flow rate. Due to the higher flow rate more volume of the tank is used causing the dead zone to disappear (1). Rather the flow occupies entire tank and flows to the outer edge. At the bottom of the tank there is a higher SLMA of the sludge that is moving back towards the sludge removal area (2). It is not possible to obtain similar precision using experiment which shows the benefit of the CFD approach.

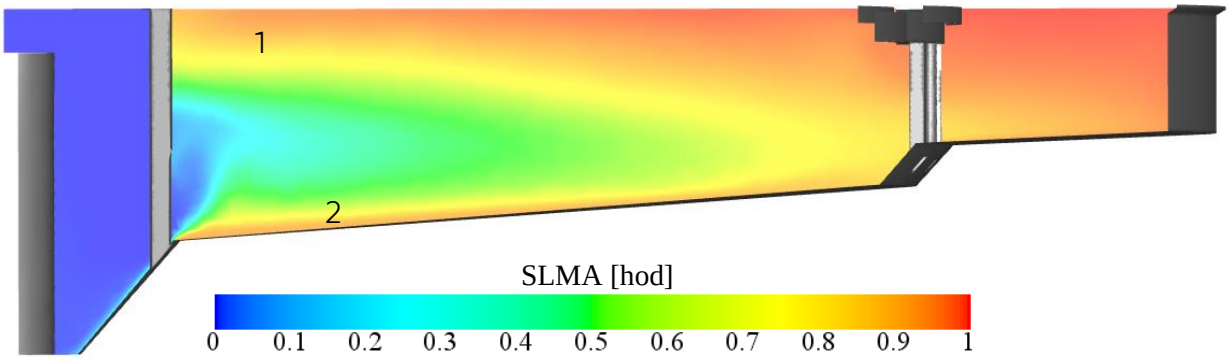

Figure 57 – Sludge local mean age scalar field for DN3 rain flow

The streamline results show clearly the increased velocity and sludge rise when leaving the inlet zone (Figure 58).

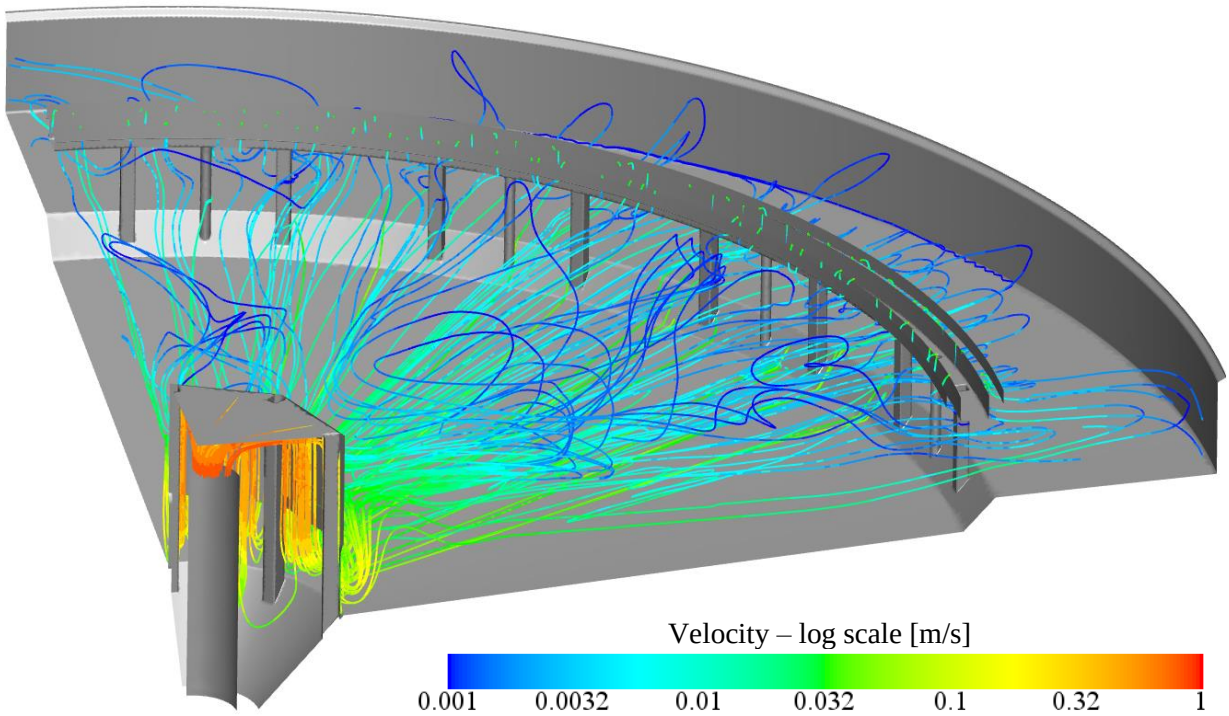

Figure 58 – Streamlines coloured by velocity for DN3 rain flow

During the DN3 validation, the CFD model showed the ability to accurately predict sludge blanket height for both nominal and increased flow rates including local phenomena such as stirred sludge area and effect of the pillars on the blanket height. Also, the SS concentration is well captured when compared to the experimental measurements. Additionally, the SLMA was presented which adds another level of insight into the behaviour of the sludge in time that is not possible to get by using other methods. It is possible to analyse potential dead zones and sludge age at any location within the tank which enables the engineers to better the design more effectively.

3.3. Settling Tank DN1 Validation

As it can be seen form the results of the DN3 tank, the problem with the inlet zone is that it points the flow rather down, then into the tank and that causes the flow to stir the already sedimented sludge going to the sludge removal area.

That led to the idea of a new inlet zone design to both increase the time for the sludge to start coagulating and also to try to change the direction of the flow coming from the inlet zone. This new design was developed and implemented in the Prague WWTP in 2015.

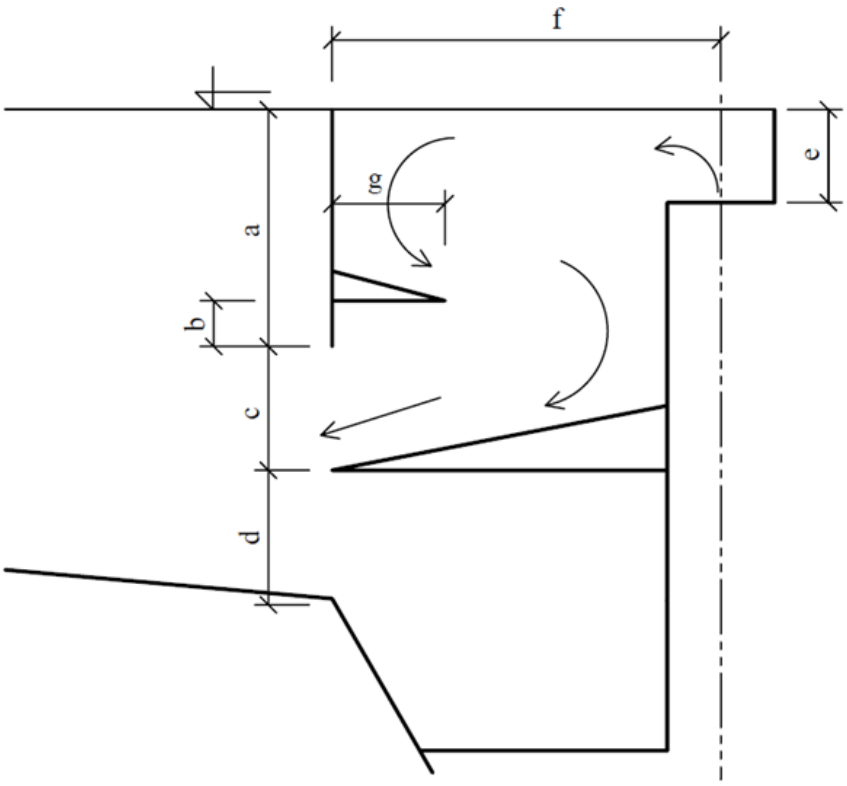

Figure 59 –Geometry of the modified inlet zone at DN1

The design is primarily made of two deflectors. The first deflector is smaller and turns the flow to the main deflector which points the flow horizontally into the tank. The exact dimensions are dependent on the tank parameters like nominal flow, height, radius etc. The main idea behind this design is that the changed direction of the flow leaving inlet zone is important during high flow rates as it does not disrupt the already sedimented sludge returning to the sludge removal area. Also, it produces lower turbulent kinetic energy which helps the settleability.

The validation was done on tank DN1 for two flow rates. The nominal flow rate and an increased flow rate when the SS concentration distribution was measured after a rain event, the same ones as under which DN3 tank was evaluated for better comparability.

For the tank DN1, two different flow rates were simulated and compared to the experimental measurements. A flow rate Q = 0,635 m3/s represents the nominal flow at the tank during normal conditions and was measured on 16.06.2016. The SVI at the tank inlet was 55 ml/g, which corresponds to the V_{0c} = 1.31 and r_{Hc} = 1.18. The increased flow rate Q = 0,870 m^3/s represents rain conditions and was measured on 16.4.2018 with the inlet suspended solids concentration of

c = 3,3 g/l. The SVI in this case was 270 ml/g with corresponding factors V_{0c} = 0.89 and r_{Hc} = 0.89.

Table 6 – Validation cases for DN1

	Flow Rate [m^3/s]	**SVI [ml/g]**	**V_{0c} [-]**	**r_{Hc} [-]**
DN1 Nominal Flow Rate	0,635	55	1.31	1.18
DN1 Increased Flow Rate	0,870	270	0.89	0.89

3.3.1. Results DN1 - Nominal Flow Rate

The sludge blanket height and suspended solids concentration was compared between CFD model and experimental data (Figure 60). The height of the sludge blanket is captured well in the model as well as the concentration of the main sludge body. The compressed sludge at the bottom of the tank shows slightly different behaviour compared to the experiment as it does not maintain constant thickness (1). The overall match is nevertheless good.

CFD Model

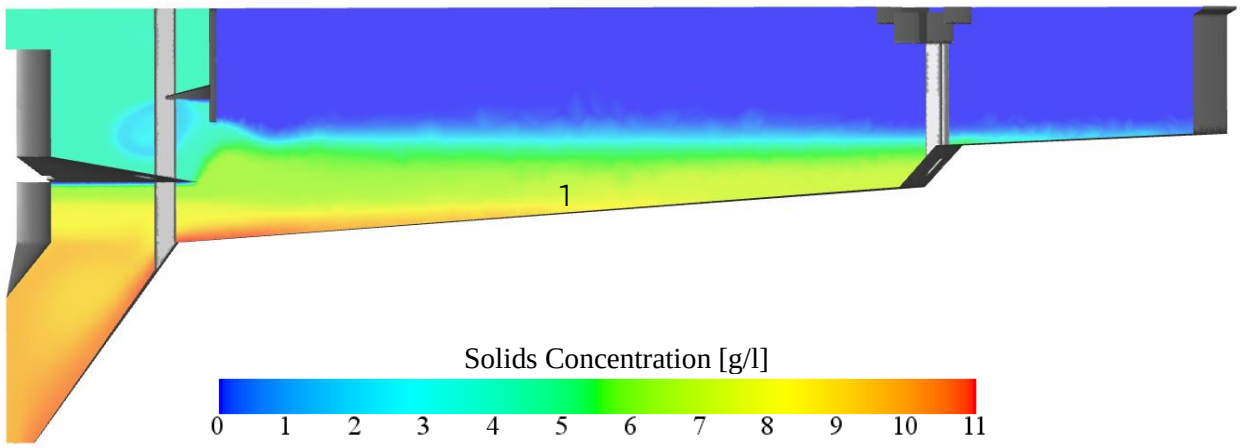

Experiment

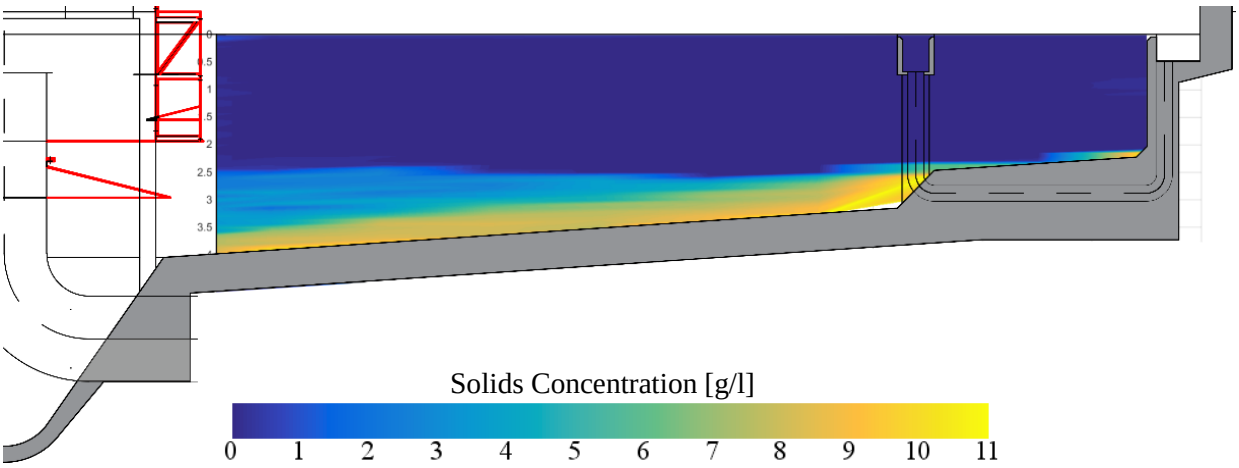

Figure 60 – Comparison of CFD model (top) and experiment (bottom) for DN1 nominal flow

From the streamlines results (Figure 61) it can be well seen the changed flow behaviour in the inlet zone.

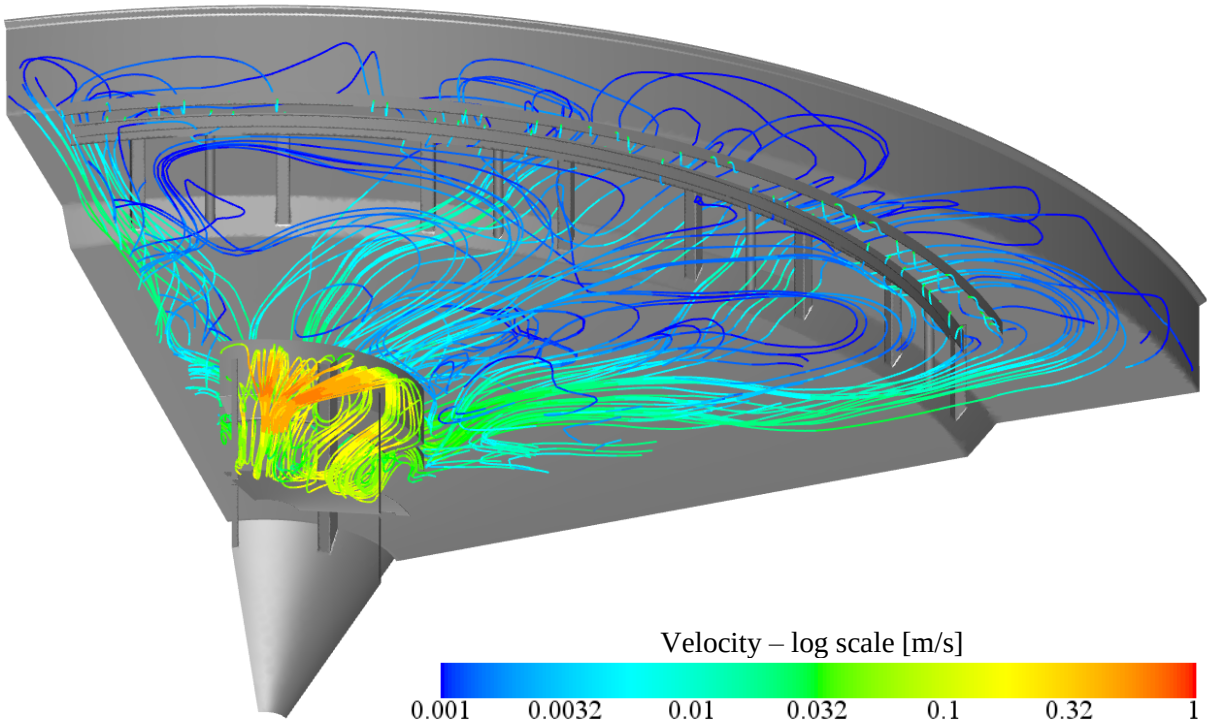

Figure 61 – Streamlines coloured by velocity for DN1 nominal flow

The vector scene is quite interesting as the main flow enters the sedimentation zone in a radial direction. The velocities are higher (0.02 m/s) than for the rest of the tank which is partly caused by the pillars that contract the flow and therefore increase local velocities.

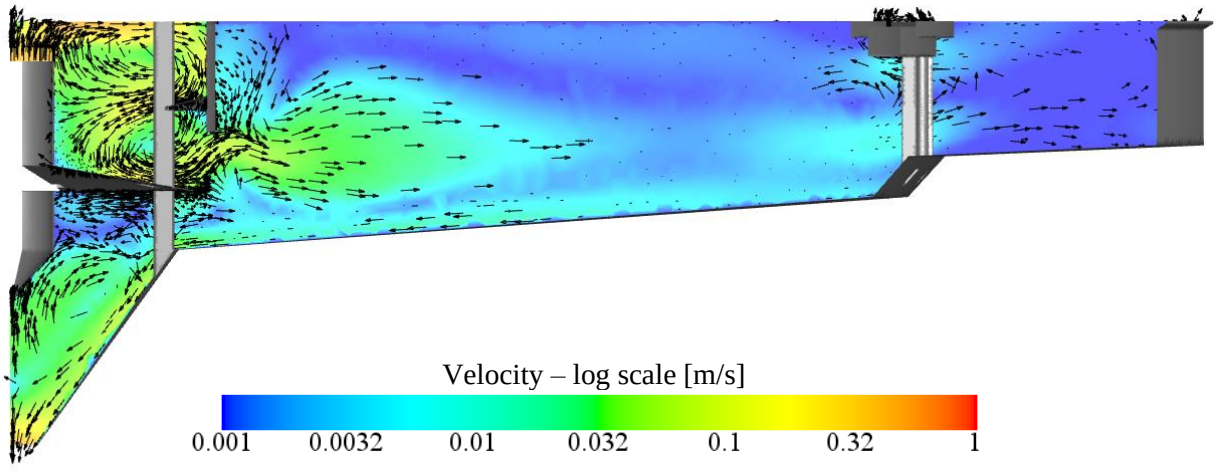

Figure 62 – Velocity vectors for the DN1 nominal flow

The SLMA scalar field shows an interesting fact that there is no old sludge on the bottom of the tank showing that rather than sedimenting at a greater radial distance it seems to be settling gradually and is not disturbed by the inflow. Also, it can be seen that compared to DN3, there is no dead zone at the top of the tank meaning the entire volume is used.

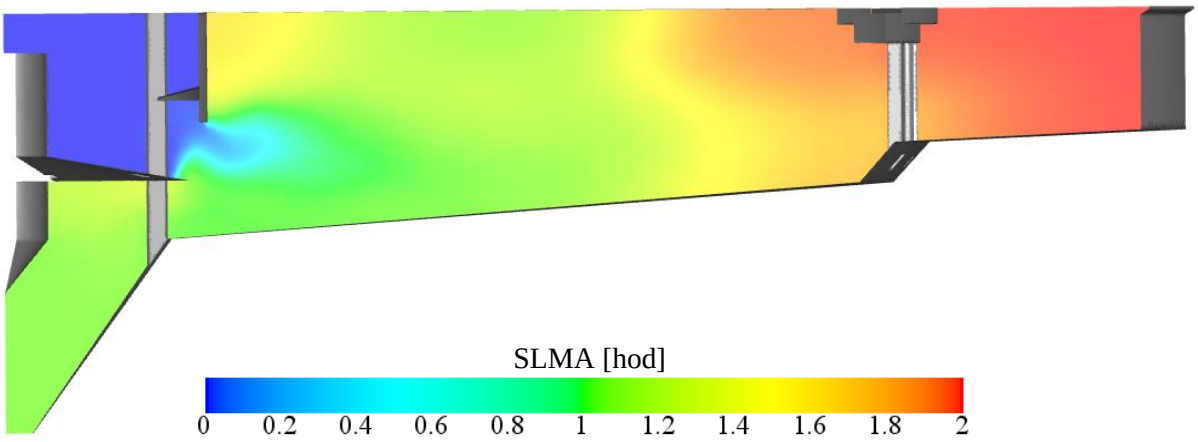

Figure 63 – Sludge local mean age scalar field for DN1 nominal flow

3.3.2. Results DN1 - Increased Flow Rate

From the results after a rain event the experiment shows an area of an increased blanket height (1). The same phenomena can be seen from the CFD results, even though the peak is more apparent. Also, the overall sludge blanket height matches well between CFD and experimental data. Compared to the DN3 tank which was measured under the same flow rate, the sludge blanket height is lower in DN1 tank showing better settling ability than the unmodified DN3 tank.

CFD model

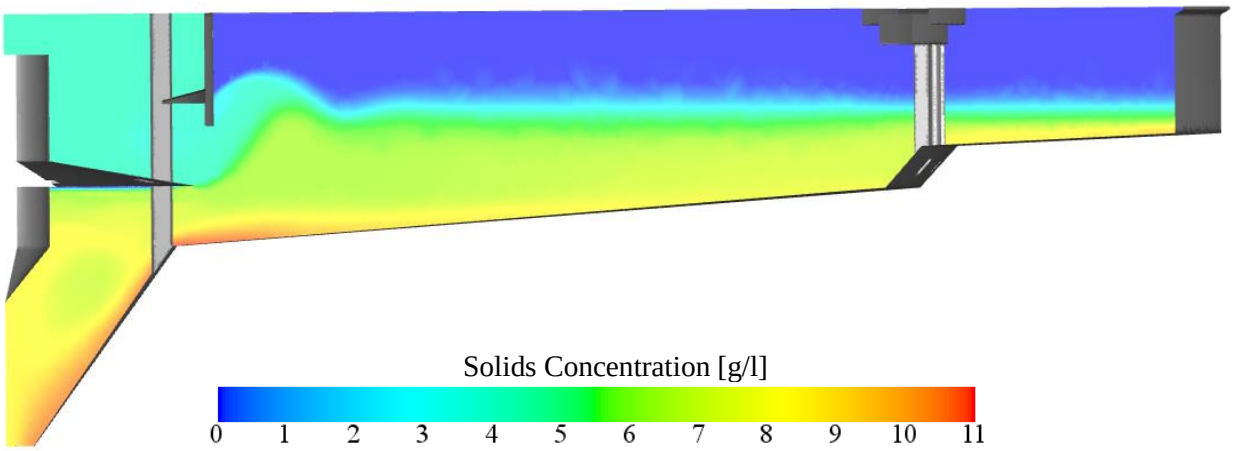

Experiment

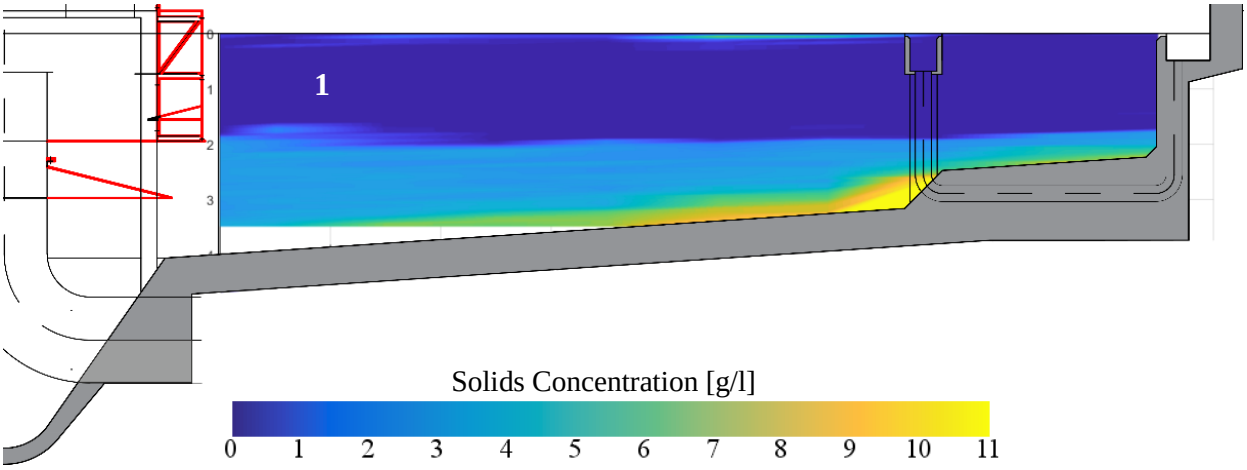

Figure 64 – Comparison of CFD model (top) and experiment (bottom) for DN1 rain flow

The Figure 65 and Figure 66 shows the isosurfaces of SS concentration for 2 g/l representing the sludge blanket height and for 6 g/l representing the interface between hindered and compress settling zones. What is apparent is the influence of the pillar mentioned previously. It increases flow velocities and also contracts the flow which has a negative impact on the function of the tank.

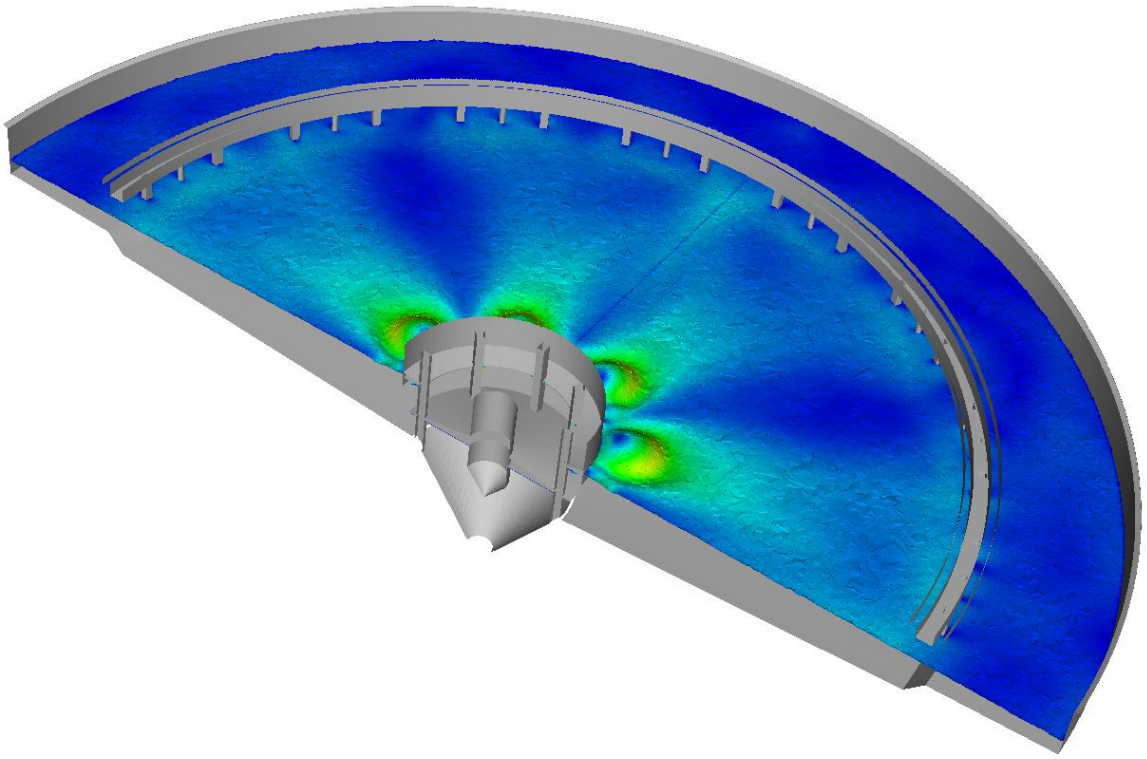

Figure 65 – Isosurface of the c = 2 g/l interpreting the sludge-water interface for DN1 rain flow

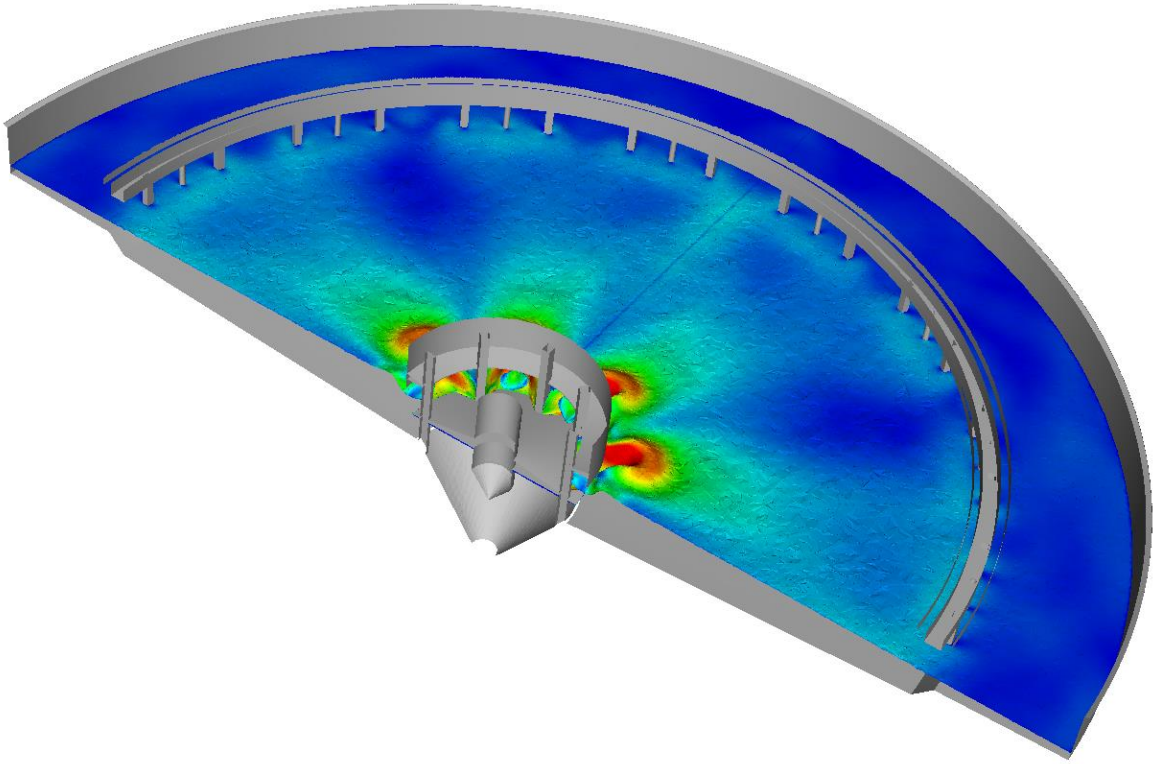

Figure 66 – Isosurface of the c = 6 g/l interpreting the hindered and compression regions interface for DN1 rain flow

The vector field show nicely how the tank functions under rain conditions. The flow coming from the inlet zone is pushed upwards and into the tank (1) whereas the bottom of the tank is not disturbed by the incoming flow (2).

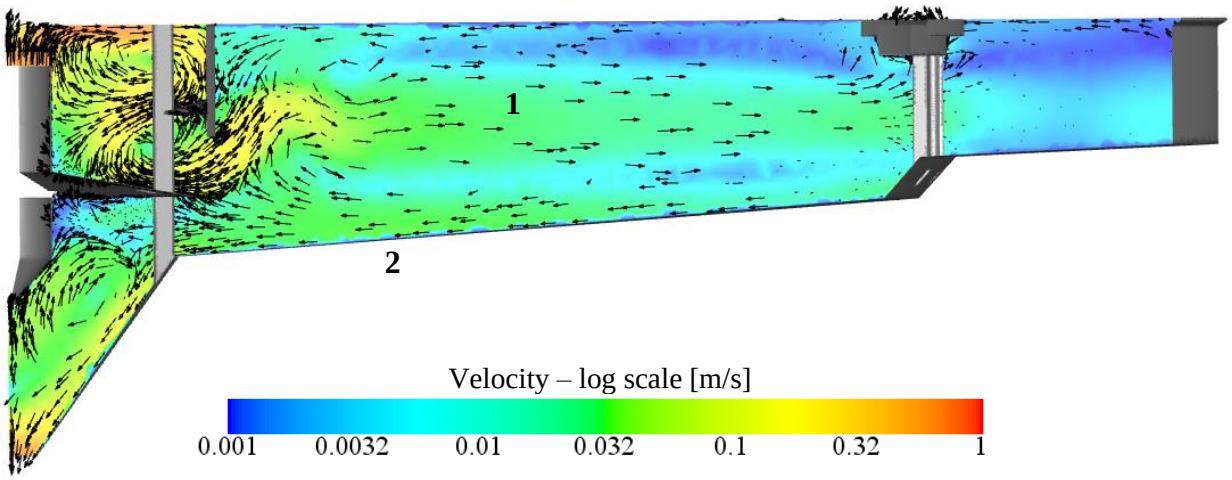

Figure 67 – Velocity vectors for the DN1 rain flow

The SLMA shows that the increased flow and corresponding velocities does not allow for a gradient sedimentation but the sludge flows to the outer part of the tank, sediments and then goes back on the bottom.

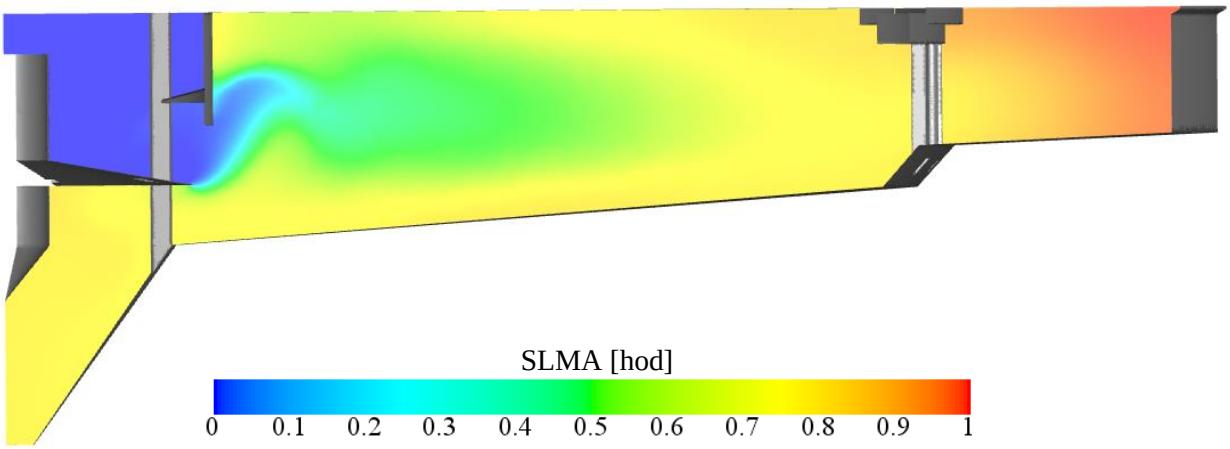

Figure 68 – Sludge local mean age scalar field for DN1 rain flow

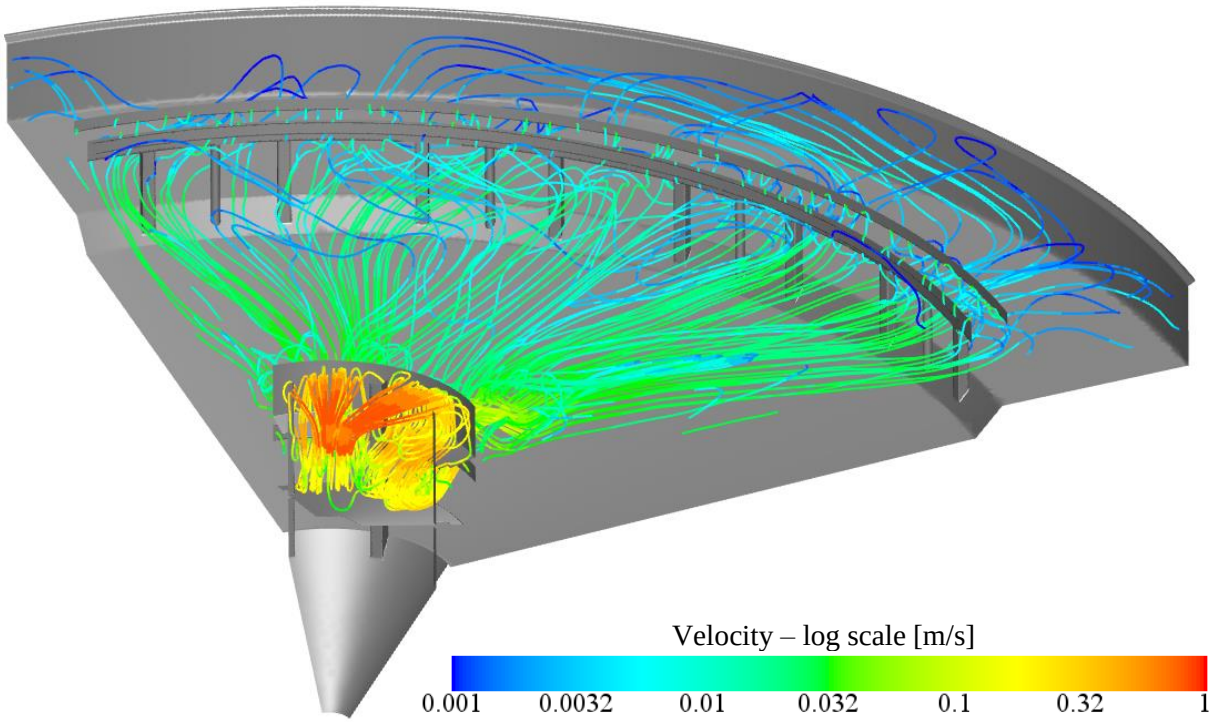

Figure 69 – Streamlines coloured by velocity for DN1 rain flow

From the streamlines results (Figure 69) it can be well seen how the flow propagates through the tank to the outer end.

4. Conclusion and Discussion

The aim of this thesis was an attempt to create a CFD model for secondary settling tanks design and optimization which would be based on an experimental data obtained through a measuring campaign but also to try to generalize the model in a way, that it would be easily adjustable for different sludge and tank conditions outside the calibrated data.

The sludge properties experimental data were gathered at the Central Waste Water Treatment Plant in Prague (CWWTP) from two different SSTs. Subsequently, the measured data were evaluated partly on-situ and partly in the laboratory. For each sample a report including all measured and calculated properties was made. The most important tests were the batch settling column test, viscosity measuring, density, solids concentration, SVI and filament index external parameters such as tank flow rates and flocculant and coagulant dosages. Also, a new technique was developed in order to measure the solids concentration profile of entire tank to provide good validation data. Due to an extensive amount of data gathered over two years, a database framework was created to process that data and to find sludge sedimentation dependencies and relations which were then used as an input for the CFD model.

Based on the measured data three different sub-model were created on top of a commercial CFD solver Ansys Fluent. The first one is a rheology sub-model that handles the non-Newtonian nature of the sludge. The model is created based on the Casson fluid type and calculates the viscosity of the sludge based on the shear rate and solids concentration to capture especially the high concentration sludge behaviour at the tank bottom. Another sub-model resolves the flocs initial aggregation phase and potential floc breakup in case of high shear gradients of the flow. It is implemented in a way, that it doesn't allow for a sedimentation in case of a very few minutes before the discrete sedimentation phase is initiated and also limits the sludge sedimentation in case of high shear rates. In order to monitor the sludge behaviour in time a new scalar is added that enables to show local sludge retention time and thus provides better insight into the dynamics of the settling tanks. The last and most important is the sedimentation sub-model that couples the solids concentration with the settling velocity thought a slip velocity term. This model also uses an innovative approach in a way that it extends the standard Takacs-Vesilind exponential equation with a correction factor based on a sample SVI. Given that, the settling model can be easily adjusted regarding the specific tank conditions, such as rain flow where the

sludge parameters differ without the need to run the batch settling test again for the specific condition.

The validation was conducted firstly using the data from a settling column test and then for 2 different settling tanks DN1 and DN3 located in a Central Waster Water Treatment Plant in Prague for 2 different flow rates, nominal and rain respectively. The results showed, that the model captures the sludge blanket height very well including important hydraulic features such as local sludge blanket rise. Thanks to the sludge local mean age model, it is possible to monitor the sludge retention time within the tank and therefore analyse potential recirculation zones. In terms of solids concentration distribution, the models predicted the low and medium solids concentrations well but underpredicts the high solids concentrations that are typical for a bottom of the tank. That is due to the fact, that the compression regime of the sludge is not resolved separately. Nevertheless, the developed model can be used due to its nature for assessing sludge flows not only in the secondary settling tanks but also for any sludge flows at WWTPs such as dividing objects and galleries or primary sedimentation tanks.

The potential future work might be then focused on validating the model at different WWTPs and potentially finding and implementing the relations between sludge age and its settling properties. Currently the model provides local sludge age information which could be added to the database in order to find new dependencies and relations.

References

Alcantara, M. R. & Moura, A. F., 1999. Rheological Data Modeling through Linear Multivariate Regression and Response Surfaces. *An. Assoc. Bras. Quim.*.

Anon., n.d. *K-epsilon turbulence model.* [Online]
Available at: https://en.wikipedia.org/wiki/K-epsilon_turbulence_model
[Accessed 2017].

Anon., n.d. *Two equation turbulence models.* [Online]
Available at: https://www.cfd-online.com/Wiki/Two_equation_turbulence_models

Ansys Inc., 2013. *ANSYS Fluent Theory Guide.* Canonsburg: s.n.

Argyropoulos, C. & Markatos, N., 2014. *Recent advances o the numerical medelling of turbulent flows.* s.l., Applied Mathematical Modelling.

Casey, P., L'Hermite & Newman, P. J., 1983. *Methods of characterization of sewage sludge : proceedings of a workshop held in Dublin.* Boston: Kluwer Academic Publishers.

Daigger, G. T. & Roper, R. E., 1985. The relationship between SVI and activated sludge settling characteristics.. *Journal of the Water Pollution Control Federation.*

Daly, B. & Harlow, F., 1970. Transport equations in turbulence. *Phys. Fluids 13*.

Das, D., 1993. Floc Breakup in Activated Sludge Plants. *Water Environment Research*, pp. 138-145.

DeClerq, B., 2003. *Computational Fluid Dynamics of Settling.* Ghent, Belgium: Deparment of Applied Mathematics, Biometrics and Process Control of Ghent University.

DIck, R. I. & Ewing, B. B., 1967. The rheology of activated sludge.. *JWPCF*.

Dick, R. I. & Vesilind, P. A., 1969. The Sludge Volume Index - What Is It?. *Water Pollution Control.*

Ekama, G. A. & International Association on Water Q, 1997. Secondary settling tanks : theory, modelling, design and operation.. *International Association on Water Quality, London.*

George, C., Scott, S., Johns, B. & McFadden, B., 2021. Optimizing a WWTP lift station using CFD modeling. *Esemag*, Issue Summer.

Glover, C., Essemiani, K. & Meinhold, J., 20016. *Modelling of wastewater treatment plants – how far shall we go with sophisticated modelling tools?.* s.l.:s.n.

Goula, A. M., Kosoglou, M. & Karapantsios, T. D., 2008. A CFD methodology for the design of sedimentation tanks in potable water treatment: Case study: The influence of a feed flow control baffle. *Chemical Engineering Journal*, Issue Issue 1-3.

Govoreanu, R., Saveyn, H., Van der Meeren, P. & Vanrolleghem, P., 2004. Simultaneous determination of activated sludge floc size distribution by different techniques. *Water Science & Technology.*

Griborio, A., 2004. *Secondary Clarifier Modeling: A Multi-process.* New Orleans, Louisiana: University of New Orleans.

Griborio, A. & McCorquodale, J. A., 2006. Optimum design of your center well: use of CFD model to understand the balance between flocculation and improved hydrodynamics.. *Proceedings of the Water Environment Federation.*

Guth, C., Zhang, S. & Taylor, R., n.d. *Utilizing CFD modeling to identify methods for improving pump station hydraulic conditions.* s.l.:s.n.

IWA, 2008. *Biological Waste Water Treatment, Principles, Modelling and Design.* London UK: IWA Publishing.

Jameson, A., n.d. *Computational Fluid Dynamics: Past, Present and Future.* [Online] Available at: http://aero-comlab.stanford.edu/Papers/NASA_Presentation_20121030.pdf

Jin, B., Wilén, B. & Lant, P., 2003. A comprehensive insight into floc characteristics and their impact on dewaterability of activated sludge. *Chemical Engineering Journal.*

Karches, T., 2012. *Computational fluid dynamics in wastewater treatment: reactor and intensification.* Budapest: s.n.

Karches, T. & Buzas, K., 2011. Methodology to determine residence time. In: Vol. 70 ed. s.l.:WIT Transactions on Engineering Sciences, pp. 117-125.

Karpinska, A. & Bridgeman, J., 2016. CFD-aided modelling of activated sludge systems – A critical review. *Water research*.

Kopal, Z., 1947. *Tables of Supersonic Flow Around Cones, Depart of Electrical Engineering.* s.l.:Center of Analysis, Massachusets Institute of Technology.

Kos, M., 2015. Termochemické zpracování čistírenských kalů. *SOVAK*, Issue 12.

Kynch, G., 1952. A Theory of Sedimentation. *Transactions of the Faraday Society,* pp. 166-176.

Landes, N., Boksiner, G. & Stencel, R., n.d. *Troubleshooting Problematic Chlorine Mixing Dynamics with CFD Analysis.* s.l.:s.n.

Li, C. & Huang, Q., 2016. Rheology-Based Computational Fluid Dynamics Modeling for De-oiling Hydrocyclone Efficiency. *Chemical Engineering & Technology*, Issue 10.1002/ceat.201500623.

Mancell-Egala, Kinnear, A., Murthy, D. & Sudhir, J., 2012. Settling Transition Concentration Measurement to Quantify Sludge Settling Behavior.. *Proceedings of the Water Environment Federation.*

Maries, A. et al., 2012. Interactive Exploration of Stress Tensors Used.

Menter, F., 1994. Two-Equation Eddy-Viscosity Turbulence Models for Engineering Applications. *AIAA Journal*.

Mills, N., 2016. *Unlocking the Full Energy Potential of Sewage Sludge - Doctor of Engineering Thesis.* s.l.:University of Surrey / Thames Water.

Monash University, 2003. *Civil Engineering Resources,* s.l.: s.n.

Morse, D., Sickza, J. & Nielsen, K., 2016. *Extending the McCoquodale Model for 3D CFD of settling tanks.*. New Orleans, USA, s.n., pp. 3673-3690.

Ozinsky, A. E. & Ekama, G. A., 1995. Secondary settling tank modelling and design Part 2:. *Water SA.*

Patankar, S. V., 1980. *Numerical Heat Transfer and Fluid Flow*.. New York, USA: Hemisphere Publishing Corporation, Taylor & Francis.

Plósz et al, B. G., 2012. A critical review of clarifier modelling: State-of-the-art and engineering practices. *Technical University of Denmark.*

Ramin, E. et al., 2014. A new settling velocity model to describe secondary sedimentation.. *Water Research*, pp. 447-458.

Roache, P. J., 1982. *Computational Fluid Dynamics*.. Albuquerque, USA: Hermosa Publishers.

Říha, J., n.d. *Jakost vody v povrchových tocích a její matematické modelování.* s.l.:NOEL 2000.

Samstag, R. W. et al., 2016. CFD for wastewater treatment: An overview.. *Water Science and Technology*.

Shawn, W., 2014. *CFD of Large Structures for Wastewater Treatment.* [Online]
Available at:
http://www.engineering.com/DesignSoftware/DesignSoftwareArticles/ArticleID/7678/CFD-of-Large-Structures-for-Wastewater-Treatment.aspx

Schmitt, F., 2007. About Boussinesq's turbulent viscosity hypothesis: historical remarks and a direct evaluation of its validity. *Comptes Rendus Mécanique*, Issue 617-627.

Steiner, A. E., McLaren, D. A. & Forster, F., 1976. The nature of activated sludge flocs. *Water Research.*

Švanda, O. & Pollert, J., 2021. CFD Modelling of a Secondary Settling Tanks: Generalization based on database relations. *Acta Polytechnica,* Issue Vol. 63.

Švanda, O., Pollert, J. & Johanidesová, I., 2018. *Development of Screening Methods for Secondary Settling Tanks Monitoring and Optimization.* Palermo, Italy.

Takacs, I., Patry, G. G. & Nolasco, D., 1991. A dynamic model of the clarification thickening process.. *Water Research.*

Vanderhasselt, A. & Vanrolleghem, P. A., 2000. Estimation of sludge sedimentation parameters from single batch settling curves. *Water Research.*

Visilind, A., 2003. *Wastewater treatment plant design.* s.l.:IWA Publishing.

Voutchkov, N., 2005. Settling Tanks. *Water Encyclopedia.*

Wendt, J. F., 2008. *Computational Fluid Dynamics: An Introduction.* s.l.:Springer Science & Business Media.

Wett, B., Buchauer, K. & Fimml, C., 2011. Energy self-sufficiency as a feasible Energy self-sufficiency as a feasible.

Wilcox, D., 2004. *Turbulence Modeling for CFD.* s.l.:DCW Industries, Inc..

Wimshurst, A., Burt, D. & Jarvis, S., 2019. *Enhanced Process Models For Final Settlement Tanks.* Birmingham, s.n.

Wright, H., n.d. *New EPA rule to drive use of UV disinfection.* [Online]
Available at: http://www.waterworld.com/articles/print/volume-22/issue-3/feature/new-epa-rule-to-drive-use-of-uv-disinfection.html

Zheng, W., Yan, C. & Liu, H., 2015. Comparative assessment of SAS and DES turbulence modelingfor massively separated flows. *Acta Mechanica Sinica 32(1).*

Zhou, S. & McCorquodale, J. A., 1992. Mathematical modelling of a circular clarifier. *Journal of Hydraulic Engineering.*

List of Tables and Figures